

VIRUSES IN CHIRONOMUS PLUMOSUS

OBSERVATIONS ON NATURALLY OCCURRING VIRUSES IN  
LARVAE OF THE MIDGE CHIRONOMUS PLUMOSUS

by

DONALD B. STOLTZ, M.Sc.

A Thesis

Submitted to the Faculty of Graduate Studies  
in Partial Fulfilment of the Requirements

for the Degree

Doctor of Philosophy

McMaster University

December, 1969

DOCTOR OF PHILOSOPHY (1969)  
Biology

McMASTER UNIVERSITY  
Hamilton, Ontario

TITLE: Observations on naturally occurring viruses in larvae  
of the midge Chironomus plumosus.

AUTHOR: Donald B. Stoltz, B.Sc. (University of Guelph)  
M.Sc. (Queen's University)

SUPERVISOR: Professor D. M. Davies

NUMBER OF PAGES: ix, 163

SCOPE AND CONTENTS:

Three new virus diseases are described in larvae of the midge, Chironomus plumosus. The intracellular development of one of these, CpV-1, in the fat body and muscle of this insect is given in detail. In addition, the ultrastructure of the virion is described. Classification of the known icosahedral cytoplasmic DNA viruses is discussed.

The development of a cytoplasmic polyhedrosis virus in the midgut is examined. Observations are discussed in relation to knowledge concerning other polyhedrosis viruses, and possible evolutionary pathways among them.

A cytoplasmic polyhedrosis of the fat body is described for the first time. The ultrastructure of the viral capsid is compared to that of the bacteriophage  $\phi$  X 174.

## ACKNOWLEDGEMENTS

I should like to express sincere appreciation to my supervisor, Dr. D. M. Davies, for generous encouragement and assistance during the course of these studies.

Thanks are also due to Dr. William Hilsenhoff, Department of Entomology, University of Wisconsin, without whose help this work could not have been done. Dr. Hilsenhoff supplied most of the insects used and in addition conducted in his laboratory some experiments suggested by the author. I am indebted to him also for helpful discussions and communications concerning the ecology and population dynamics of C. plumosus.

Dr. E. A. MacKinnon, Department of Microanatomy, Ontario Veterinary College, University of Guelph, suggested altering the Na:K ratio in glutaraldehyde used in the fixation of insect tissue culture cells. Mr. Charles Chow advised and assisted in colorimetric tests for viral nucleic acids. I thank Dr. J. F. Mustard for allowing me to make use of the excellent facilities of the Department of Pathology electron microscope lab, and Mr. Tom Bistricki for instruction in the use of the Philips EM 300. I should also like to acknowledge the assistance of Dr. H. F. Stich, under whose supervision these studies were begun.

## TABLE OF CONTENTS

	Page
Introduction . . . . .	1
Materials and Methods . . . . .	10
I. Insects . . . . .	10
II. Detection and Examination of Viruses . . . . .	12
III. Autoradiography of CpV-1 Infected Larvae . . . . .	19
IV. Purification of CpV-1 . . . . .	20
V. Chemical Degradation of CpV-1 Particles . . . . .	22
VI. Colorimetric Tests for Nucleic Acids in Purified CpV-1 Particles . . . . .	24
VII. Transmission of CpV-1 . . . . .	25
VIII. Reagents . . . . .	28
Results . . . . .	32
I. <u>Chironomus plumosus</u> Virus #1 (CpV-1) . . . . .	32
II. Cytoplasmic Polyhedrosis Virus in the Midgut Epithelium . . . . .	88
III. Cytoplasmic Polyhedrosis of the Fat Body . . . . .	114
Discussion . . . . .	118
Conclusions . . . . .	151
References . . . . .	152
Appendix . . . . .	164

LIST OF FIGURES

Number	Title	Page
1	Fourth-instar <u>C. plumosus</u> larva; uninfected	34
2 to 5	Larvae infected with <u>C. plumosus</u> Virus-1 (CpV-1)	34
6	Uninfected fat body; Feulgen-stained fat body	37
7	Infected fat body showing Feulgen-positive cytoplasmic inclusion bodies	37
8	Uninfected fat body; orcein squash preparation	37
9 & 10	Infected fat body showing cytoplasmic inclusion bodies stained with orcein	37
11 & 12	Uninfected fat body	39
13 to 16	Early foci of CpV-1 infection in fat body	40
17 to 19	Fat body showing later stages of infection	41
20 to 23	Mature cytoplasmic inclusion bodies and extracellular virus	42
24 to 27	Radioautographs of infected fat body showing localization of H <sup>3</sup> -CH <sub>3</sub> -thymidine incorporation over cytoplasmic inclusion bodies	44
28 to 31	Infected fat body showing nucleolar hypertrophy	45
32	Uninfected muscle	47
33 to 37	Infected muscle	47
38 & 39	Ultrastructure of uninfected fat body	50
40 & 41	Ultrastructure of uninfected muscle	50
42	Ultrastructure of uninfected muscle	51
43 & 44	Ultrastructure of cytoplasmic inclusion bodies containing virus particles	53
45	Purified virus particles visualized by phase-contrast microscopy	54
46	Purified virus particles, negatively stained	54

LIST OF FIGURES (continued)

Number		Page
47	Extracellular virus particles <u>in situ</u>	54
48 to 50	Ultrastructure of early foci of infection in fat body	55
51 to 54	Ultrastructure of virogenic stromata	57
55	Infected fat body: small and large inclusion bodies	58
56 to 59	Infected fat body: changes in nuclear ultrastructure	60
60 & 61	Aberrant synthesis and/or assembly of viral components in cytoplasmic inclusion bodies	61
62	Release of virus particles by cell lysis	62
63 & 64	Infected fat body: phagocytosis of virus by as yet uninfected cells	64
65 & 66	Phagocytosis of virus by hemocytes	65
67 & 68	Rickettsia-like bodies in infected fat body	66
69	Ultrastructure of CpV-1-infected muscle	69
70 to 76	Virogenic stromata and maturation of virus particles in infected muscle	70 71 72 73
77 to 85	Quadrangular, pentagonal, hexagonal, and circular profiles of sectioned virus particles	74 75
86	Negatively-stained virus particle in 3-fold projection	78
87 to 90	Negatively-stained CpV-1 (Wisc.), CpV-1 (Toronto) and "CIV"	80
91 & 92	Collapse of pronase-treated CpV-1 and CIV capsids	81
93 to 95	Equilateral triangular and other fragments derived from collapsed CpV-1 and "CIV" capsids	84

LIST OF FIGURES (continued)

Number		Page
96 - 98	Triangular fragments derived from collapsed capsids	85
99 & 100	Subunits released from mercaptoethanol-treated viral capsids	86
101	Combined transverse and tangential section of uninfected midgut epithelium	90
102-105	Cellular detail of uninfected midgut epithelial and regenerative cells	91
106	Ultrastructure of the apical cytoplasm of an epithelial cell	92
107	Lateral septate junctions between adjacent epithelial cells	93
108	Uninfected midgut epithelium: nuclear ultrastructure	94
109	Ultrastructure of the basal cytoplasm of an epithelial cell	96
110	Microbodies in the basal cytoplasm of an uninfected epithelial cell	97
111	Ultrastructure of a regenerative cell	98
112-115	Infected midgut epithelial cells containing cytoplasmic inclusion bodies	99
116-117	Formation of large cytoplasmic inclusion bodies	101
118	Breakdown of infected midgut epithelium	101
119-121	Ultrastructure of cytoplasmic inclusion bodies showing free viruses, "coated" particles, and polyhedra	102 103
122	Virus particles associated with an electron dense component of a virogenic stroma	105
123-126	Ultrastructure of intra- and extracellular virus particles	106

LIST OF FIGURES (continued)

Number		Page
127-129	Ultrastructure of "coated" virus particles	107 108
130	Occlusion of polyhedra	111
131	Polyhedra and "coated" particles	112
132	Free virions in microvilli and vesicles derived from microvilli	113
133&134	Larvae with cytopolyhedrosis of the fat body	116
135-136	Polyhedra in infected fat body	116
137	Ultrastructure of a polyhedron, showing occluded virions	117
138-140	Negative-stained cytoplasmic polyhedrosis virus particles viewed along various axes of symmetry	117
141	Diagrammatic representation of sectional profiles of an icosahedron	120
142	Diagram of proposed structure of <u>Sericesthis</u> iridescent virus	122
143	Diagrammatic representation of cytoplasmic polyhedrosis virus maturation in <u>C. plumosus</u>	140
144	Diagrammatic representation of possible evolutionary pathways among the cytoplasmic polyhedrosis viruses	142
145	Diagrammatic representation of possible evolutionary pathways among the granulosis and nuclear polyhedrosis viruses	144

LIST OF TABLES

Number	Title	Page
1	Results of colorimetric tests for nucleic acids in CpV-1 virus particles	87
2	The icosahedral cytoplasmic DNA viruses	129

## INTRODUCTION

A list of virus diseases in 127 species of insects was published in 1960 (82); only four references to virus diseases in the Diptera were given. This is perhaps surprising in view of the fact that certain Diptera, for example, the chironomids (midges) and culicids (mosquitoes), have become important laboratory animals. The chironomids, because of their giant salivary gland chromosomes, have been particularly useful in studies of chromosome structure and function, developmental cytology, and hormone action (12, 33, 121). Certainly, a search for viruses in the Chironomidae, and similar nematoceros flies, might be expected to provide useful tools for the study of at least some biological processes.

In Rhynchosciara angelae, for example, a nuclear polyhedrosis virus induces nuclear and cellular hypertrophy (97). Chromosomes that were already polytene and large in size, show a considerable increase in polyteny in virus-infected nuclei. It seems possible that such a virus could be used meaningfully in an investigation of the mechanisms underlying the induction of polyteny and cellular hypertrophy.

It was with such considerations in mind that a search was initiated for new viruses in the genus Chironomus<sup>1</sup>. This

---

<sup>1</sup> A pox virus has been reported in C. luridus (45).

thesis describes the results of that endeavour. The viruses discovered, while apparently unique, are nevertheless thought to belong to well-defined "groups" of insect viruses, namely the Iridoviridae (15) and the cytoplasmic polyhedrosis viruses (110). Such viruses are therefore briefly introduced below:

### I. The Iridescent Insect Viruses (Iridoviridae)

The virus family name, Iridoviridae, was coined in 1962 as part of Iwoff, Horne, and Tournier's scheme of viral classification (78). While only one virus, Tipula iridescent virus (TIV), was included in the family, other iridescent insect viruses have since been discovered (29,31,41,120), and together seem to form a well-defined group (15). Tipula, Chilo and Sericesthis iridescent viruses are large, ranging in size from 130 to 180  $\mu$  depending on the amount of hydration, contain double-stranded DNA, possess icosahedral symmetry and form, and may or may not accidentally acquire an envelope (15). All multiply only in the cytoplasm. The names of the family, and of the proposed type genus (Iridovirus) are derived from the fact that infected tissues, and pellets of purified virus, invariably iridesce; the phenomenon is due to the formation of microcrystalline arrays of virus particles (66).

Virions typically consist of electron-dense cores enclosed by shells consisting, according to various

interpretations, of one or two layers (86,120,127,128,137). Some evidence has been presented (86,128) for the existence of a negatively-charged 50 m $\mu$  electron-translucent surface coat around virus particles, but this remains to be determined. The chemical nature of the shell is uncertain; reports of lipid being present (126) have been interpreted as host contaminants (13). Polysaccharide components were not detected by Thomas (126), but, according to Mercer and Day (86) may be present. As yet, there is no convincing chemical evidence for this proposal. Until recently, it had been assumed that the capsid of TIV was composed of 812 capsomeres (109). It is now known that at least one iridovirus capsid contains approximately 1562 capsomeres arranged so as to form an icosahedron (142). Iridovirus DNA is double-stranded, with molecular weights ranging from 126 to 134 million daltons, and G + C contents of from 28 to 32% (14,15,16). Aside from this, almost nothing is known about the molecular biology of these viruses.

Most of what is known concerning the replication of iridoviruses is derived from electron microscopic work. The replication of Sericesthis iridescent virus (SIV) (13,72) which has been studied by means of electron microscopic autoradiography (72), is probably typical of the group as a whole. Virus particles are apparently taken up in phagocytic vesicles. Following this, an undetermined sequence of events results in the disappearance of recognizable virus, and later,

in the appearance of fibrogranular virogenic foci near the nuclear membrane.

Nothing definite is known about how virus particles are actually assembled. Incomplete shells are often seen in areas of viral replication, and have been interpreted as representing stages in viral morphogenesis (145), the shell presumably remaining open until a full complement of DNA is enclosed. Complete but empty shells are also seen; these have been interpreted by Bird (21) as being profiles of particles cut above or below the core, or as artefacts resulting from extraction of the core during preparation of material for electron microscopy. The most detailed study is probably that of Xeros (145). This author describes the presence of a microvesicular element in the virogenic stroma, and states that these may be involved in the formation of viral shells.

Methods of transmission of iridoviruses in nature are unknown in most instances. In the laboratory, diseases are very efficiently induced by inoculation of virus into the hemolymph; feeding of virus results in a much lower incidence of infection (74,88,141). Recent work on mosquito iridescent virus (MIV) suggests that transovarial infection may be the predominant mode of transmission for that virus (74).

## II. The Cytoplasmic Polyhedrosis Viruses

The cytoplasmic polyhedroses constitute a very common form of infectious viral disease in insects. First described

in 1950 (107), diseases in over 80 species of insects have since been found (110). The viruses seem rarely to affect insects other than the Lepidoptera; only one convincing case of cytopolyhedrosis in the Diptera has been previously reported (32). Virions are small, about 50-70 m $\mu$  in diameter (8,60), and possess isosahedral symmetry; projections occur at each vertex (60). The nucleic acid is a double-stranded RNA (89), probably occurring in the form of linear fragments (73). RNA polymerase activity is associated with intact purified virus particles (73); the enzyme appears to be a transcriptase.

Multiplication of cytoplasmic polyhedrosis viruses takes place only in the cytoplasm of the midgut epithelium<sup>1</sup>. Regenerative cells of that tissue are apparently immune (26). The disease is often more debilitating than lethal (26,117), presumably because the regenerative cells are able to replace the virus-killed cells up to a point, which seems to depend on the time of acquisition of infection (26). Most larvae that become infected during the earlier instars are killed. At a terminal stage of disease, the midgut becomes chalky-white, owing to a massive accumulation of polyhedra in infected cells. This change is readily observed through the integument of some insect larvae, and constitutes the major symptom of disease.

---

<sup>1</sup> Exceptions: (a) Cytopolyhedrosis in ovarian tissue cultures of the silkworm has been reported and, (b) the present study includes a brief account of a cytopolyhedrosis of the fat body in a single C. plumosus larva.

The first sign of infection is the development of Feulgen-negative virogenic stromata (144). Mature virus particles become occluded in large masses of crystalline protein in the form of polyhedra. Little is known about the mechanics of this phenomenon. In only three previous studies was any attempt made even to describe what happens (8,23,117). Bird (23) states that the polyhedral protein diffuses into "relatively large masses of virus particles and crystallizes to form polyhedra". Arnott et al. (8) suggest that polyhedra develop within a "crystallogenic matrix". Such matrices, however, seem to be derived from the original stromata which, perhaps at a later stage, somehow become more involved in occlusion than in replication of viruses. Occlusion of particles appears to occur by a process of accretion of polyhedral protein around virus particles, after those have established a close association with the growing polyhedron (8). It is assumed that the occlusion of viruses within polyhedra is a device whereby viruses can remain viable in an extracellular environment for extended periods of time. The protein, in fact, is known to be remarkably resistant to bacterial proteases (39).

### III. Biology of *Chironomus plumosus*

*Chironomus plumosus* is a holarctic species, the larvae of which live primarily in eutrophic bodies of water. In Wisconsin, oviposition occurs in the spring and late summer,

there being two generations per year (55). The eggs are embedded in a jelly-like matrix. Egg masses, originally deposited on lake surfaces, soon absorb water and then sink to the bottom. Larvae hatch in 3 to 14 days and often remain in the egg mass for 24 hours, perhaps feeding on the gelatinous matrix. First-instar larvae, upon leaving the egg masses, are apparently free-swimming. Larvae of all other instars (total of 4), however, construct U-shaped burrows in the bottom mud and at temperatures above 5°C feed indiscriminately on particles trapped by a filtering apparatus (132). This filter is composed of salivary gland secretion and is concave in shape, being attached in the center by a thread connected with the larval mouthparts. Water is caused to flow through the filter by means of undulations of the larval body. All particles over 12 $\mu$  in size are retained on filters, which are periodically eaten and replaced (132). In addition, larvae have been known to feed at the mud surface near their burrows (55). Limnetic swimming behaviour, however, seems to be rare, so that extensive population movements probably occur mainly during the first instar, depending on the suitability of the surface substrate. Wind direction and velocity also appear to be important factors in determining the final distribution of larval populations (55).

Progeny from the spring emergence of adults will pupate about 7 weeks after hatching, assuming average lake bottom temperatures. At typical temperatures of 23 to 25°C in July

and August, the pupal stage lasts from 1 to 2 days. The progeny of the second (late summer) generation are usually in the fourth instar by October, and overwinter as such.

Populations of C. plumosus larvae fluctuate drastically not only from year to year, but also from one part of a lake to the other. Such changes are not all accounted for by larval migration or wind conditions (57). Larvae are subject to heavy predation by fish and, to a lesser extent, by a leech (54). First- and second-instar larvae may also be an important source of food for other chironomid larvae belonging to the predacious subfamily Tanypodinae (57). Indeed, adult emergences of the latter often follow closely upon hatching of C. plumosus larvae.

Diseases of C. plumosus larvae have not been studied in any detail. Excluding the results of the present study, the only other pathogen known for this insect is a microsporidian parasite (56). Although this protozoan has occasionally been found to infect as many as 50% of fourth-instar larvae, it is generally the case that only 5% are infected. Hilsenhoff (57) regards "unidentified bacterial, fungal or viral diseases" as being probably the most important factors involved in population fluctuations of the insect.

During the past 5 years, larval samplings in Lake Pepin, Wisconsin, have indicated an extensive mortality, from unknown causes, of fourth-instar larvae. Such larvae normally range in length from 15 - 30 mm and do not pupate until they

are at least 23 mm long (55). Fat body does not develop significantly until larvae have grown to 21 mm or more. From 1962, through 1964, the numbers of larvae of different lengths taken from Lake Pepin have been tabulated (Hilsenhoff, personal communication). In late June, following the May emergence, populations of 15-20 mm fourth-instar larvae averaged 104 per square foot. In July, August, and September, however, populations of larvae greater than 21 mm never exceeded 3 per square foot. A similar, but less drastic, reduction in numbers also occurred in the progeny of the September emergence, with overwintering populations of larvae greater than 21 mm averaging less than 10 per square foot. In March of 1967, 40% of collected fourth-instar larvae were found to exhibit abnormal fat body coloration; instead of being transparent, the tissue was white and opaque. The observations suggested the presence of a disease of epidemic proportions.

The present studies began with an attempt to characterize the agents responsible for the above-mentioned<sup>1</sup> and certain other diseases in C. plumosus larvae.

---

<sup>1</sup> The majority of the work presented here is concerned with this disease, now known to be caused by a virus which appears to be closely related to the Iridoviridae. For the sake of clarity of communication in the following, the virus has been designated as CpV-1 (for C. plumosus virus #1).

## MATERIALS AND METHODS

### I. Insects

C. plumosus larvae were reared, or collected, by Dr. W. L. Hilsenhoff of the Department of Entomology, University of Wisconsin, Madison, Wisconsin. Techniques for rearing larvae in the laboratory have already been described in detail (58). Briefly, larvae were maintained in aquaria (75 gallon capacity; 48 x 20 x 14 inches high) containing a 3 inch layer of lake mud covered by 9 inches of aerated water at 23.5°C. Following emergence, adults were induced to swarm and mate by controlled light conditions: an intensity of 0.5 ft-c from overhead incandescent lamps for 75 mins. each morning, followed by normal fluorescent room lighting for 15 hours, and 8 hours of darkness. Swarming and mating occurred in a large (4 1/2 x 5 1/4 x 7 foot high) polyethylene cage surrounding the aquaria. Eggs deposited in aquaria hatched and completed larval development within five weeks. Food was found to be necessary for the initiation of pupation and emergence, although larvae could develop to the fourth-instar without it. Generally, however, food (powdered dog biscuits) was added every two days. Aquaria were originally stocked with fourth-instar larvae reared from egg masses taken from female flies at Lake Winnebago, Wisconsin.

Field-collected larvae were sampled mainly from Lakes Winnebago and Pepin by means of a 6 inch Ekman dredge. Various sites on these lakes were marked with buoys during the summer, and with wooden poles embedded in the ice during the winter when weather and ice conditions were favourable. Samples have been collected by Dr. Hilsenhoff during the past seven years as part of a study of the ecology of C. plumosus, and other aquatic invertebrates, in a total of 14 Wisconsin lakes.

Permission to import larvae was obtained from the Canada Department of Agriculture, Plant Protection Division, Ottawa, and attempts were made to have them shipped from Madison to Hamilton. It was soon made apparent that very few larvae were sufficiently hardy to withstand the usual customs procedures. Thereafter, larvae were shipped to Roswell Park Memorial Institute, in Buffalo, where they were picked up by the author and personally transported without incident across the United States - Canadian border. All larvae were sent in polyethylene bags containing water.

Upon arrival in Hamilton, larvae were either used immediately, or else placed in plastic containers with 3 inches of Lake Winnebago mud and supplied with running tap water at 17-18°C. Food was added weekly.

In addition, a few C. plumosus larvae collected at Hanlon's Point, Lake Ontario, were made available by Dr. R. O. Brinkhurst of the University of Toronto. These,

too, were examined for virus infections.

## II. Detection and Examination of Viruses

Insects (almost always fourth-instar larvae) were suspected of having viral, or other, diseases on the basis of discoloration of various tissues<sup>1</sup>, such as fat body, muscle, or gut. Since it was originally assumed that symptoms of diseases caused by any of several possible agents (i.e. bacteria, fungi, protozoa and viruses) might in some cases be similar, a standard procedure was developed in order that some indication of the nature of the infectious agent could be achieved quickly and simply.

Each larva was placed on blotting paper to eliminate as much surface moisture as possible, and then transferred to a small watch glass. Using hooked minuten pins taped securely to 6" applicator sticks, larvae were quickly ripped open along the lateral integument. Immediately after drawing off a drop of hemolymph with a Pasteur pipette, larvae were flooded with Grace's modified insect tissue culture medium (Grand Island Biological Co., Grand Island, New York) at 4°C. The hemolymph was prepared for electron microscopy by negative staining. Samples of various tissues, dissected out under culture medium, were then quickly placed in freshly prepared Kahle's fixative<sup>2</sup>.

---

<sup>1</sup> Symptoms of viral diseases are described fully in RESULTS.

<sup>2</sup> For details concerning composition and sources of chemicals not given in text, see REAGENTS.

The insect was then flooded with 3.5% glutaraldehyde in mammalian phosphate buffer at 4°C. Tissues<sup>o</sup> dissected out under glutaraldehyde were transferred with a Pasteur pipette to small test tubes containing fresh cold fixative. Tubes were stoppered and kept at 4°C.

Tissues in Kahle's fluid were transferred to 45% acetic acid on microscope slides and squashed. Coverslips were sealed with a mixture of equal parts beeswax and paraffin. Such slides were examined by phase-contrast microscopy immediately after scanning of negatively stained hemolymph in a Zeiss EM 9A electron microscope. Occasionally, it was desirable to preserve certain squash preparations. In such cases, slides were first placed on dry ice for 5 min., or else dipped in liquid nitrogen for 1 min. Coverslips were then quickly removed with a razor blade, and the slides immediately placed in 2% orcein (in 45% acetic acid) for 10 min. Slides were dehydrated in alcohol and then mounted in Canada balsam.

These operations were continued until a consistent symptomatology, as detected by examination of diseased insects under a dissecting microscope, became apparent, and in all cases of uncertainty as to the cause of disease. Advantages were two fold: first, insects with suspected and presumed viral diseases could be immediately segregated from those having protozoan or bacterial infections, on the basis of phase-contrast microscopy of Kahle-fixed, squash preparations; secondly, the presence of particular types of virus particles

could actually be confirmed in many cases by the simplest of electron microscopic techniques.

At the same time, samples of tissues of all insects under examination were fixed in glutaraldehyde. Such material, when from insects with confirmed (virus in hemolymph) or suspected (lack of non-viral agents and/or presence of intracellular inclusions) viral disease, could then be further processed for fine structural studies.

## 1. Light and Phase-Contrast Microscopy

Almost all histological work involved an examination of thick sections prepared from material embedded for electron microscopy. In addition to this, fat body from several CpV-1-infected and uninfected fourth-instar larvae was fixed in Carnoy's fluid for 1 hour, embedded in paraffin, sectioned, hydrolyzed for 10 min. in 1 N HCl at 60°C, and stained with Feulgen's reagent.

## 2. Electron Microscopy

### (a) Negative Staining Techniques

Perforated copper grids were obtained from E. F. Fullam, Inc., Schenectady, New York. They were first coated with parlodion and then stabilized with carbon, using an Edwards evaporating unit (Model E12E4). Parlodion was used as a 0.4% solution in iso-amyl acetate; the chemical was obtained in strip form from Mallinckrodt Chemical Works, St. Louis.

Hemolymph samples were allowed to stand on grids for 30 sec., whereupon the drops were removed by touching to filter paper. Four drops of 3% ammonium molybdate at pH 6.8 (92) were added and removed in succession in order to stain the samples and also to wash out salts, sugar, etc., from grid surfaces. Alternatively, 2% uranyl acetate was used as a negative stain (61). Samples in this case were added to grids, left 30 sec. and partially blotted. Grids were then inverted while still wet over a drop of water and left for 5 min. After a second rinse, a drop of stain is added, and removed after 1 min.

In some cases, insect tissues other than hemolymph were examined by negative staining. Tissues were minced in a drop of distilled water; cell fragments and cytoplasm released by osmotic shock were then picked up on a grid inverted over the drop. Staining was as outlined above.

#### (b) Fixation, Embedding, and Sectioning Techniques

Tissues from both infected and uninfected larvae were prefixed for 20 to 30 min. in 3.5% glutaraldehyde in phosphate buffer (0.1 M; pH 7.2-7.4) at 4°C. Post-fixation was in 2% osmium tetroxide in veronal acetate buffer (0.1 M; pH 7.4) at the same temperature. Washing of tissues prior to post-fixation in osmium was found to be unnecessary unless after prolonged, e.g. overnight, storage of material in glutaraldehyde. In that case, tissues were rinsed for 4 hours

in as many changes of phosphate buffer. A few samples of CpV-1-infected fat body were fixed in osmic acid only.

Dehydration was accomplished using a graded series of ethanol concentrations: 2 changes, 10 min. each, in 50%, 70%, and 95% ethanol, followed by 3 10 min. changes of absolute ethanol. The alcohol was replaced by 3 changes, for 10 min. each, of propylene oxide (Eastman Organic Chemicals, Rochester, New York). The infiltration sequence was as follows:

- (a) 2 parts propylene oxide:1 part Epon 812 (no accelerator) - 1 hour,
- (b) same, but with 2% accelerator - 1 hour,
- (c) 1 part propylene oxide:2 parts Epon 812 (with accelerator) - 2 hours.

After infiltration, each piece of tissue to be embedded was placed on a drop of Epon in the bottom of a gelatine capsule. Capsules were then filled with Epon, which was allowed to polymerize for at least 12 hours in an oven at 60°C.

Insect tissue cultures<sup>1</sup> were processed in much the same way, except for the fact that cells were handled as a pellet, obtained by a 10 min. centrifugation at 800 rpm. It was, however, found that very poor fixation resulted from the use of glutaraldehyde in the usual mammalian phosphate

---

<sup>1</sup> Techniques for the cultivation of insect cell lines will be found in section VII.

buffer. Thus the ratio of K and Na ions in the buffer was adjusted so as to approximate that in Grace's insect culture medium. Glutaraldehyde in "insect" phosphate buffer was found to give acceptable fixation of tissue culture cells.

Glass knives, for sectioning, were made from 400 x 25 x 6 mm glass strips (LKB) with an LKB 7800 B Knifemaker. Troughs were fashioned with masking tape and sealed with wax. Thick sections (about 0.5  $\mu$ ) were cut from all blocks for purposes of orientation and identification of tissues. Sections were cut with a Reichert Om U2 ultramicrotome. Sections were transferred with a platinum wire loop to clean microscope slides, dried on a hot plate, and stained 30 secs. in warm toluidine blue. They were examined by phase-contrast microscopy.

Thin sections showing grey to silver interference colours (500 to 600 Å) were picked up on uncoated 300 mesh copper grids and stained with uranyl acetate and lead citrate for 15 min. and 30 secs. respectively.

### (c) Electron Microscopes

Either of three electron microscopes were used: Zeiss EM9A, RCA EMU-3H, and Philips 300. Calibration of the Zeiss and RCA microscopes was checked with either a grating replica (E. F. Fullam) ruled to 54,800 lines/inch, or a suspension of latex particles (188 m $\mu$ , Dow Chemical).

(d) Photography

Photographs of larvae were taken with a single-lens reflex camera equipped with electronic flash; Kodak Panatomic-X film was used, and developed in Microdol.

Light and phase-contrast photography was performed with an Olympus camera back mounted on a Zeiss Standard GFL microscope equipped with Neofluor objectives. Hi-Contrast Copy film was used, and also developed in Microdol.

Details of emulsions used in electron photomicrography, and their processing, are as follows:

Zeiss EM9A: Agfa-Gevaert Scientia film, 7 x 7 cm., developed 4 min. in undiluted D-19 at room temperature.

RCA EMU-3H: Kodak Contrast Projector plates (glass), 2 x 10", developed 5-7 min. in undiluted Dektol.

Philips 300: Kodak Contrast Projector plates (glass), 3 1/4 x 4" developed 4-5 min. in undiluted Dektol, or 6-8 min. in undiluted D-11.

Occasionally, reverse contrast prints were made of some micrographs. This was accomplished simply by printing from a positive slide made from the original negative. The final image is a negative.

### III. Autoradiography of CpV-1-Infected Larvae

Larval integuments were ripped open in cold insect tissue culture medium. The larvae, still alive, were then transferred to incubation medium in small vials and held at 18°C. Medium contained 10  $\mu\text{C}/\text{cc}$  of  $\text{H}^3\text{-CH}_3\text{-thymidine}^1$  and 5% Antheraea pernyi hemolymph. After one hour, infected and uninfected larvae were rinsed in isotope-free medium, and then fixed and embedded in Epon as described previously. Thick sections (about 0.75  $\mu$ ) were cut and transferred, unstained, with a platinum wire loop to clean glass slides and dried on a hot-plate at 60°C. Slides were left overnight at 40°C to ensure thorough drying and attachment of sections to the glass, and then stored in slide boxes with Drierite.

Further treatment of sections closely followed the recommendations of Hendrickson et al. (53). Slides were immersed in 0.1 N NaOH for 5 minutes at room temperature, and then washed in distilled water. They were then placed in 1% periodic acid ( $\text{HIO}_4$ ) for a similar interval, and washed, followed by air drying.

Slides were coated with Ilford K-5 emulsion<sup>2</sup>, by means of the dipping method (67). The emulsion was melted for 15 min at 55°C and then diluted with an equal volume of distilled water at the same temperature. Coated slides

---

<sup>1</sup> New England Nuclear Corporation, Boston. Specific Activity: 1.00 mC per 0.12 mg.

<sup>2</sup> Ilford Ltd., London, England.

dried in a light-tight box containing a variable speed electric air blower (modified hair dryer). Air at room temperature was gently directed at the non-emulsion side of the slides for one hour. Following this, slides were placed in light-tight slide boxes containing Drierite, and exposed at 4°C for 1-2 months.

Slides were developed in undiluted Kodak D-19 for 4 minutes, rinsed in distilled water, fixed in Kodak Rapid Fixer for 5 minutes, washed in running tap water for one hour, rinsed in distilled water, and air dried at room temperature. All chemicals were used at room temperature.

Sections were stained for 10 minutes in 0.075% Azure B<sup>1</sup> at room temperature, rinsed in tap water, air dried, and mounted under Canada balsam.

#### IV. Purification of CpV-1

Infected larvae were dissected in small amounts of borate-HCl buffer (0.01 M; pH 7.5) on depression slides. Infected tissues (fat body and muscle) were transferred to small test tubes on ice. Buffer was added to make up a volume of 5-10 cc. The tissues were then vigorously triturated for 3-4 min. with a 1 cc tuberculin syringe. Larval skins, if present, floated to the surface and were easily removed from the preparation.

---

<sup>1</sup> Allied Chemical Corporation, New York.

Preliminary purification of virus was accomplished by differential centrifugation at 4°C. Bacteria, cellular debris, and virus aggregates were spun out in a Sorvall RC2-B centrifuge at 7000 rpm (5900 g) for 15 min. Additional virus could be extracted from such sediments by repeated trituration, followed by differential centrifugation. Virus in supernatant fluids was pelleted by centrifugation at 15,000 rpm (27000g) for 20 min., resuspended in buffer, subjected again to differential centrifugation, washed once in distilled water, and finally resuspended in either distilled water or in tissue culture medium, containing 200 µg penicillin and 200 µg streptomycin per cc. Suspensions prepared in this way were judged to be essentially free of cellular contaminants both by phase<sup>1</sup> and electron microscopy.

Further purification was performed by layering virus suspensions on linear sucrose (5-40% in borate buffer) density gradients, and spinning in a Spinco SW 25-1 swinging bucket rotor at 15000 rpm (22,889 g) for 20 min. A Beckman model L2-65 ultracentrifuge was used. Virus suspensions were dialysed overnight against borate buffer or distilled water.

Virus preparations were sterilized by Millipore filtration (450 mµ pore size) using a Swinny filter holder attached to a 10 cc syringe equipped with a Luer-lock tip. Storage of virus was at 4°C.

---

<sup>1</sup> Virus particles are quite readily visualized at 1000 X magnification.

A virus similar to that found in diseased larvae from Lake Pepin, Wisconsin, was isolated from 2 larvae collected from Lake Ontario. A virus suspension was prepared in insect tissue culture medium by trituration of infected tissues. The material was stored at 4°C and not purified further. The isolate is referred to as CpV-1-Toronto.

#### V. Chemical Degradation of CpV-1 Particles

In an attempt to produce and characterize substructural components of the CpV-1 virion, purified virus suspension in distilled water were exposed to several chemical agents. All the chemicals listed below were diluted 1:1 with virus. Final concentrations are those given. Exposure to enzymes was at room temperature or at 37°C, for 20 min. Virus was at a final concentration of 0.5 mg/cc. For purposes of comparison, CpV-1-Toronto and "CIV"<sup>1</sup> were also used.

#### Enzymes:

1. Pronase (Calbiochem), 200 µg/cc in Dulbecco buffer, pH 7.4. This enzyme was predigested at 37°C for 120 minutes.

---

<sup>1</sup> Actually, several iridescent insect virus stocks, labelled at TIV, SIV, or CIV were made available from the Insect Pathology Research Institute, Sault Ste. Marie, Ontario. However, they were all serologically identical; CIV is regarded as being the dominant virus in these preparations (J. C. Cunningham, personal communications). Contamination of iridescent virus stocks with CIV has also been reported by Gibbs (cited in 16).

## Enzymes (continued):

2. Trypsin (Bacto-Difco), 1000 µg/cc, Dulbecco buffer, pH 7.4.
3. Pepsin (Worthington), 500 µg/cc, Dulbecco buffer, pH 7.4.

## Protein-denaturing agents:

4. Urea, 7.6 M, six minutes at room temperature.
5. 2-mercaptoethanol (Eastman Organic Chemicals, Rochester), 7 M, 5 minutes at room temperature.

## Nasal Decongestants (muco-solvents?):

6. "Otrivin" (CIBA, Dorval, Quebec), containing 0.1% xylometazoline.
7. "Nafrine" (Schering Corporation, Pointe Claire, Quebec) containing 0.05% oxymetazoline hydrochloride. Virus was exposed to decongestant for 1-4 days at room temperature.

## Agents thought to alter the structure of water:

8. Dimethylsulfoxide, 50 and 80%, 10 minutes at 4°C.
9. Formamide, 30%, 30 minutes at room temperature.

## Lipid solvents:

10. Chloroform, 5%, 10 minutes at 4°C.

## VI. Colorimetric Tests for Nucleic Acids in Purified CpV-1 Particles

Equivalent volumes of virus suspension in distilled water and 1 N perchloric acid (PCA) were mixed, heated at 90°C for 15 min., and then cooled. The precipitated protein was spun down at 10,000 rpm for 10 min. The supernatant fluid was used for nucleic acid determinations. Two-fold dilutions (two tubes of each) of supernate were made up in 0.5 N PCA, to a final volume of 0.5 cc.

For the detection of DNA, the method of Sekiguchi and Takagi (103) was used. Samples prepared as above, were diluted 1:2 with diphenylamine reagent, heated at 100°C for 10 min., cooled, and read at 590 m $\mu$ . PCA (0.5 N solution) served as a control. Standards were prepared from calf thymus DNA (Calbiochem) in concentrations ranging from 20-200  $\mu$ gm/cc in 0.5 N PCA.

For the detection of RNA, the orcinol method (85) was used. To each sample, 0.15 cc of orcinol reagent (100 mg orcinol in 1 cc of 95% ethanol) and 1.5 cc of 0.1% FeCl<sub>3</sub> (in conc. HCl) were added. Tubes were heated at 100°C for 30 min., cooled, and read at 670 m $\mu$ . Controls were as above. Standards were made using yeast RNA (Worthington) at concentrations ranging from 10-100  $\mu$ gm/cc in 0.5 N PCA. All readings were taken with a Beckman model DU spectrophotometer.

## VII. Transmission of CpV-1

### 1. Feeding

Several attempts were made to achieve transmission of virus by making it available for ingestion by larvae under normal laboratory rearing conditions. Essentially, this consisted simply of adding infected fourth-instar larvae, either intact or macerated, to aquaria containing presumably uninfected eggs, first-instar larvae, or fourth-instar larvae.

### 2. Injection

In preparing microneedles for injection of larvae, the following equipment was used:

- (a) a microburner made from thick-walled glass tubing with an aperture about 3 mm in diameter,
- (b) heparinized capillary tubing (I.D. = 1.1 - 1.2 mm).

Microneedles were drawn out over the burner to a final diameter of approximately 0.05 mm; they were stoppered with cotton and then autoclaved. For injections, the broad end of a microneedle was inserted tightly through a piece of rubber, which in turn was connected to a flexible length of tubing. Virus was taken up into the microneedle by capillary action; delivery was accomplished simply by blowing through the assembly.

Larvae to be injected were surface sterilized for 30 seconds in 70% alcohol; this also anaesthetized them. They were then placed on a dissecting microscope stage, which

had been previously washed with alcohol. Using forceps, larvae were drawn onto microneedles and injected with either virus suspension<sup>1</sup> or insect tissue culture medium. Injections were not quantitative, but it is estimated that 1-5 µl quantities were delivered into the hemocoel. After injection, larvae were placed in tap water for 1 hour to allow the wound to heal, and then transferred to substrate in other containers.

All larvae injected within CpV-1 were taken from Lake Winnebago.

### 3. Insect Tissue Culture

Attempts were made to grow CpV-1 in insect cells cultured in vitro. Two different cell lines were used. Grace's (46) Antheraea eucalypti<sup>2</sup> cells were obtained from Dr. P. Faulkner of the Department of Microbiology, Queen's University, Kingston, Ontario. These cells had already been adapted by Yunker et al. (147) to medium free of hemolymph, and were subcultured here in the same medium (available from Gibco). A cloned subline of Grace's Aedes aegypti<sup>3</sup> cells was made available by Dr. E. C. Sutor of the Naval Medical Research Institute, Bethesda, Maryland.

---

<sup>1</sup> Virus was suspended in modified Grace's insect tissue culture medium containing antibiotics. Particle counts were not determined.

<sup>2</sup> Lepidoptera: Saturniidae (moths)

<sup>3</sup> Diptera: Culicidae (mosquito)

These cells were shipped in Grace's medium (Gibco) supplemented with 1% Philosamia cynthia<sup>1</sup> hemolymph, and were subcultured here in medium supplemented with Antheraea pernyi<sup>1</sup> hemolymph, a gift of the Insect Pathology Research Institute, Sault Ste. Marie, Ontario.

The mosquito cells were adapted to hemolymph-free medium (Grace's modified medium) by gradual replacement of hemolymph by fetal calf serum over a period of a month. Sera were always inactivated at 56°C for 15 min before adding to media. All experimental work was done with the resulting "adapted" line.

Cells were seeded, upon receipt, at a concentration of  $10^5$ /cc in 3 or 6 oz. Sani-Glas bottles (Brown's Bottles and Supplies, Montreal, Quebec) and held at 27°C. At the end of one week, cells were diluted 1:1 with fresh medium, and allowed to grow for a second week after which they were spun down, resuspended and diluted in fresh medium and seeded again in bottles. Although these cell lines were originally established in media at pH 6.5 (approx.) they seemed to grow well at pH 7.0 - 7.2 which is the pH of media available from Gibco.

Attempts to infect cells with CpV-1 were made using Leighton tubes (Bellco Glass Inc., Vineland, New Jersey). Ten minutes after subculturing into tubes, most cells were attached to the glass substrate. The medium was

---

<sup>1</sup> Lepidoptera: Saturniidae (moths)

then poured off and 0.5 cc of purified virus suspension was added. After one hour, 1.5 cc of fresh medium was added to that already present. Tubes were kept at either room temperature (ca. 22°C) or at 27°C in an incubator. Samples were drawn off periodically during a period of 3-4 weeks for examination of live cells by phase-contrast microscopy. At the end of 4 weeks, samples were fixed for electron microscopy, and examined for signs of virus multiplication.

In other experiments, diseased fat body and muscle was dissected out under sterile conditions and added to cell cultures. These were examined as above.

#### VIII. Reagents

Kahle's Fixative:	formaldehyde	2 parts (by volume)
	95% ethanol	5 parts
	glacial acetic acid	1 part

These chemicals are made fresh and in order of listing.

Carnoy's Fixative:	95% ethanol	3 parts
	glacial acetic acid	1 part

Feulgen's Reagent:	basic fuchsin	0.5 gm
	distilled water	100 cc

Boil 15 min., cool to 50°C and add:

1 N HCl	10 cc
$K_2S_2O_5$	1 gm

Store 24 hours in dark, and filter.

## Glutaraldehyde:

Stock phosphate solutions (0.1 M in 500 cc distilled water).

A = 7.10 gm  $\text{Na}_2\text{HPO}_4$

B = 6.80 gm  $\text{KH}_2\text{PO}_4$

C = 8.70 gm  $\text{K}_2\text{HPO}_4$

D = 6.40 gm  $\text{NaH}_2\text{PO}_4$

Mammalian phosphate buffer - 7 parts A:3 parts B  
(by volume)

Na:K = 2.75:1

Insect phosphate buffer - 19 parts C:16 parts B:15 parts D.

K:Na = 7:1

Fixatives are made fresh before use by adding 14 cc of 25% glutaraldehyde (Eastman Organic Chemicals, Rochester, New York) to 86 cc of either of the above two buffers, giving a final concentration of 3.5% glutaraldehyde, with a pH 7.2 to 7.4.

## Osmium tetroxide:.

Veronal buffer - sodium veronal (barbital)	1.5 gm
sodium acetate, $3\text{H}_2\text{O}$	1.0 gm
distilled water	50 cc
Fixative - distilled water	30 cc
buffer	10 cc
0.1 N HCl	10 cc
$\text{OsO}_4$	1 gm



Lead citrate:	double distilled water	10 cc
	10 N NaOH	0.1 cc
	lead citrate (K & K Labs)	0.035 gm

Uranyl acetate:	uranyl acetate (B.D.H.)	1.5 gm
	absolute methanol	25 cc

Borate-HCl buffer (0.01 m):

sodium borate	3.81 gm
sodium azide	0.52 gm
sodium chloride	5.85 gm
distilled water	1000 cc

Adjusted to pH 7.5 with 1 N HCl

Dulbecco Buffer:	sodium trichloroacetate	27.8 gm
	Tris	6.05 gm
	E.D.T.A.	0.93 gm
	NaCl	2.92 gm
	sodium citrate	0.68
	distilled water	500 cc

pH 7.4

Diphenylamine reagent:	diphenylamine	1.0 gm
	glacial acetic acid	100 cc
	conc. H <sub>2</sub> SO <sub>4</sub>	2.75 cc

This is stored in darkness. Before use, 0.25 cc of 0.07 M acetaldehyde is added to 40 cc of the reagent.

## RESULTS

A total of three virus-induced diseases<sup>1</sup> were found in fourth-instar larvae of Chironomus plumosus. These diseases, and their presumed causative agents, are described below in order of discovery.

### I. Chironomus plumosus Virus #1 (CpV-1):

#### (a) Symptomatology

This virus infected fat body and/or muscle of fourth-instar larvae; these tissues then became hypertrophied. With respect to muscle, generally only the large abdominal muscles were affected. However, light infections of the midgut muscularis were recently found in two specimens. Infected areas of individual muscularis fibers were hypertrophied and projected out into the hemocoel. This symptom distinguished this disease from a second disease of the midgut (cytopolyhedrosis) in which no hypertrophy of infected tissue occurred.

In Lake Pepin, Wisconsin, only the fourth-instar larvae exhibited symptoms of disease. A similar disease was found

---

<sup>1</sup> "Virus" for the purposes of this thesis, refers to any group of homogeneous particles, clearly related in morphology to previously characterized viruses, and associated with definitive tissue pathologies.

in two (out of 50) larvae collected from Lake Ontario; one of these was a third-instar larva. In Wisconsin, only larvae from Lake Pepin had this particular viral disease. Two other viral diseases were found only in larvae from Lake Winnebago.

Uninfected tissues always appeared more or less translucent under a dissecting microscope (Fig. 1); when infected, however, they appeared white and opaque (Figs. 2 and 3). At higher magnifications, infected fat body appeared mottled (Fig. 4) while infected muscle was more or less uniformly white (Fig. 5). The normal outlines of infected tissues were clearly delineated in infected insects such that diseased individuals were readily distinguished without the aid of any microscope. Massively infected insects were quite capable of normal movements and activity.

(b) Transmission:

Feeding experiments<sup>1</sup>: Efforts to produce infection in the larvae by making virus available as food were mostly negative. The following combinations were tried:

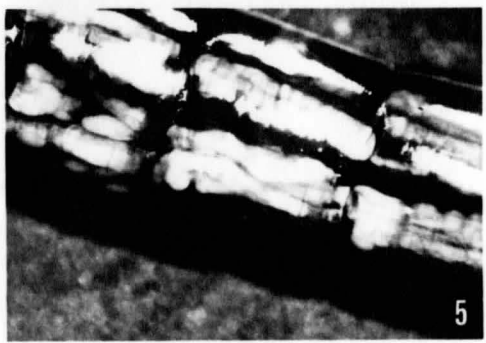
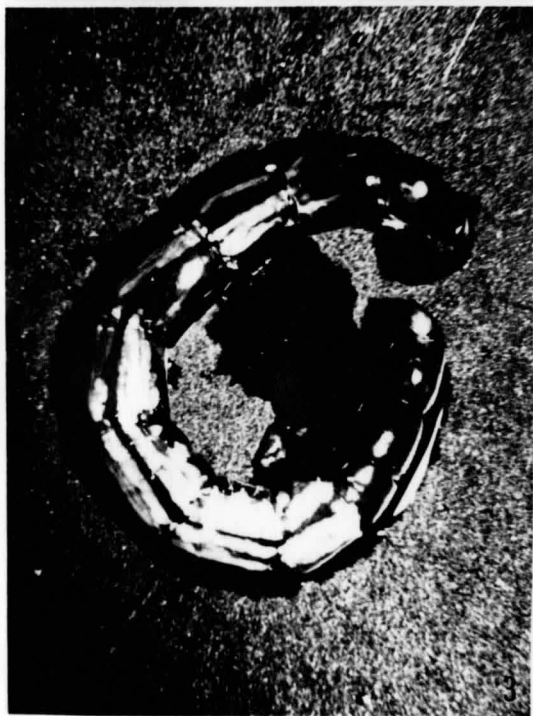
1. 10 live infected larvae added to an aquarium containing 1/2 egg mass.
2. 10 live infected larvae added to an aquarium containing 500 first-instar larvae.

---

<sup>1</sup> While certain of these experiments were suggested by the author, they were all carried out by Dr. Hilsenhoff in Wisconsin.

Figures 1-5. Fourth-instar C. plumosus larvae

- Fig. 1. Uninfected larva; 8 X.
- Fig. 2. Larva with CpV-1 infection of the fat body; 8 X.
- Fig. 3. Larva with CpV-1 infection of the muscle; 8 X.
- Fig. 4. Appearance of diseased fat body; 20 X.
- Fig. 5. Appearance of diseased muscle; 15 X.



3. 20 macerated infected larvae added to an aquarium containing 500 first-instar larvae.

4. Control: 1/2 egg mass.

Of these, only tests 3 and 4 gave positive results: in test 3, 7 of 226 larvae became diseased (during the fourth instar) and in test 4, 5 of 168 larvae were infected. The percentages of infection were more or less identical (3.1 and 3.0% respectively). Attempts at infecting fourth - instar larvae by similar methods gave negative results.

Injections: The purposes of injections were two-fold:

1. to prove that the filterable agent seen in the electron microscope had biological activity (i.e. was a virus), and
2. to ensure a supply of this agent for further studies.

Unfortunately, larvae lost too much blood, especially after withdrawal of the needle, and in most cases died, either from this cause, or from bacterial septicemia occurring in the first week after injection.

Injections of virus were administered to 40 fourth-instar larvae; a similar number of larvae were given injections of Grace's insect tissue culture medium. After 2 1/2 weeks only six of the virus-injected larvae were alive; of these, two were heavily infected. Of the control larvae, nine survived, but none were infected.

Tissue cultures: No signs of infection were seen in the Antheraea or Aedes cell lines inoculated with

CpV-1 whether by phase-contrast microscopy of living cells, or by electron microscopy at the end of four weeks. Neither purified virus<sup>1</sup> nor pieces of fat body had any effect on these cells. In an attempt to see whether or not the virus might adapt to these cell lines, some infected cultures were maintained and serially subcultured for a period of three months, again with negative results.

(c) Light and Phase-Contrast Microscopy

Samples of infected and uninfected fat body were embedded in paraffin and stained by the Feulgen reaction for DNA. In uninfected fat body (Fig. 6), only the nuclei were stained. Large Feulgen-positive inclusion bodies were present in the cytoplasm of infected cells (Fig. 7). Nuclei of such cells appeared to be somewhat heterogeneous in size, and frequently pycnotic.

Permanent squash preparations were made of uninfected and infected fat body which had been fixed in Kahle's fluid and stained with orcein. Uninfected cells (Fig. 8) lacked cytoplasmic inclusion bodies. The cytology of infected cells, however, could be determined in more detail than was possible with paraffin-embedded material. In fact, two different types of cytoplasmic inclusions would be detected. The smaller, shown in Fig. 9, stained darkly and homogeneously. The larger appeared finely granular (Fig. 10).

---

<sup>1</sup> The virus preparation used to inoculate tissue cultures was the same as that injected into larvae.

Figures 6 and 7. Feulgen-stained fat body.

Fig. 6. Uninfected fat body; 2000 X.

Inset shows a typical nucleus; 8000 X.

Fig. 7. Infected fat body; I, Feulgen-positive cytoplasmic inclusion body; 1700 X.

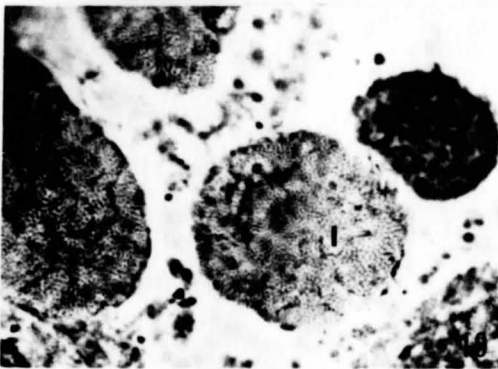
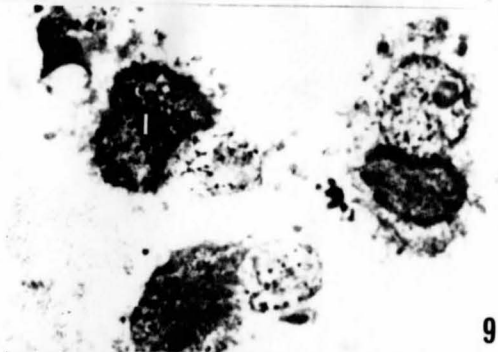
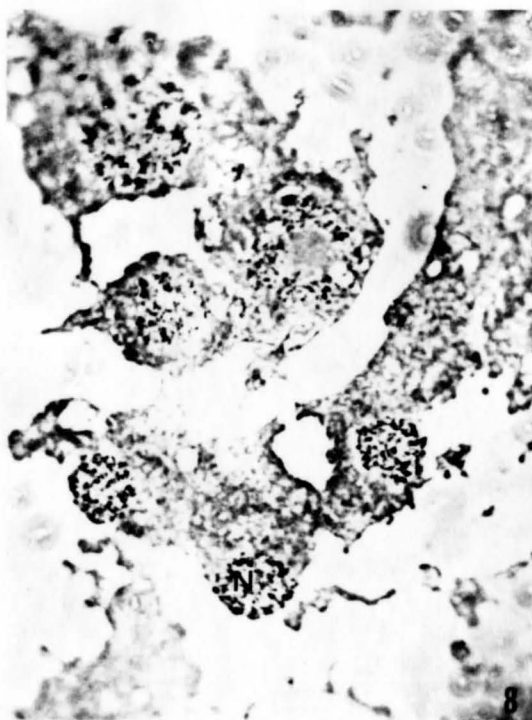
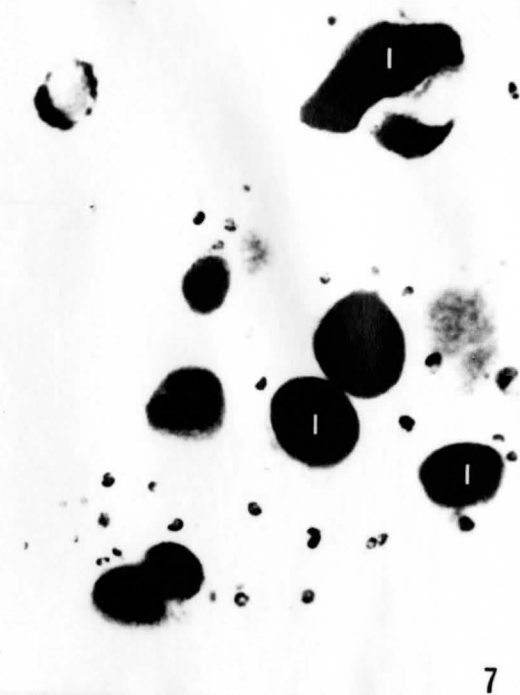
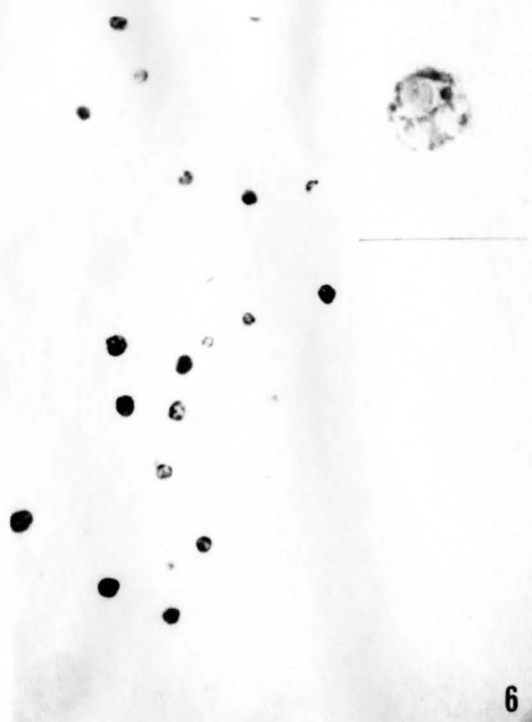
Inset shows pycnosis and margination of chromatin in a nucleus; 7000 X.

Figure 8 to 10. Orcein-stained fat body.

Fig. 8. Uninfected fat body; N, nucleus; 8000 X.

Fig. 9. Infected fat body; I, cytoplasmic inclusion body; 8000 X.

Fig. 10. I, finely granular cytoplasmic inclusion bodies; 8000 X.



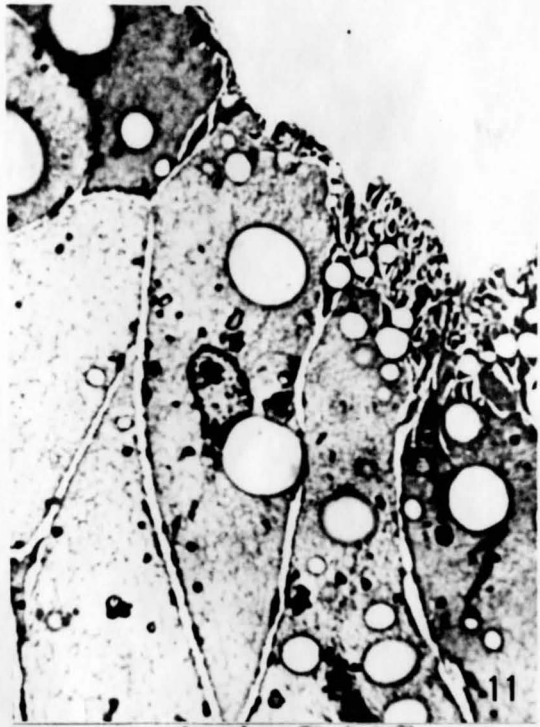
Cytological detail was, of course, best preserved in material that had been fixed and embedded for electron microscopy. Thick sections of both fat body and muscle were stained with toluidine blue and examined with a phase-contrast microscope. Generally, the cytoplasm of uninfected fat body cells stained extremely lightly, except in the immediate area of the nucleus (Figs. 11 and 12). Unidentified granules were always present, as were large droplets of what is presumably lipid. The latter were often extracted during processing for electron microscopy. Peripheral areas of fat body cytoplasm often contained what appeared to be many invaginations of the plasma membrane. Nucleoli were small. The only unusual features of these cells was the fact that many had more than one nucleus (Fig. 12).

Striking changes were seen in both the cytoplasm and nuclei of infected fat body cells. Cytoplasmic inclusion bodies (Figs. 13 to 23) were of several types, comprising a spectrum of morphological entities, the two extremes of which are shown side by side in Fig. 16. These correspond to the types of inclusion body (IB) revealed in squash preparations (Figs. 9 and 10). The smallest IB's (Figs. 13 to 16) were circular in outline and contained several dark granules of varying size. Larger IB's (Figs. 17 to 19) contained lighter areas in addition to the relatively dark and homogeneous matrix seen in the smallest IB's. The former predominated in the largest IB's, examples of which are shown in order of

Figures 11 and 12. Uninfected fat body; toluidine blue. Nuclei are surrounded by a darkly-staining rim. Two nuclei can be seen in a cell in Fig. 12 (arrows).

Fig. 11. 7000 X.

Fig. 12. 6000 X.



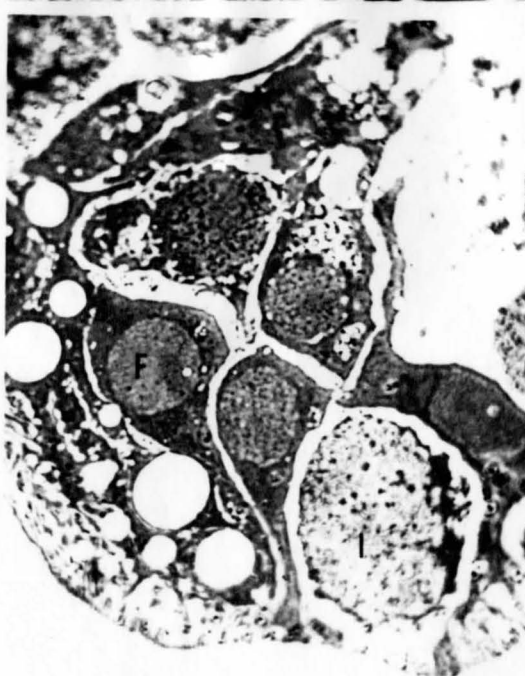
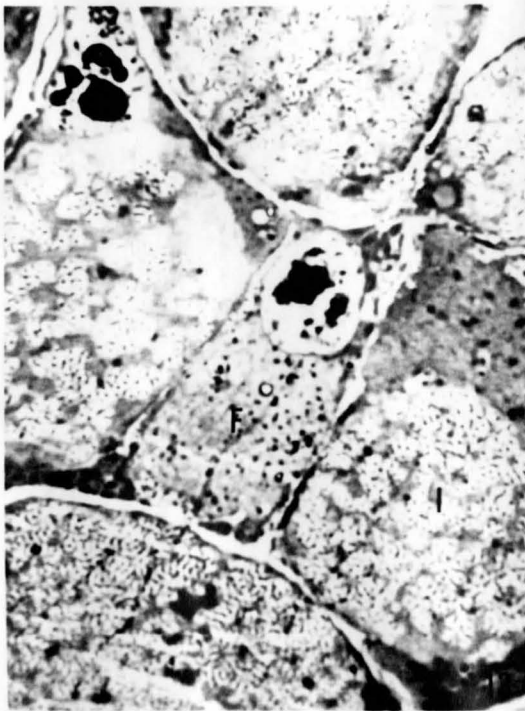
Figures 13 to 16.

Early foci of CpV-1 infection in fat body.

Early foci (F) are more or less circular in outline, and well-delineated within the cytoplasm. Such foci occur together with what are regarded as mature inclusion bodies (I). L, lipid.

Figs. 13, 14 and 16. 9000 X.

Fig. 15. 7000 X.



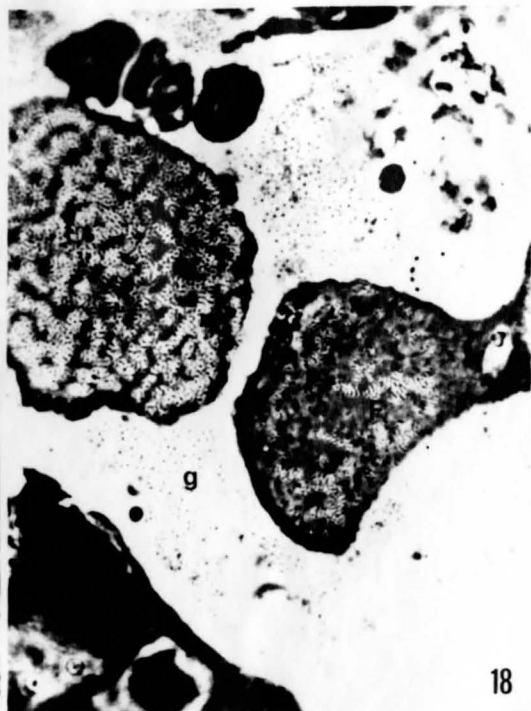
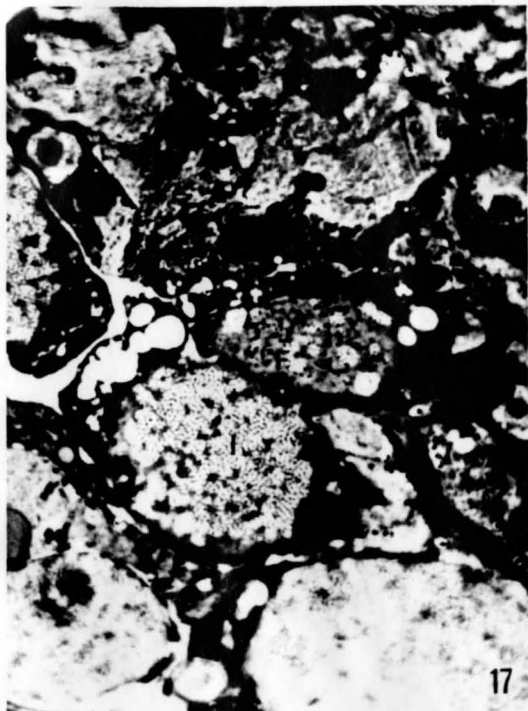
Figures 17 to 19.

Later stages of infection in fat body.

Small islands of material identical to that in mature inclusion bodies (I) appear in the foci (F). Note tiny extracellular granules (g) in Fig. 18; each granule is surrounded by a light circular halo.

Figs. 18 and 18. 8000 X.

Fig. 19. 9000 X.



17

18

19

Figures 20 to 23.

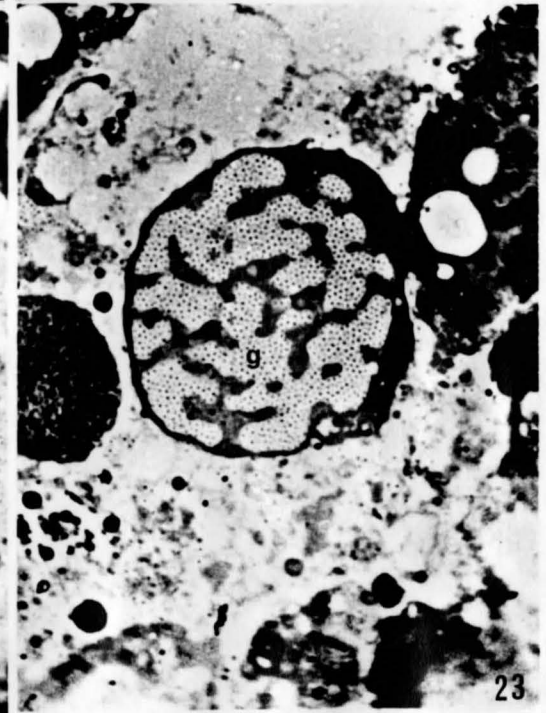
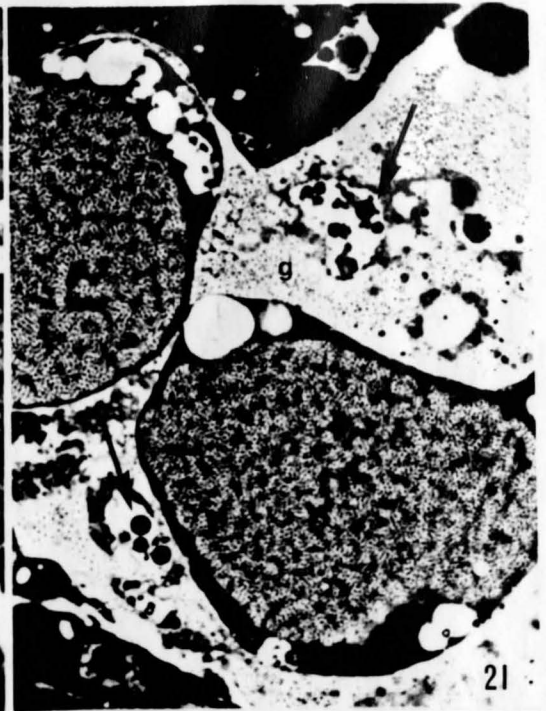
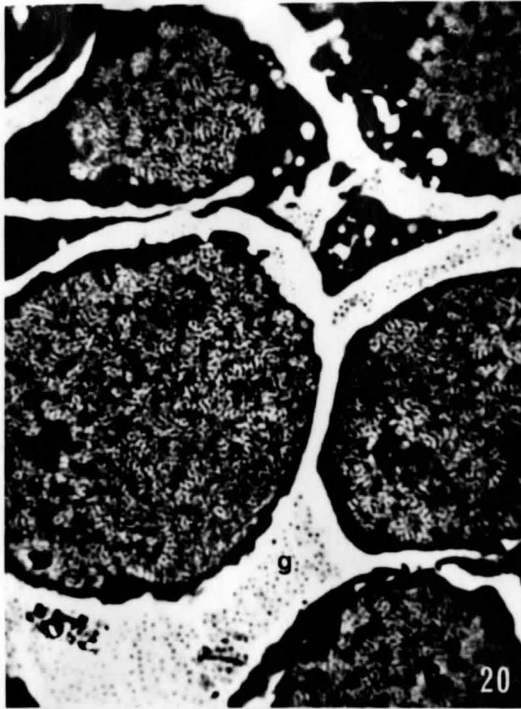
Mature inclusion bodies, as shown in sections of decreasing thickness. Extracellular granules (g) are present.

Fig. 20. 7500 X.

Fig. 21. Nuclei from lysed cells contain lipid droplets (arrows); some granules appear to have halos. 7000 X.

Fig. 22. Hemocytes (H) are present. 7000 X.

Fig. 23. Intracellular granules (g) with halos. 7500 X.



decreasing thickness (approx. 0.8 to 0.5  $\mu$ ) in Figs. 20 to 23. Such light areas contained many granules of uniform size, identical to similar granules often seen in extracellular spaces (several figures). Granules, particularly those in extracellular spaces, were often surrounded by a light "halo". This is especially evident in Fig. 21, but can be seen elsewhere, for example around the intracellular granules shown in Fig. 23.

Inclusion bodies were further characterized by means of radioautography, using  $H^3$ -methyl-thymidine as a marker for DNA synthesis. Infected cells were found to incorporate label only in the cytoplasm (Figs. 24 to 27). Cytoplasmic labelling was confined to discrete foci, identifiable as the IB's described above. However, not all inclusion bodies incorporated thymidine to the same extent. Generally, the smallest ones incorporated most label, and the largest, very little. Those of intermediate size and morphology rarely incorporated much label; those that did appeared to be labelled primarily over the more darkly staining component of the inclusion body (Fig. 26). Uninfected fat body showed no incorporation of label over either the cytoplasm or nucleus.

Nuclear changes were also evident in virus-infected fat body cells. Invariably associated with the disease was a marked nucleolar hypertrophy, particularly apparent in those cells that were either as yet uninfected or at least not heavily infected (Figs. 28 to 31). Compare, for example,

Figures 24 to 27.

Radioautographs of infected fat body showing localization of  $H^3$ - $CH_3$ -thymidine incorporation over cytoplasmic inclusion bodies.

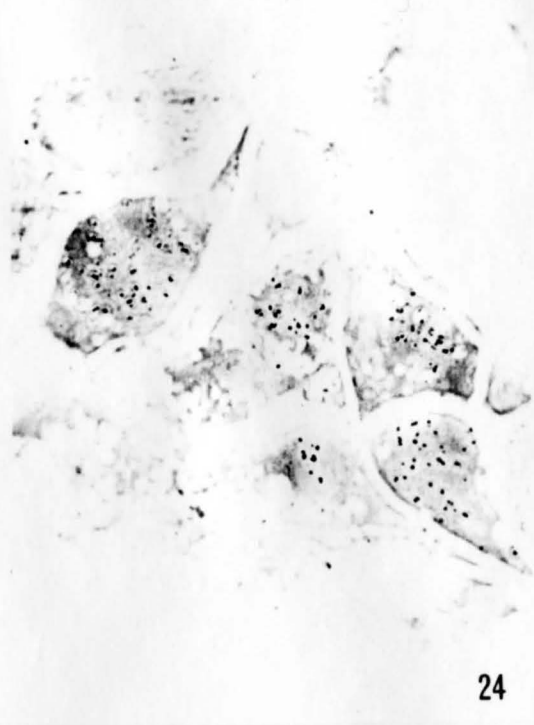
Fig. 24. Early foci of infection. 7000 X.

Fig. 25. Early foci (labelled), and mature inclusion bodies (I, unlabelled).

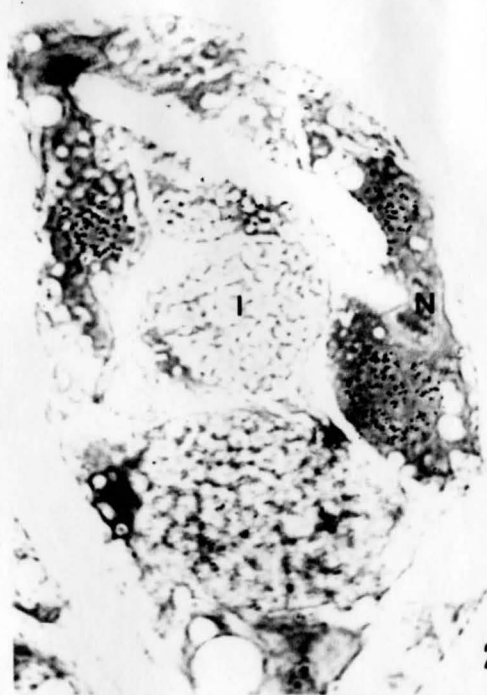
There is no incorporation over a nucleus, N. 7000 X.

Fig. 26. Inclusion body of intermediate morphology. Label is primarily over the dark component of the inclusion body. A nucleus (N) is unlabelled. 7000 X.

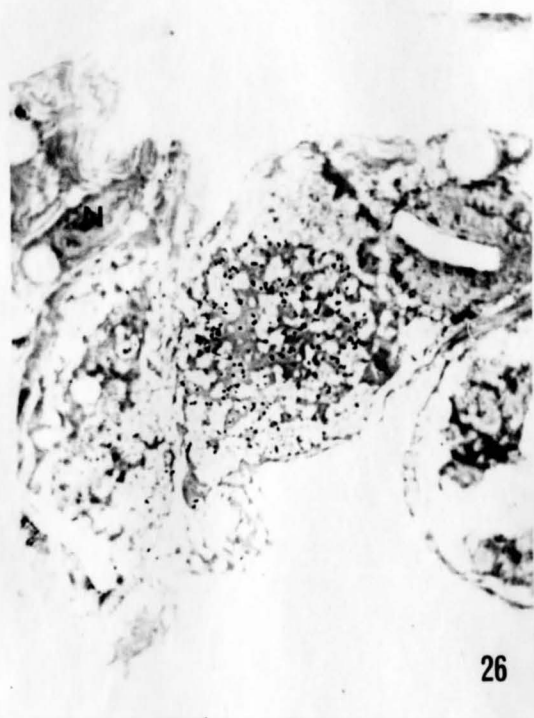
Fig. 27. Included to show that granules (g) can be visualized through the emulsion, and distinguished from label. 7000 X.



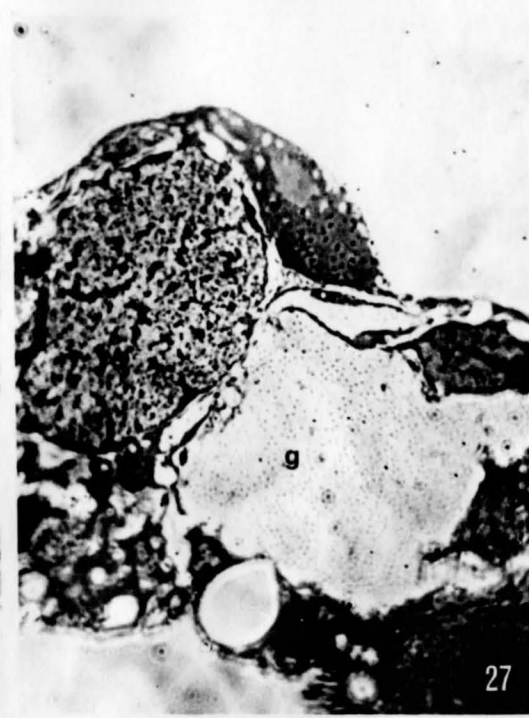
24



25



26



27

## Figures 28 to 31.

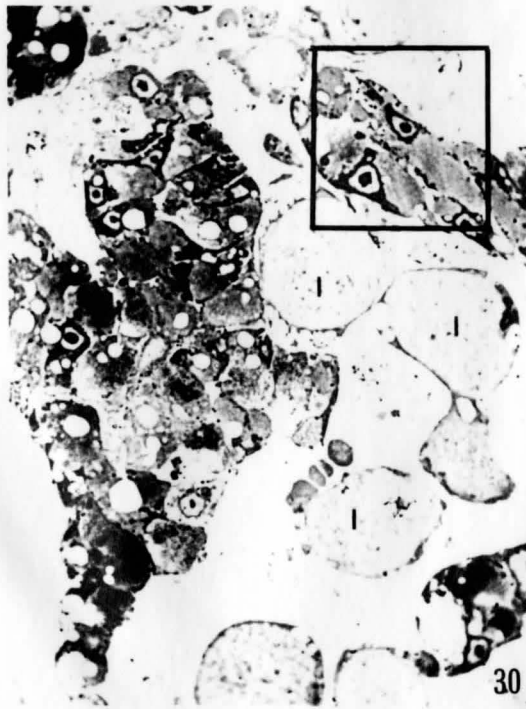
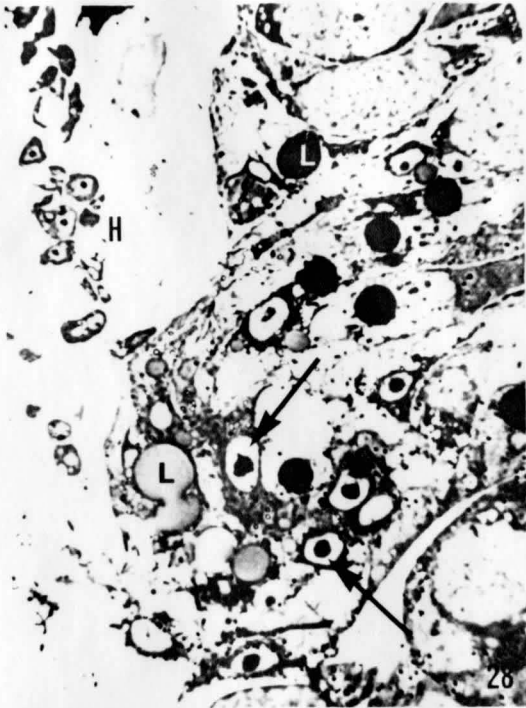
Infected fat body: nucleolar hypertrophy in uninfected cells.

Fig. 28. Hemocytes (H) are present at the edge of the fat body. Arrows indicate nucleoli. L, lipid. 6000 X.

Fig. 29. Uninfected cells in proximity to mature inclusion bodies (I) and extracellular granules (g). 7000 X.

Fig. 30. Low magnification micrograph showing an area of uninfected fat body, and several large inclusion bodies (I). The bracketed area is shown at higher magnification in Fig. 31. 3000 X.

Fig. 31. Uninfected cells showing nucleolar hypertrophy. Arrow indicates lipid in nucleus from lysed cell. n, nucleoli. 7000 X.



Figs. 11 and 31 which are reproduced at equivalent magnifications. Nuclear changes in heavily infected cells were more difficult to interpret at the level of the light microscope. Feulgen-stained nuclei showed condensation of chromatin (Fig. 7). However, chromatin typically stains very lightly in thick sections of material prepared for electron microscopy, so that morphological changes are difficult to determine. Bizarre conformations of the nucleolus, however, were readily detected and appeared commonly in infected cells (Figs. 14 and 19). Also characteristic of heavily infected cells was the presence of highly refractile material, presumably lipid, in the nucleus (Fig. 13). This was especially evident in the extracellular nuclei released by cell lysis (Fig. 21). No lipid-like material was ever detected in nuclei of uninfected cells.

Infected and uninfected abdominal muscles were also embedded in Epon and examined by phase-contrast microscopy. Figures 32 and 33 show, respectively, uninfected and infected muscle at low magnification. Infected tissue could be clearly distinguished by the presence of darkly staining material both in the peripheral sarcoplasm and also running between the myofibrils. The morphology of cytoplasmic inclusion bodies was less clear than in infected fat body; inclusion bodies were much more irregular in outline. However, inclusions roughly corresponding to the types previously described in fat body were found (Figs. 34 to 37). Nuclear changes were

Figure 32. Uninfected muscle. 3000 X.

Figures 33 to 35. CpV-1-infected muscle. Note darkly staining material near peripheral nuclei and between myofibrils.

Fig. 33. 3000 X.

Fig. 34. Probable early focus (F) of infection. 7000 X.

Fig. 35. Virogenic stromata (S), early (bottom) and mature (top). Encircled material from an early stroma is probably homologous with islands of material seen in early foci of infection in fat body (compare with Fig. 17). 7000 X.



32



33



34

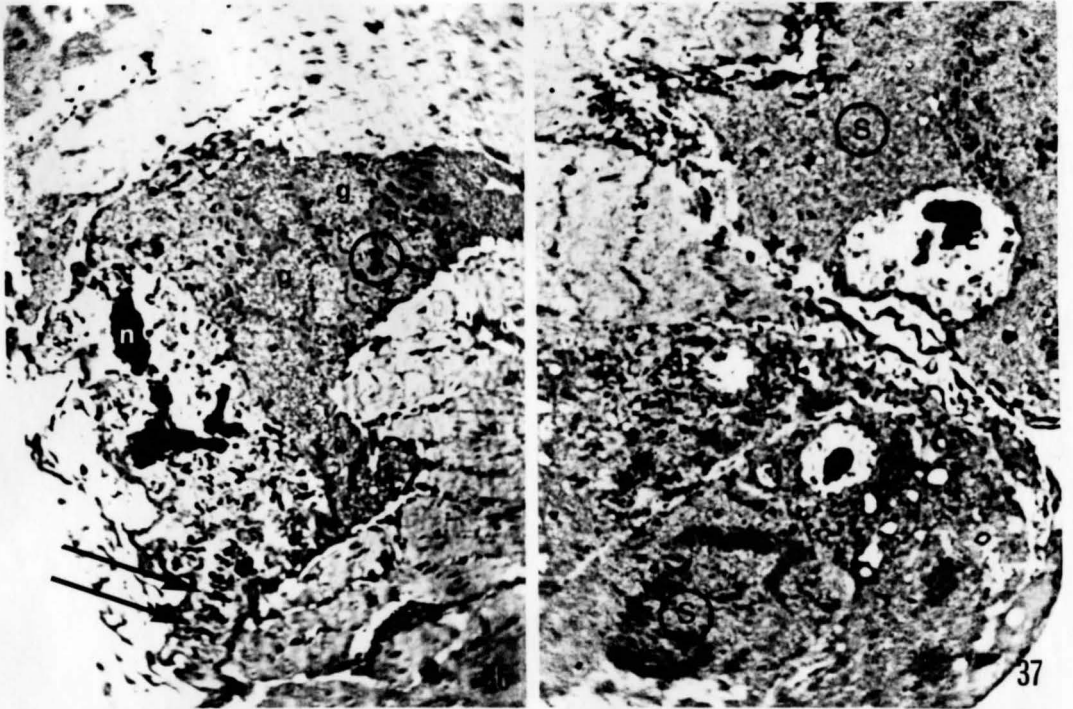


35

Figures 36 and 37. Mature virogenic stromata (S).

Fig. 36. Areas of granular material (g) are visible within the stroma. Note banded polytene chromosomes in markedly hypertrophied nucleus. Arrows indicate chromosome bands. n, nucleolus. 7000 X.

Fig. 37. Mature virogenic stromata (S) near nuclei. Upper stroma consists of granular material only. Blocs of granular material can be visualized in the lower stroma. 7000 X.



less evident; limited observations, however, suggested that hypertrophy of both nuclei and nucleoli was characteristic of infected muscle fibers. A greatly hypertrophied nucleus, containing large polytene chromosomes, is shown in Fig. 36. No lipid-like material was ever detected in muscle nuclei.

(d) Electron Microscopy

For purposes of comparison with CpV-1-infected tissues, uninfected fat body and muscle were examined in the electron microscope. These tissues differed little from those described in previously published works (96,133).

Examples of uninfected fat body are shown in Figures 38 and 39. In all samples examined, this tissue had the appearance of a storage organ, with little synthetic apparatus. There were abundant deposits of glycogen and lipid; dense, unidentified granules were present. Endoplasmic reticulum, ribosomes, and mitochondria were sparse and generally showed only a perinuclear distribution. In this area also were found a few bodies resembling bacteria (Fig. 38). Nucleoli were somewhat small, and of rather indistinct morphology.

Muscle fiber structure (Figs. 40 to 42) was similar to that described for other arthropod species (133). A, Z, and I, but not H or M, bands were readily identified. However, sarcomeres were poorly organized and lateral fusion of Z-band elements was incomplete. The ratio of thin to thick myofilaments was approximately 6:1. Large reserves of glycogen were found in the peripheral sarcoplasm and between myofibrils.

Figures 38 and 39. Electron micrographs of uninfected fat body.

Fig. 38. Note perinuclear distribution of RER. Arrow indicates a rickettsia-like body. L, area of extracted lipid. 14,000 X.

Fig. 39. Unidentified granules (G) in cytoplasm. n, nucleolus. 15,000 X.

Figures 40 and 41. Uninfected muscle.

Fig. 40. A, I, and Z bands are indicated. The peripheral sarcoplasm is filled with glycogen granules (gly). 15,000 X.

Fig. 41. m, mitochondrion. 17,000 X.

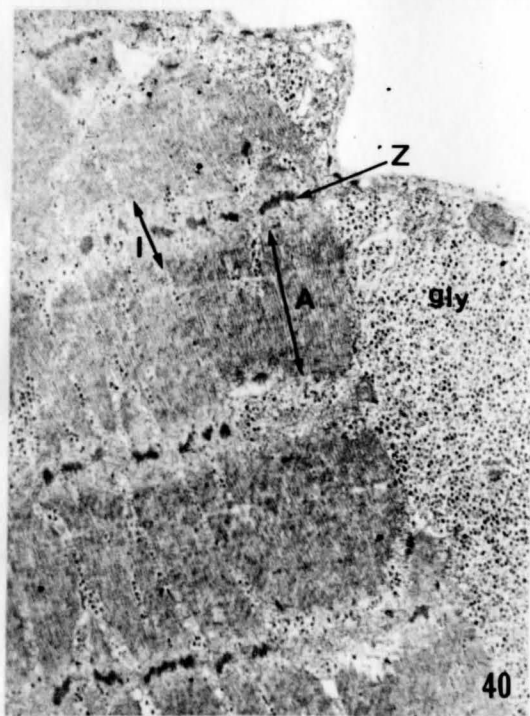
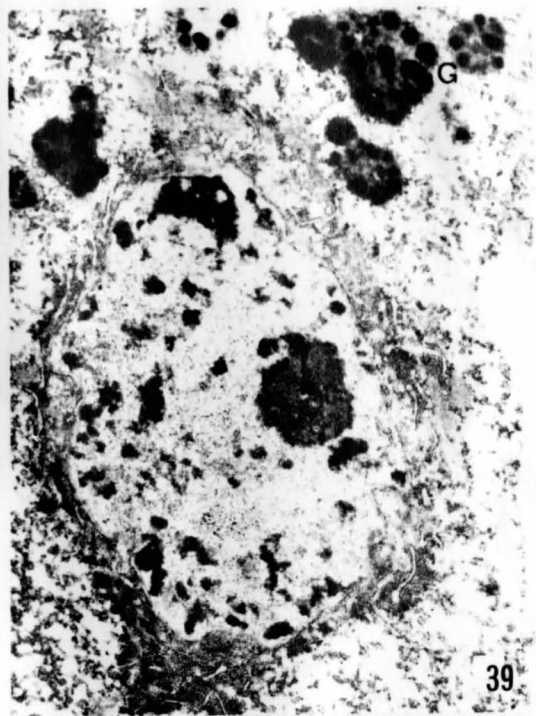
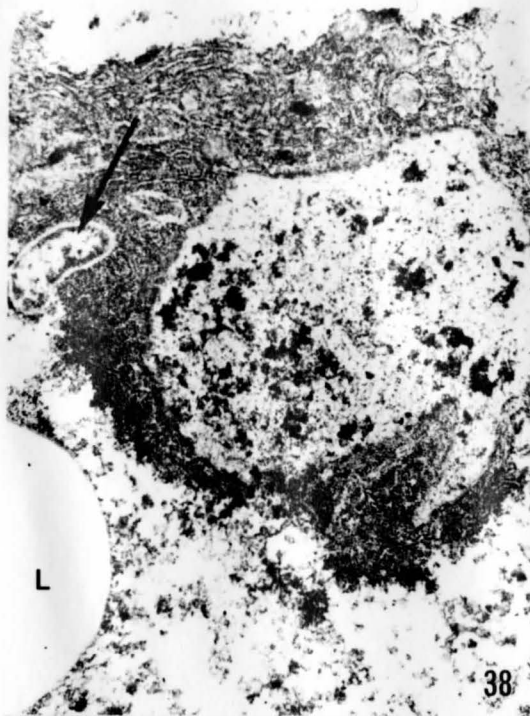
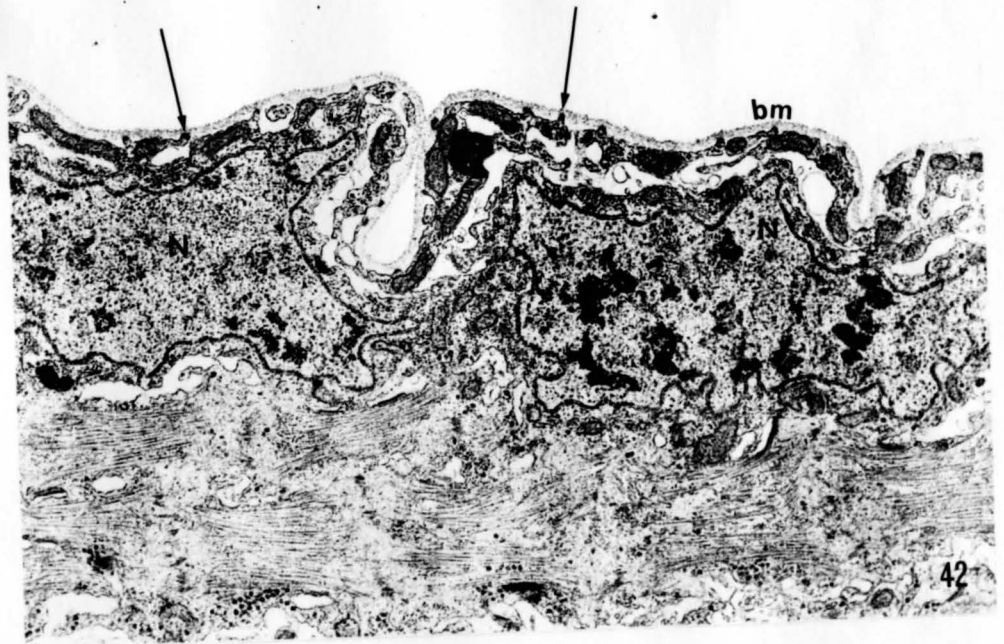
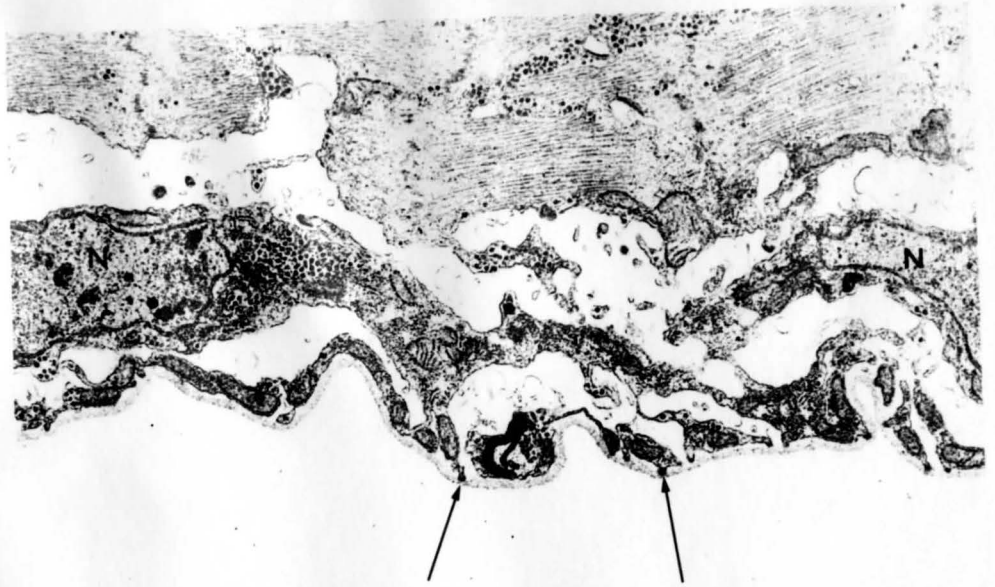


Figure 42. Uninfected muscle. Nuclei (N) are present in the peripheral sarcoplasm. Hemidesmosomes are indicated by arrows. Bm, basement membrane. 16,000 X.



Nuclei, having irregular outlines, were seen only in the peripheral sarcoplasm. Each muscle fiber was invested with a thick basement membrane. At points of contact with the basement membrane, the sarcolemma was differentiated into typical hemidesmosomes (Fig. 42).

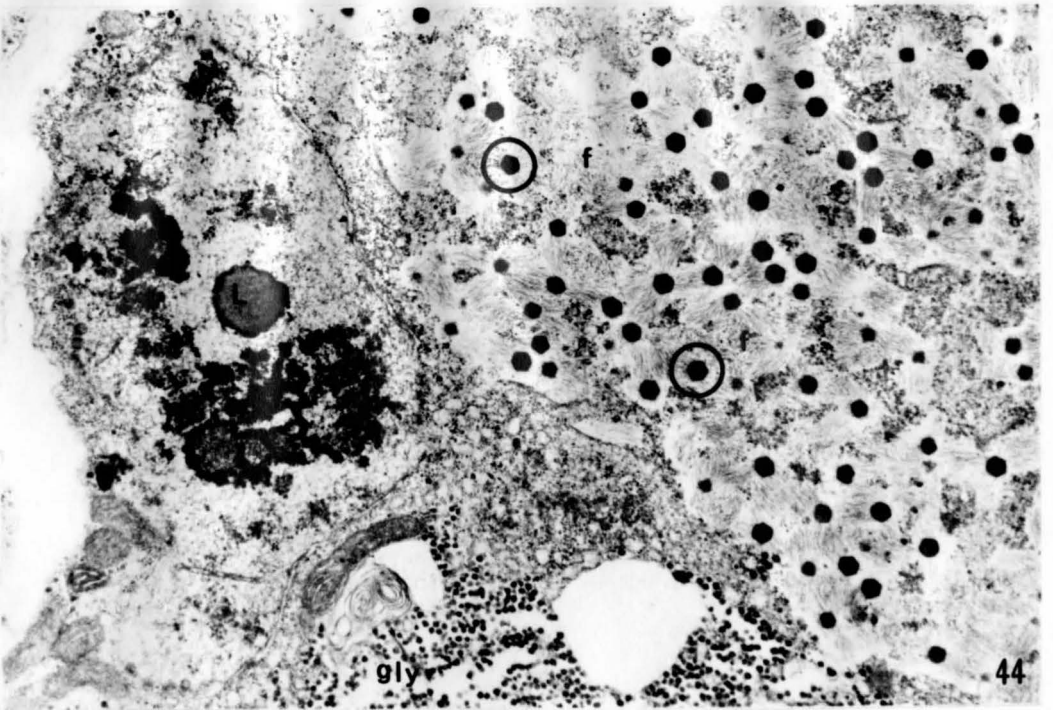
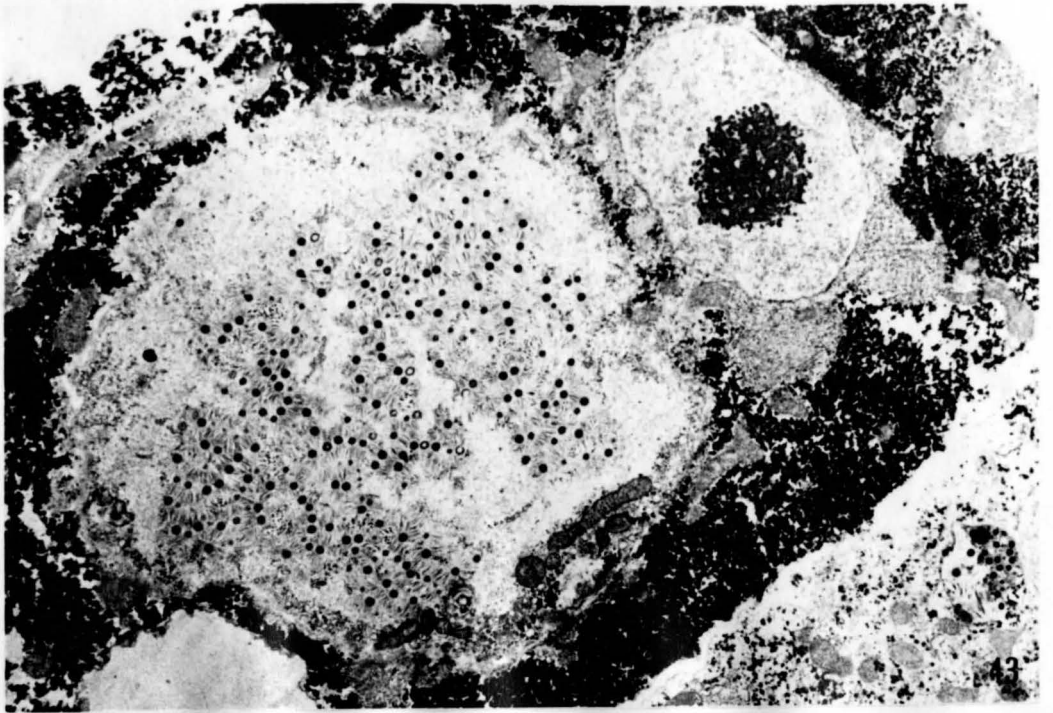
Examination of diseased fat body in the electron microscope confirmed the presence of a virus (Figs. 43 and 44), which had been previously assumed to exist simply because no other types of microorganisms could be detected by phase microscopy. It subsequently became apparent that this virus could be readily visualized at the level of the light microscope (Figs. 45, 46 and 47). The fine "granules" seen, for example, in Figures 21 and 23, were therefore regarded as virus particles.

With this in mind, it was possible to relate the types of inclusion bodies seen by phase-contrast microscopy to homologous structures detected at much higher magnification in the electron microscope. Examples of the smallest IB's so detected are shown in Figures 48 to 50. Such IB's appeared to consist of an area of amorphous material and were generally surrounded by a rim of rough endoplasmic reticulum (RER). Occasionally, dilated cisternae of RER, containing amorphous material similar in electron density to that composing the IB, were seen peripherally (Fig. 49). Such profiles were more commonly seen in "mature" inclusion bodies containing many virus particles; in these, most of the peripheral RER

Figures 43 and 44. Cytoplasmic inclusion bodies containing virus particles.

Fig. 43. The extremely electron-dense material is glycogen. 8000 X.

Fig. 44. Virus particles appear to be in close association with numerous fine fibrils (f). Hexagonal and pentagonal virus outlines (circled) are present. L, nuclear lipid; gly, glycogen granules. 18,000 X.

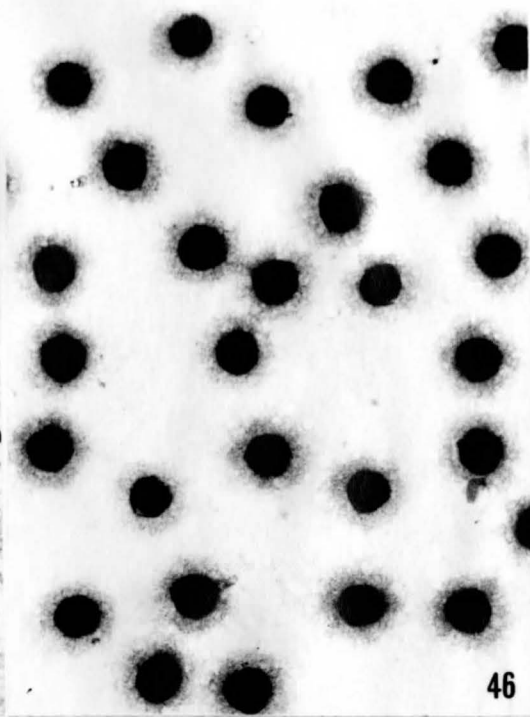
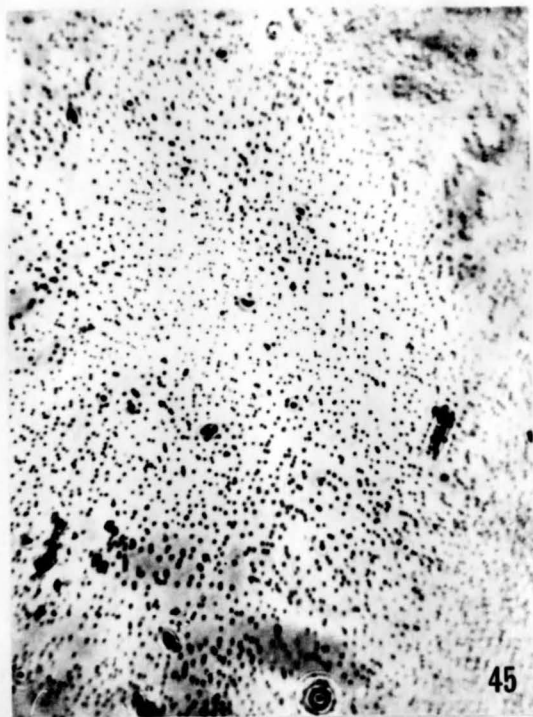


Figures 45 to 47. Extracellular virus particles.

Fig. 45. Phase-contrast micrographs of virus particles purified by differential centrifugation. 7500 X.

Fig. 46. Electron micrograph of virus particles from same preparation. 30,000 X.

Fig. 47. Sectioned virus particles. Note that extracellular particles retain fibrils. 30,000 X.

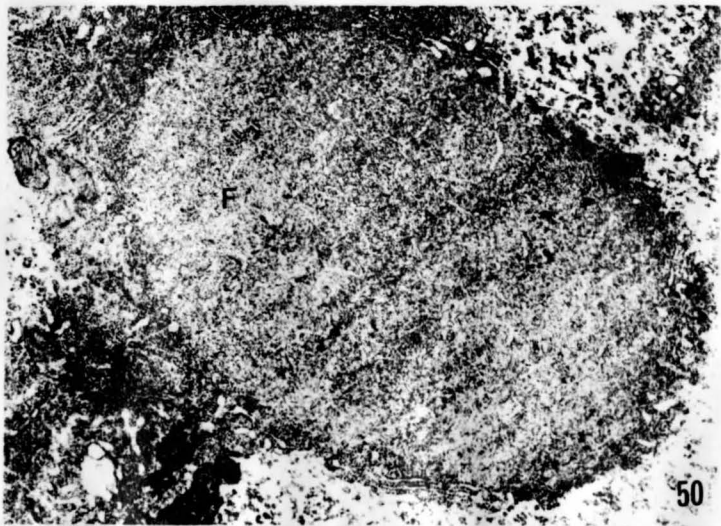
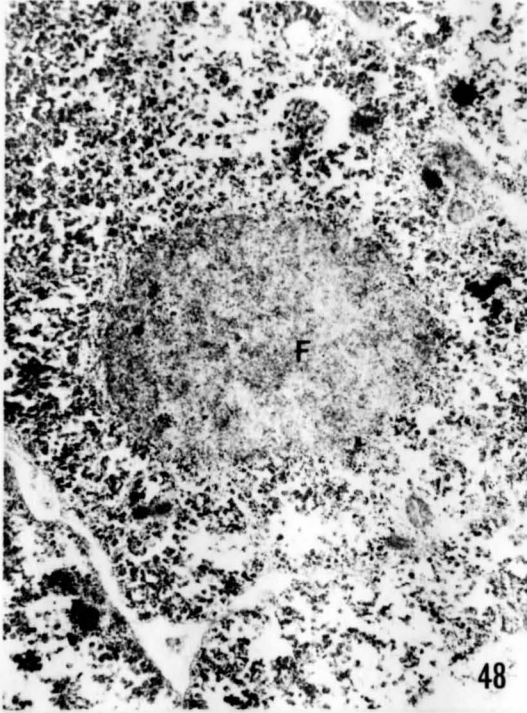


Figures 48 to 50. Ultrastructure of early foci (F) of infection.

Fig. 48. 15,000 X.

Fig. 49. Vesicular profile of RER (arrow) contains material similar in appearance to that in the focus (F). 16,000 X.

Fig. 50. Note abundance of peripheral RER and ribosomes. 15,000 X.



was vesiculate (Figs. 44 and 54). Micrographs of typical areas within larger inclusion bodies are reproduced in Figures 51 to 54. Such inclusions often contained islands of polyribosomes (Figs. 51 and 52). Virus particles appeared to be in greatest concentration at the periphery of these islands. In many inclusion bodies, membranous profiles were common (Fig. 54); these were occasionally circular in outline but more often resembled cups or "W's". Material contained within, or in the vicinity of, such profiles was less electron dense than the general matrix of the inclusion body. Both these materials, however, resembled very closely the contents of intact microsomes (vesiculate RER); compare, for example, Figures 52, 53 and 54). It must be noted here that not all inclusion bodies had such membranous profiles, nor were they ever found in infected muscle. When found, they were most common in tissue fixed in  $\text{OsO}_4$  only.

Light areas containing virus particles are seen in Figures 53, 54 and 55 (compare with Fig. 17). Virus particles apparently segregated into these "clear" areas bear a fringe of fine fibrils (Fig. 54, inset). These fibrils appear identical to those seen on extracellular virus particles (Figs. 46 and 47).

Figure 55 is included to show the general features of infected fat body in a single micrograph. It will be seen that all the nuclei contain lipid-like material, and two show "spotted" nucleoli. Both these features were characteristic

Figures 51 to 54. Ultrastructure of virogenic stromata.

Fig. 51. Virus particles (arrows) are most numerous on edges of islands of polyribosomes. 6000 X.

Fig. 52. Same, at higher magnification. 15,000 X.

Fig. 53. The peripheral RER is vesiculate. The contents of large microsomes (mic) resemble the ground substance of the virogenic stromata (compare with Fig. 52). 18,000 X.

Fig. 54. Membranous profiles in virogenic stromata. Material within circular profiles, and in the immediate vicinity of open profiles resembles the contents of the microsomes shown in Fig. 53. 13,000 X.  
The inset shows segregated virus particles with fibrils. 20,000 X.

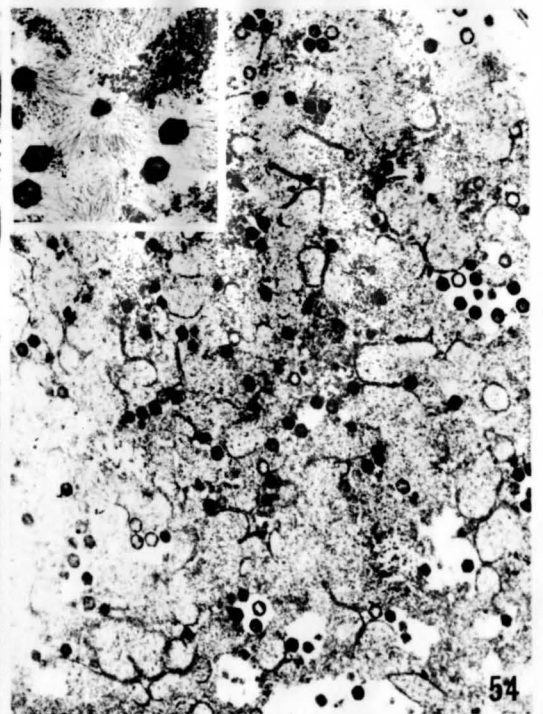
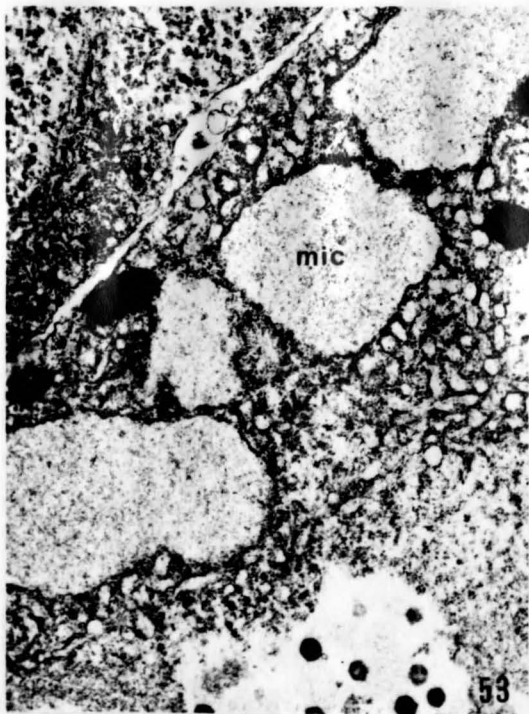
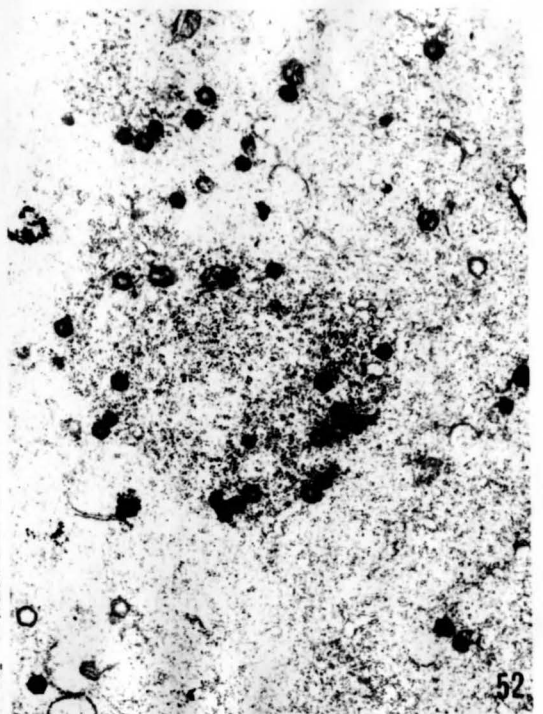
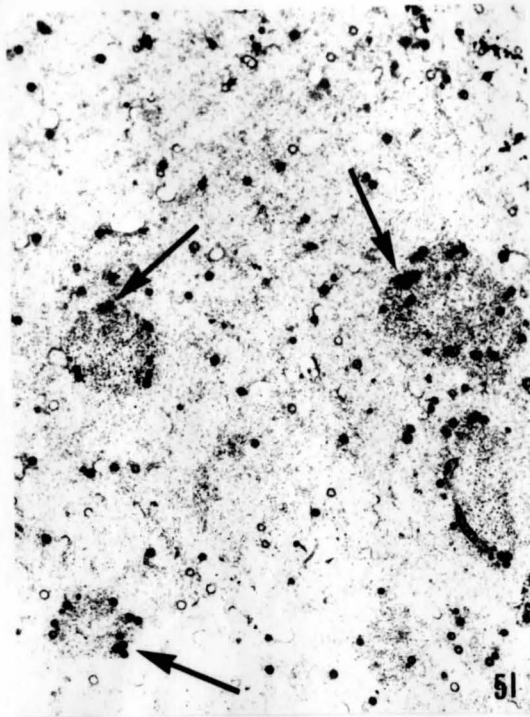
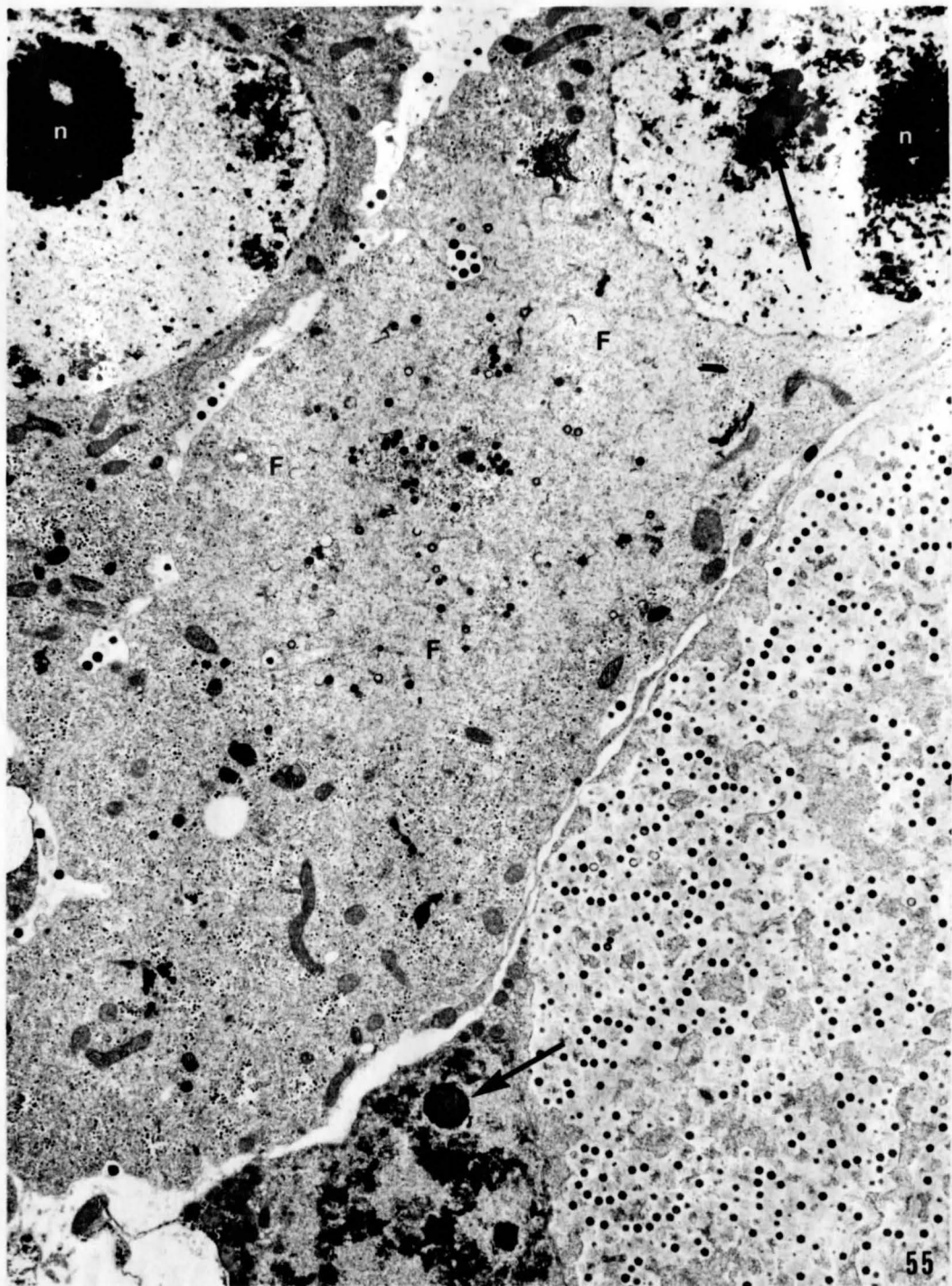


Figure 55. Survey micrograph of infected fat body. An early focus of infection (F) is present, along with an inclusion body composed primarily of mature virions. Nucleoli (n) are "spotted". Arrows indicate nuclear lipid. 7200 X.



of infected fat body. The granular component of the normal nucleolus (Fig. 56) appears, in infected cells (Figs. 57 to 59), to have condensed, giving rise to the "spotted" character. Generally, nuclear aberrations were more severe, or extensive, in those cells which contained what were regarded as mature inclusion bodies, namely those composed primarily of virus particles.

Since it is shown more clearly in muscle tissue, stages in viral maturation are not given here. Of interest, however, were rare cases of incomplete and/or bizarre assembly of virus particles. Assembly of capsids apparently took place in the absence of cores (Fig. 60), but few closed capsids were then produced. Synthesis of virus-associated fibrils predominated in one cell (Fig. 61).

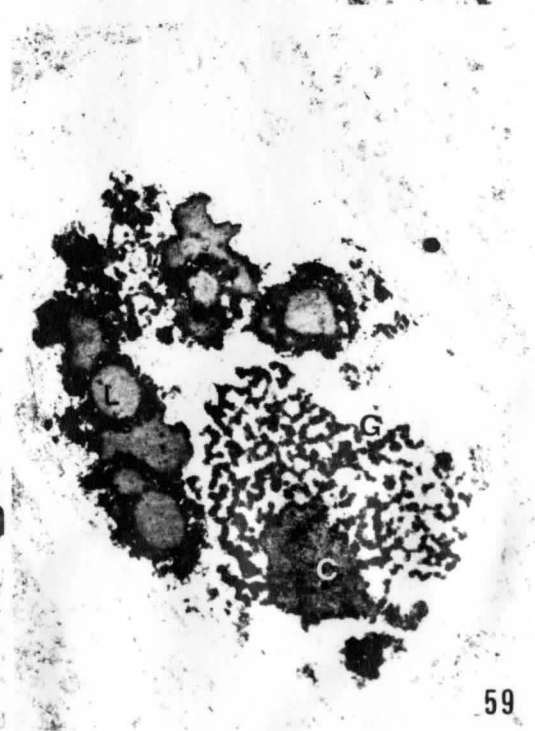
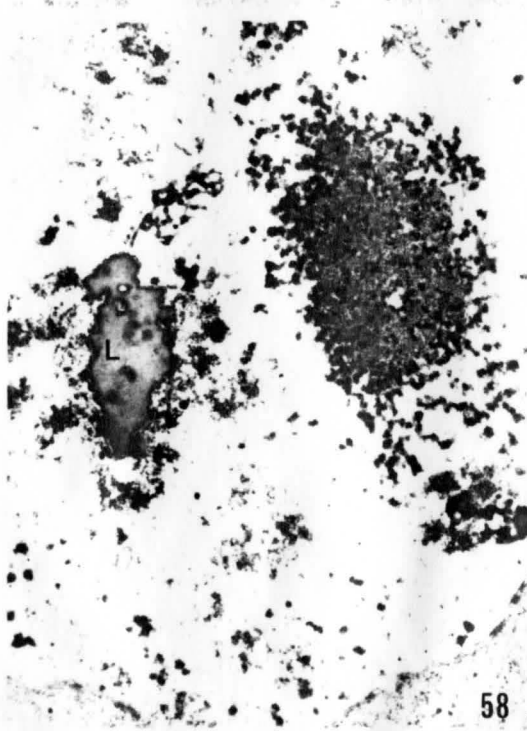
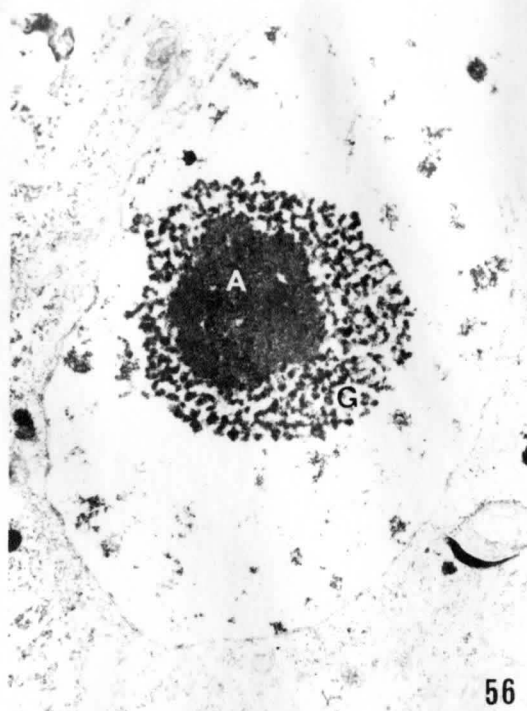
Virus particles appeared to gain entrance to the extracellular milieu as a result of cell lysis (Fig. 62); budding of virus particles at plasma membranes was never observed. In accordance with this observation was the finding of large numbers of virus particles in negatively-stained hemolymph. Two types of virus particles were seen in extracellular spaces, and could be distinguished by fibril<sup>1</sup> length (Fig. 62). Long fibrils were at least 270  $\mu$  long, while short ones (Figs. 46 and 47) ranged from about 130 to

---

<sup>1</sup> Fibrils appeared clumped in many areas of tissue fixed only in  $\text{OsO}_4$  and, for unknown reasons, in muscle fixed with both glutaraldehyde and  $\text{OsO}_4$ . Doubly-fixed fat body invariably showed unclumped<sup>4</sup> fibrils.

Figures 56 to 59. Changes in nuclear ultrastructure  
in infected fat body.

- Fig. 56. Nucleus showing nuclear hypertrophy;  
the cell was as yet uninfected.  
Amorphous (A) and granular (G) regions  
of the nucleolus are well differentiated.  
14000 X.
- Fig. 57. Spotted nucleolus. 14,000 X.
- Fig. 58. Spotted nucleolus and nuclear lipid.  
14,000 X.
- Fig. 59. Fragmentation and dispersal of condensed  
granular nucleolar material (G); the  
fibrous core (C) of the nucleolus  
remains unaltered. L, nuclear lipid.  
14,000 X.



Figures 60 and 61. Aberrant synthesis and/or assembly of viral components in cytoplasmic inclusion bodies.

Fig. 60. Adjacent cells, one containing normal mature virions (V), and the other showing an aberrant assembly (arrows) of capsids in the apparent absence of core material. cm, cytoplasmic membranes. 17,000 X.

Fig. 61. Abnormal inclusion body containing fibrils (f) as the main component. 18,000 X.

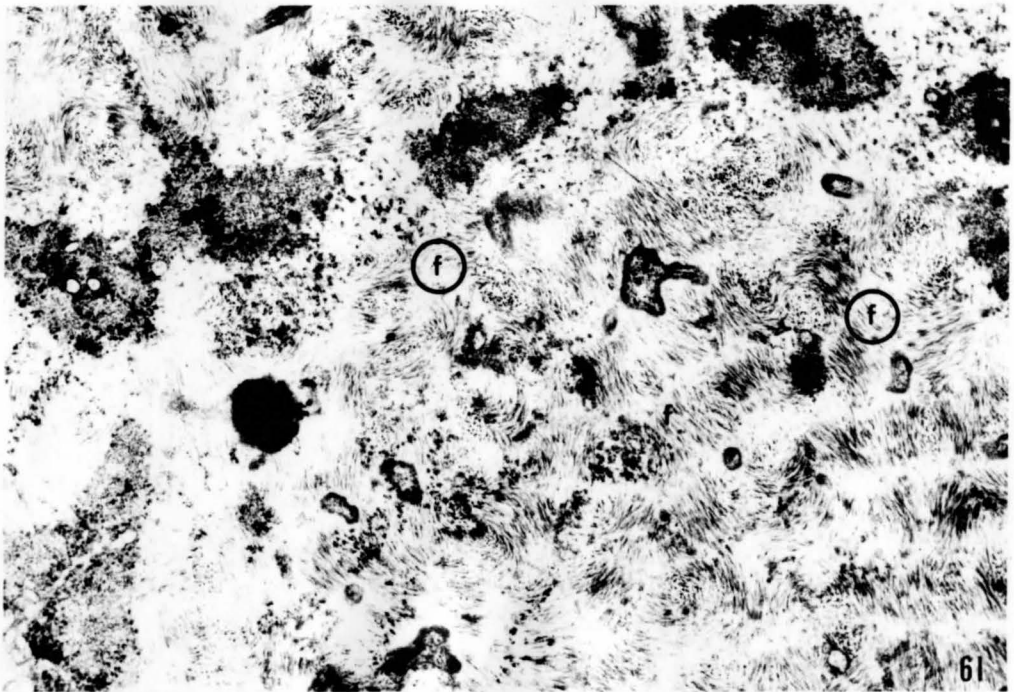
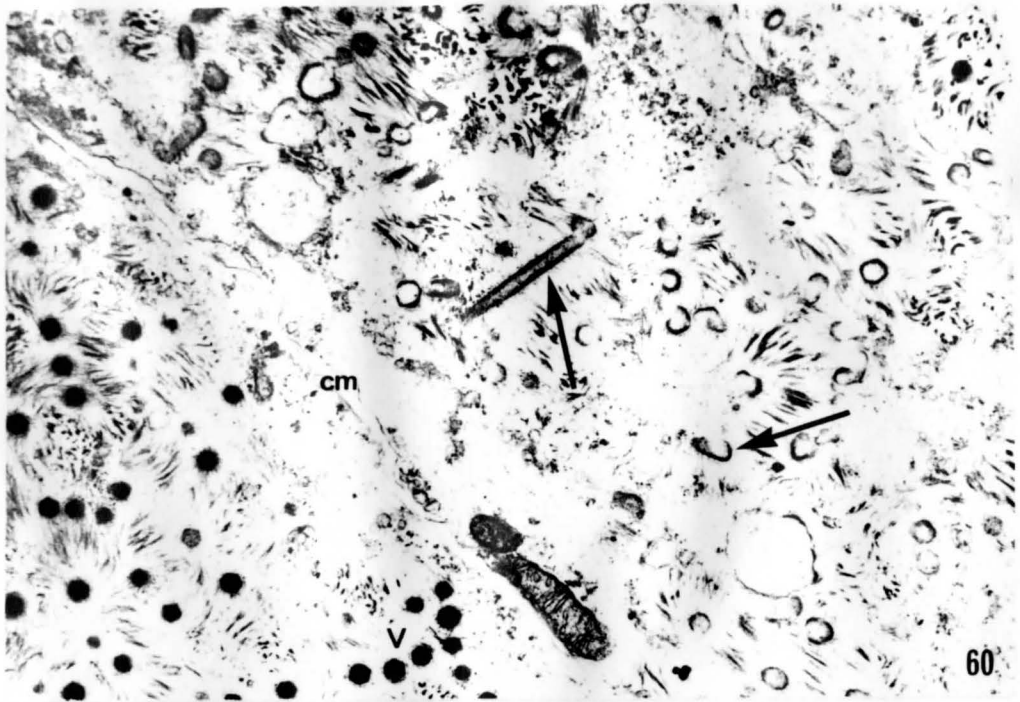


Figure 62. Release of virus particles by cell lysis. The arrow indicates an apparently abnormal inclusion body. Most extracellular particles in this case have long fibrils; two virions with short fibrils are circled. 7000 X.

The inset shows negatively-stained virions of different fibril lengths. 45,000 X.



170  $\mu$  in length. Only 4.3% of virus particles isolated by differential centrifugation were of the long fibril type (500 counted). It was unfortunately impossible to determine fibril length on intracellular particles in sectioned tissue.

It was originally hoped that uptake of virus and very early stages of infection might be followed in vitro; however, all attempts to grow the virus in either Antheraea or Aedes cells were negative. Thus an attempt was made to find cells in early stages of infection within obviously diseased tissue in situ. The results of this were disappointing and rather inconclusive, although nucleolar enlargement of apparently uninfected cells within infected fat body was confirmed (Fig. 63; compare with Figs. 38 and 39). Little can be said other than that virus particles were readily phagocytosed by such cells (Figs. 63 and 64). Hemocytes (Figs. 65 and 66) also phagocytosed virus particles, often in large numbers (Fig. 65). No multiplication of virus occurred in these cells; instead, viruses were apparently degraded within heterolysosomes (Fig. 66).

In all samples of fat body examined, both infected and control, were found bacteria-like bodies (Figs. 38, 67, and 68). These contained ribosomes and fine fibrillar material, and were surrounded by a rippled profile of RER presumably derived from the host cell. Such bodies were not seen in extracellular spaces, nor in muscle tissue. No evidence for multiplication could be found.

Figures 63 and 64. Phagocytosis of virus by as yet uninfected cells. •

Fig. 63. Phagocytosed viruses are indicated with arrows. 8000 X.

Fig. 64. Many phagocytosed viruses can be seen. One particle (circled) lies in a pocket of cell cytoplasm. 7200 X.

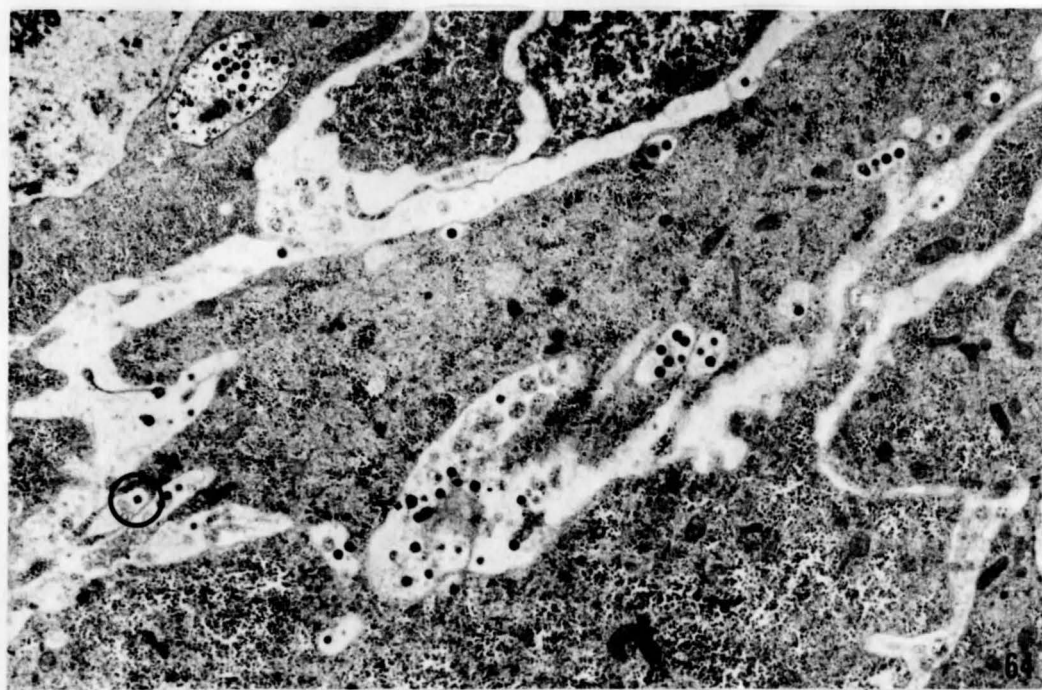
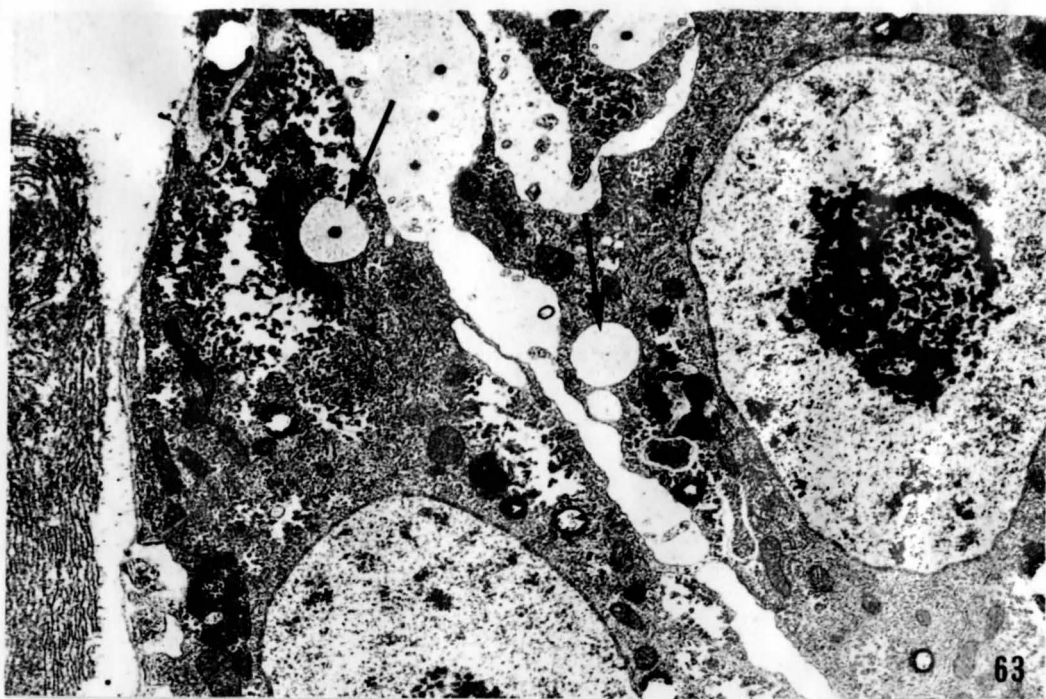


Figure 65. Hemocyte containing many virus particles in a phagocytic vesicle. 7500 X.

Figure 66. Virus particles in lysosome (ly) of a hemocyte. Arrow indicates an extracellular virus particle. G, Golgi apparatus. 20,000 X.

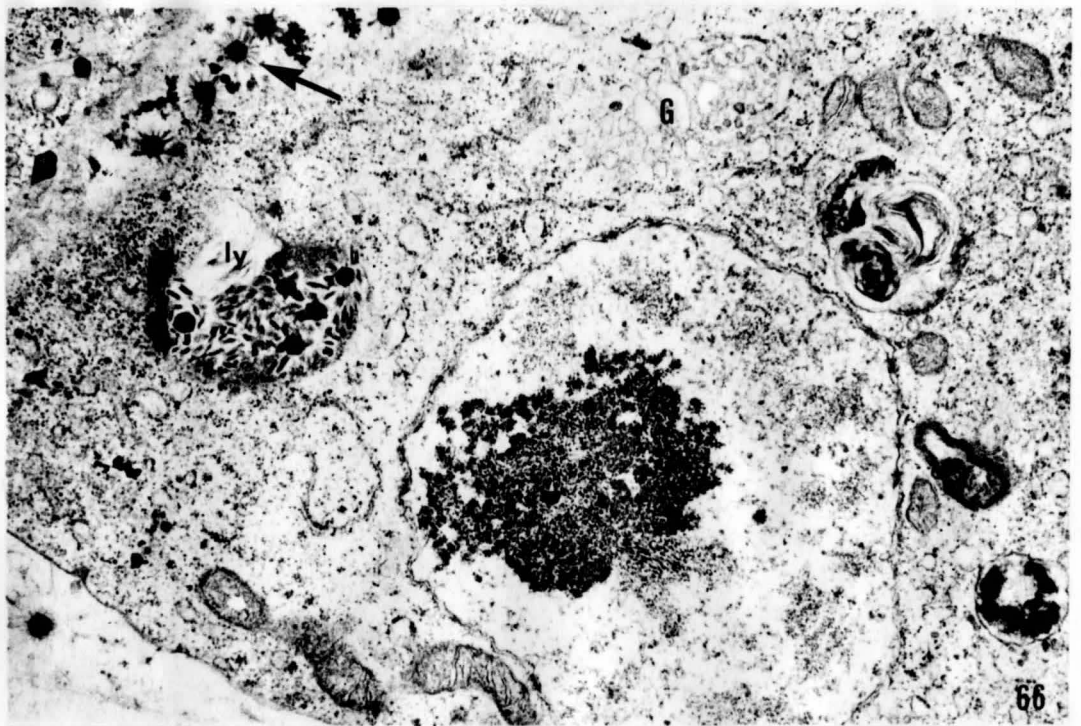
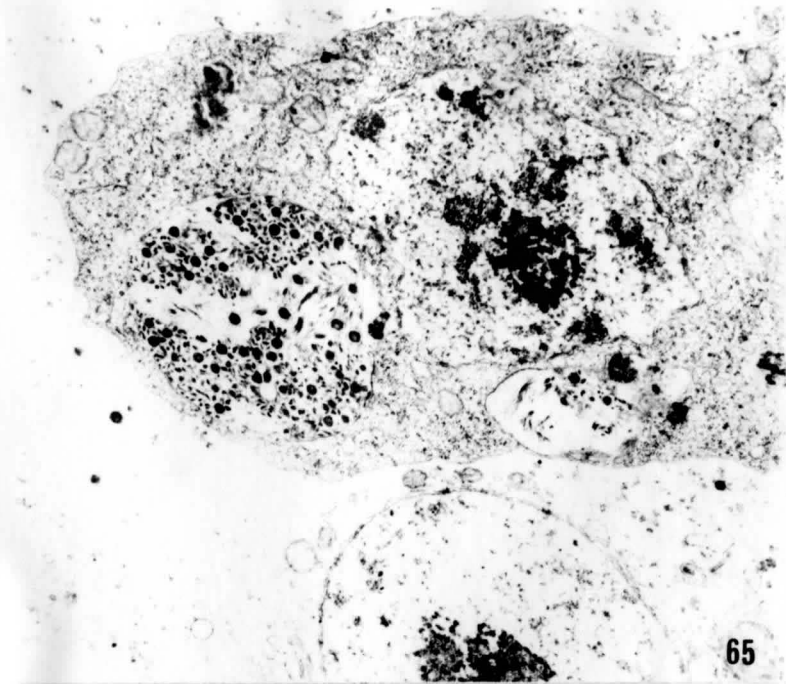
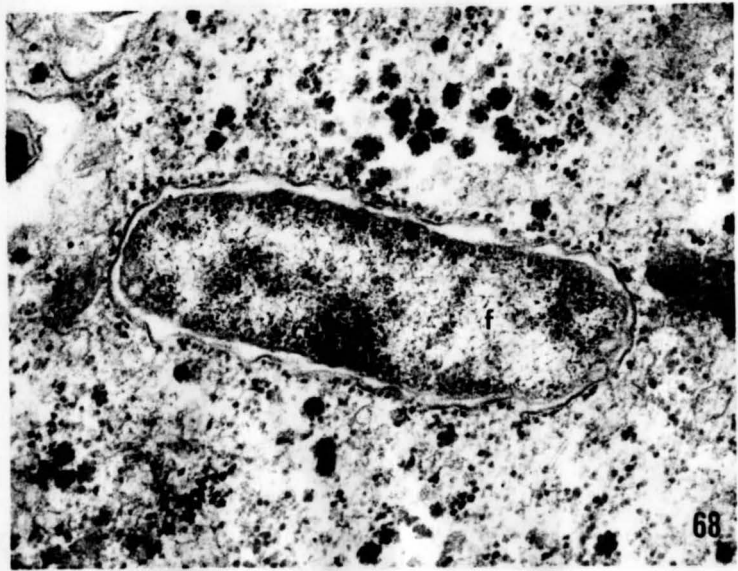
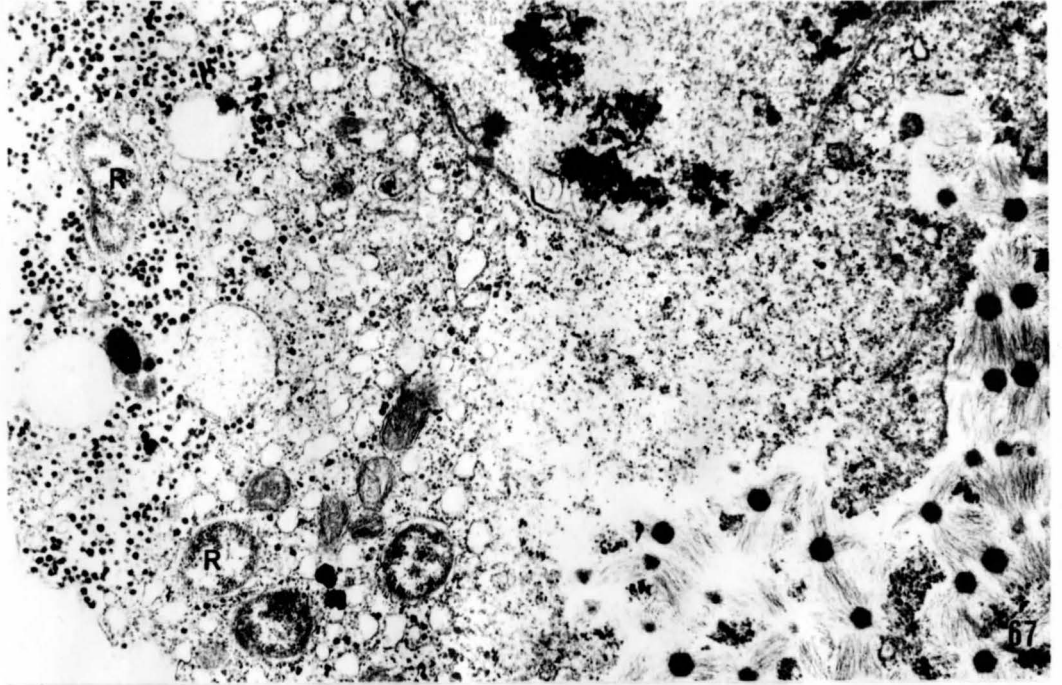


Figure 67. Rickettsia-like bodies (R) in the cytoplasm of a virus-infected cell.  
22,000 X.

Figure 68. Rickettsia-like body apparently lying within a vesicle of RER. The microorganism has a fibrous core (f), and an abundance of peripheral ribosomes (r).  
50,000 X.



Since symptoms of infection were also detected in muscle by phase-contrast microscopy, this tissue was also examined in the electron microscope. Virus particles were found in great abundance, especially in areas that in uninfected cells contained large deposits of glycogen; that is, near the nuclei, between myofibrils, and in the peripheral sarcoplasm. Areas of infected muscle fibers are shown in Figures 69 and 70. Virus particles appeared to develop in association with islands of polyribosomes embedded within masses of amorphous fibrogranular material. Only virus particles that were not embedded within, or not found close to the periphery of, fibrogranular matrices, bore fibrils.

Details of "virogenic stromata"<sup>1</sup> in muscle are shown in greater detail in Figures 71 to 76. Lengthy membranous profiles, common in some fat body stromata, were not found in muscle; however, other membranous components were visible. In addition to the usual profiles of rough and smooth ER (Figs. 71 and 73), appreciably thicker "membranes" were found; these took the form either of clusters of microvesicles (Fig. 71) or of elongate structures (Fig. 74). The latter often terminated in angular profiles, the dimensions of which resembled those seen in viral capsids (Fig. 74). Such components also resembled what were regarded as incomplete

---

<sup>1</sup> So-called because of a presumed involvement of amorphous material, polyribosomes, etc., in virus synthesis and maturation

capsids (Figs. 71 to 74, and 76). The latter were found only in association with virogenic stromata.

Complete, but "empty", capsids were also found, most commonly in such matrices (Figs. 71, 72, 74 to 76), and often in groups (Figs. 75 and 76). It was of interest to note that empty capsids were generally larger than those which contained electron-dense cores (Fig. 75). The content of incomplete shells resembled that of empty capsids, and in many preparations appeared as fine anastomosing fibrils (Fig. 72). A few particles had small cores (Figs. 71, 72 and 76).

The morphology of mature virions was examined in both sectioned and negatively-stained material. A typical survey micrograph of sectioned virus particles in fat body cytoplasm is shown in Figure 77. While most virions were clearly hexagonal, others had quadrangular, pentagonal, or roughly circular outlines (Figs. 78 to 85). Those particles with quadrangular outlines were diamond-shaped with a dark band running across the shorter dimension; those with pentagonal outlines, on the other hand, were regular<sup>1</sup> polygons. Both types of particle were smaller and generally less electron-dense than the hexagonal particles, and were regarded as being tangential, or near tangential, sectional

---

<sup>1</sup> "Regular" polygons are those having equal sides enclosing equal angles. Its 3-dimensional analogue is a regular solid, which is "a polyhedron whose faces are congruent regular polygons arranged so that the same number of faces occurs at each vertex." (2)

Figure 69. Ultrastructure of infected muscle.  
Virogenic stroma (S) is seen near the  
nucleus. 14,000 X.

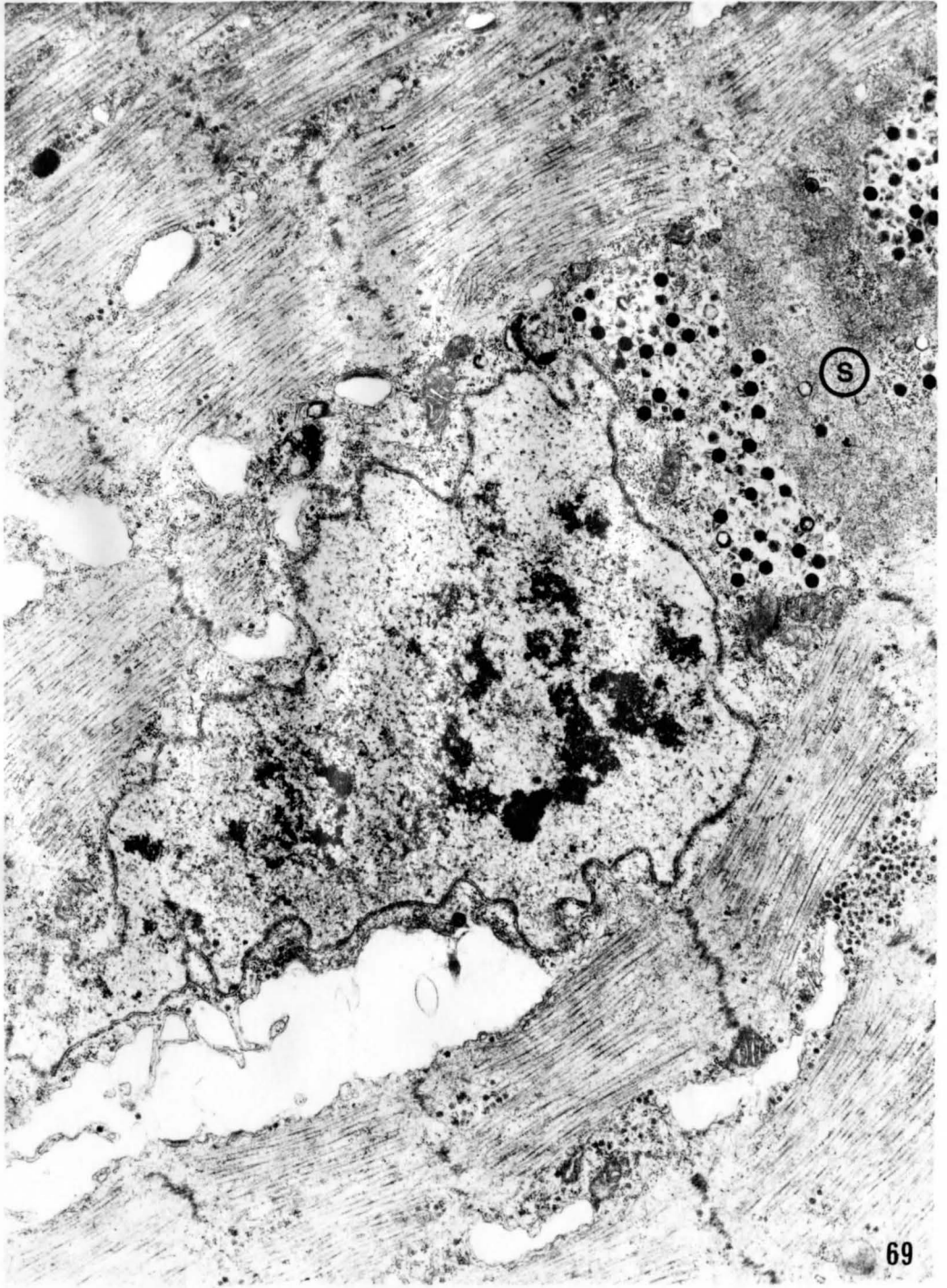


Figure 70. Detail of virogenic stroma (S) in muscle. Virus particles develop in association with clusters of polyribosomes (pr) within or on the edges of the stroma. myo, myofibril. 18,000 X.

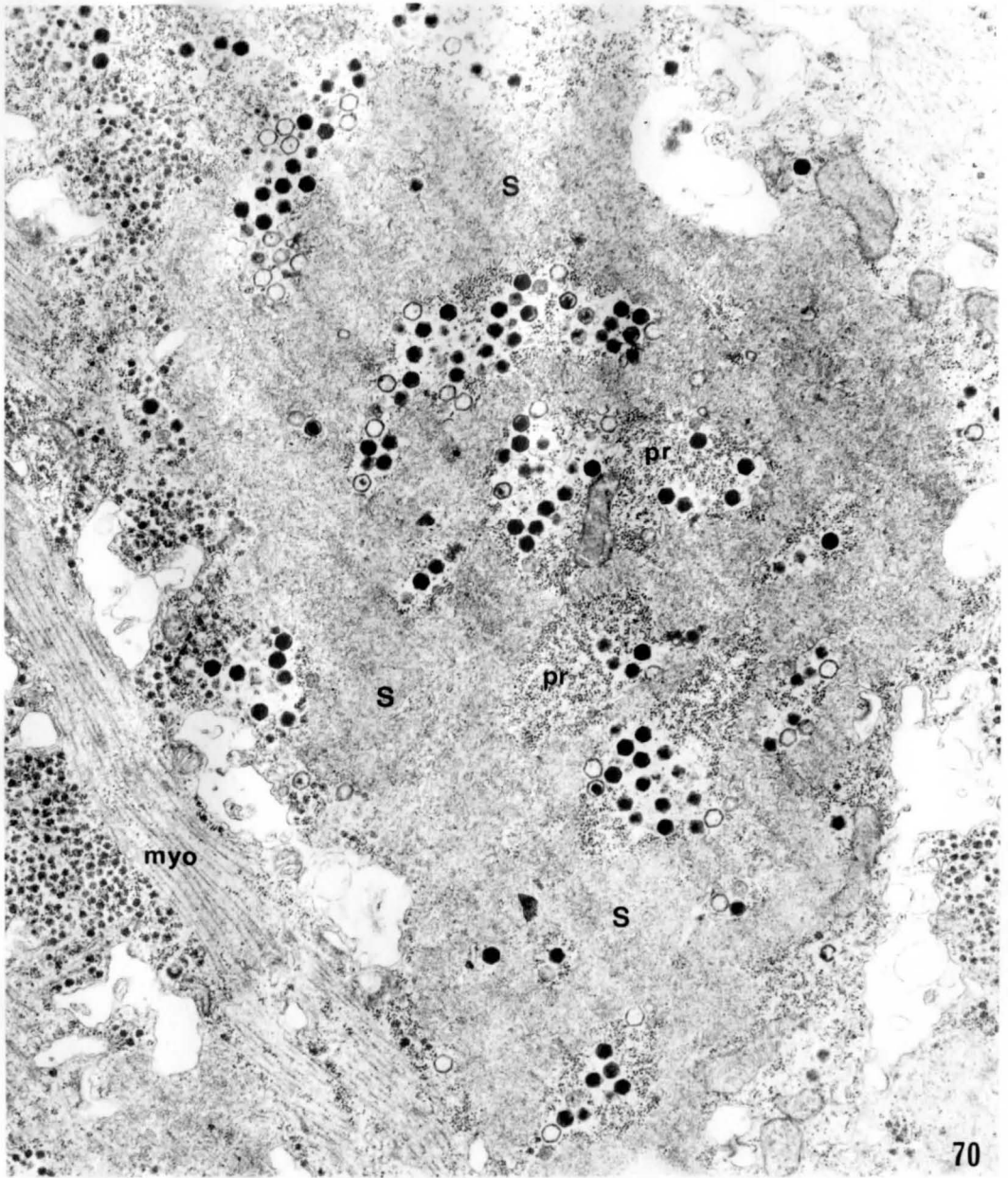
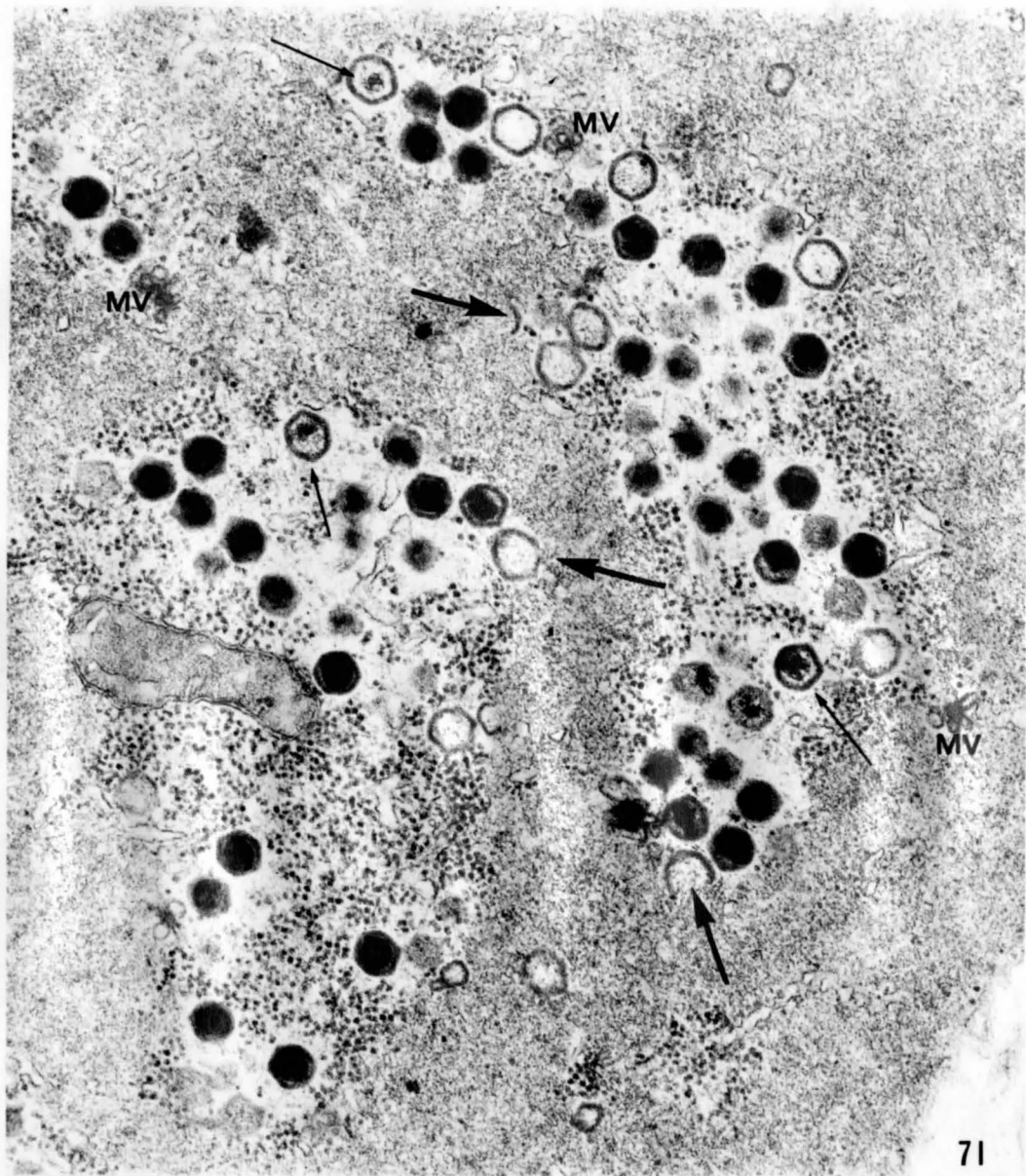


Figure 71. Enlarged area taken from Fig. 70.

Incomplete capsids (large arrows) are present on the edges of fenestrae within the stroma; multivesicular elements (MV) are present in the same areas. Some particles have small cores (small arrows). A few profiles of RER are present. 52,000 X.



MV

MV

MV

Figures 72 to 75. Developmental forms of virus particles.

Fig. 72. Mature virions with large electron-dense cores are present, together with an incomplete shell (large arrow) and a complete shell (small arrow) lacking a dense core. The incomplete shell seems to be enclosing stroma material. 60,000 X.

Fig. 73. Incomplete shell (large arrow) beside ER (small arrow). Note that the shell is thicker than the membranes of the ER. 60,000 X.

Fig. 74. Identity of material composing angular profiles and viral shells. 63,000 X.

Fig. 75. Particles lacking dense cores are larger than mature virions; such particles contain fine fibrillar material. 60,000 X.

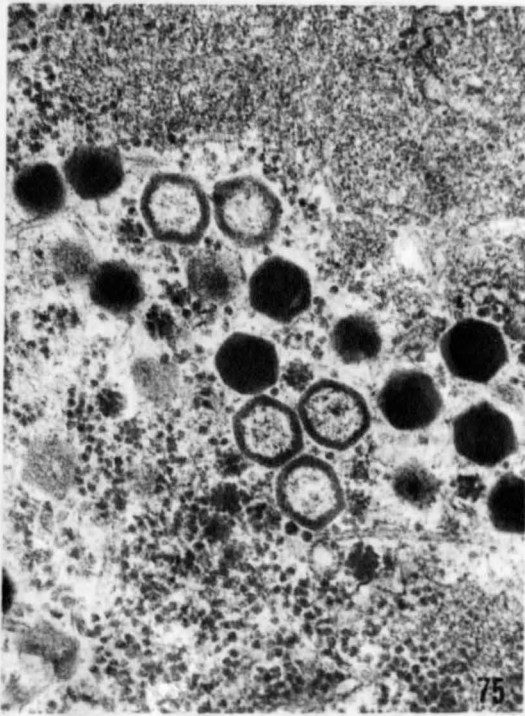
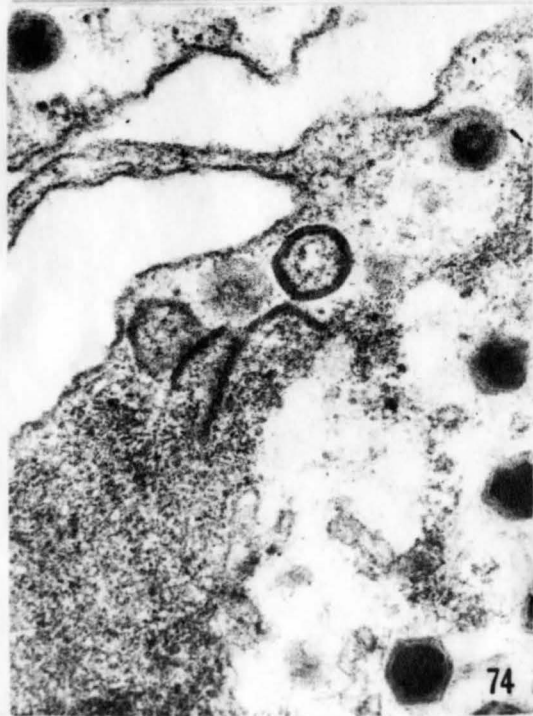
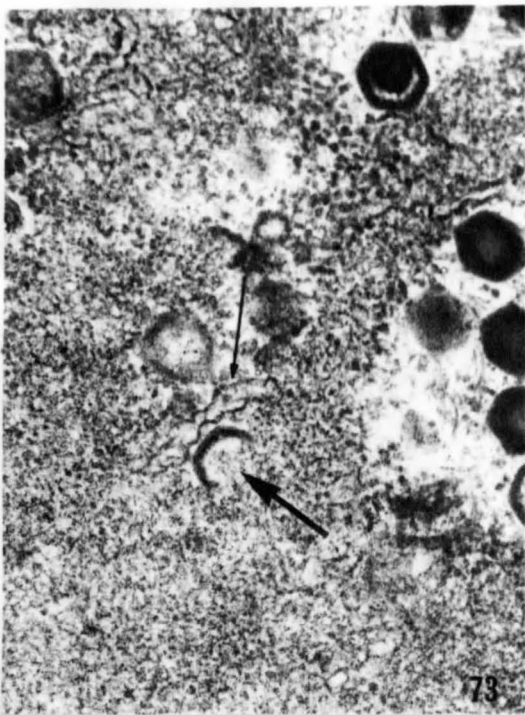
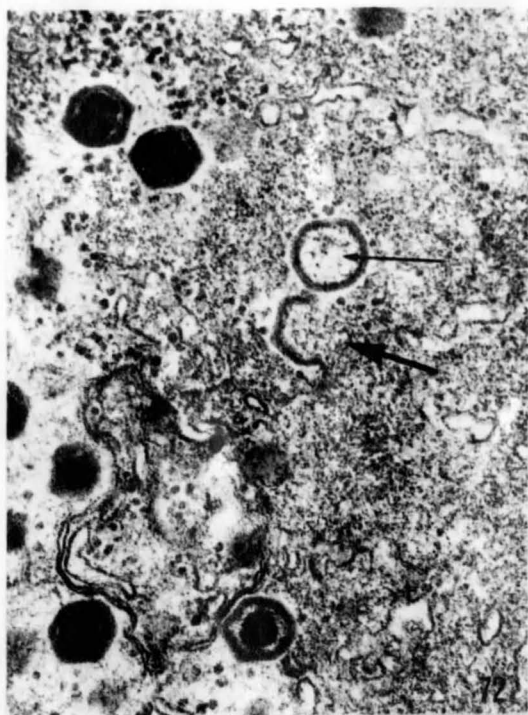


Figure 76. Assembly of viral shells within stroma. One complete shell shows condensing core material (arrow). Note that virus particles free from association with the stroma have dense, well-defined cores. 48,000 X.

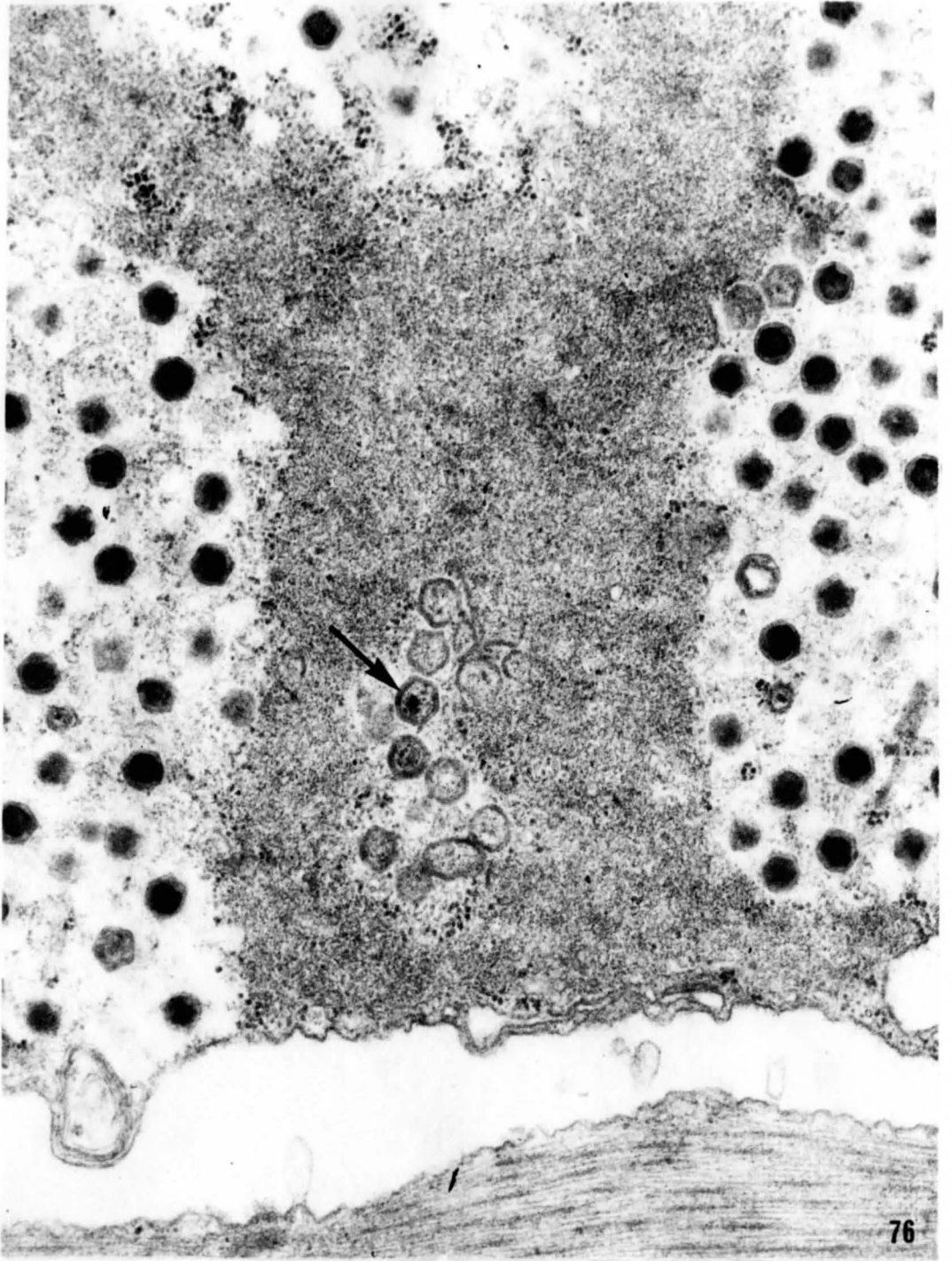
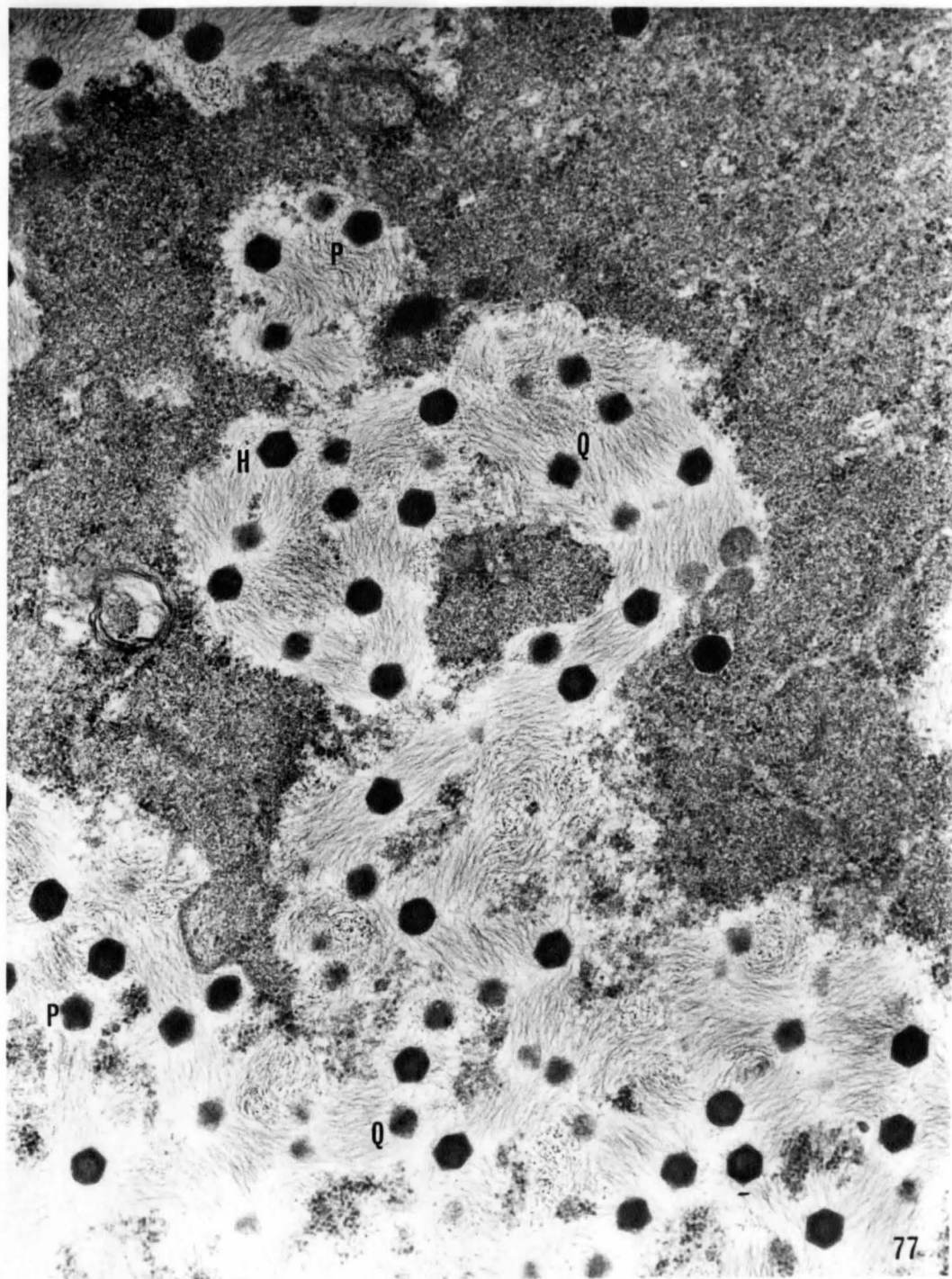


Figure 77. Survey micrograph of sectioned virus in fat body cytoplasm. Viruses with hexagonal (H), pentagonal (P), and quadrangular (Q) outlines can be seen. 42,000 X.



Figures 78 to 85. Sectional profiles of virus particles.

Figs. 71 to 81. Non-regular hexagonal and quadrangular profiles. Note dark band across shorter dimension of quadrangular particles (arrows).

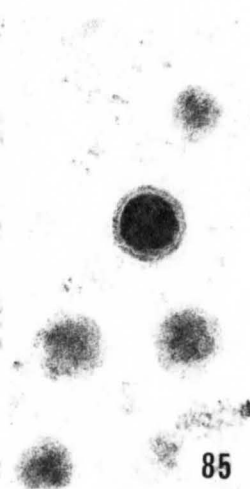
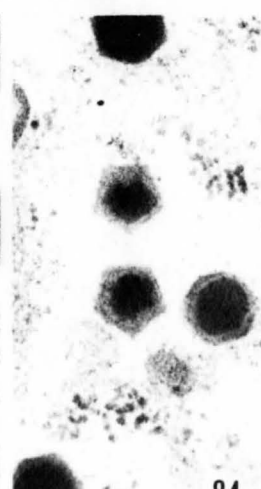
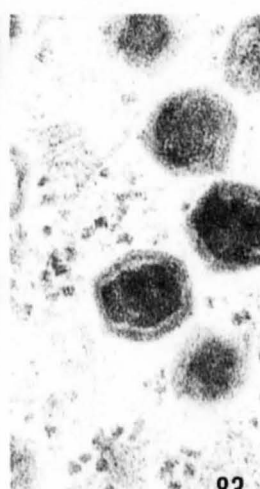
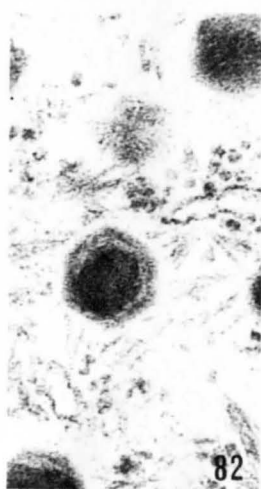
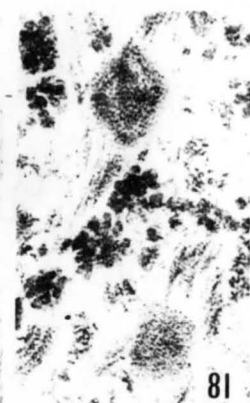
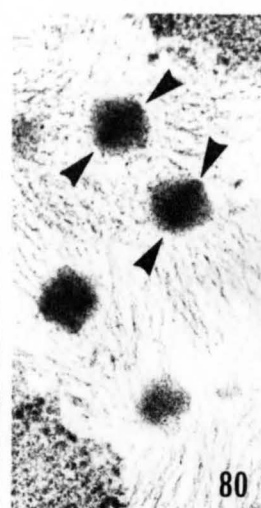
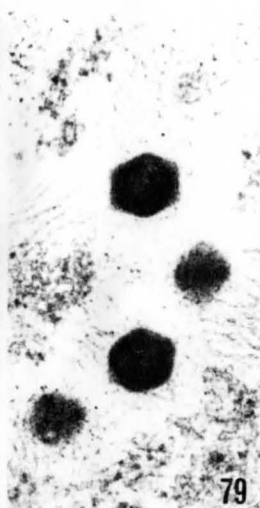
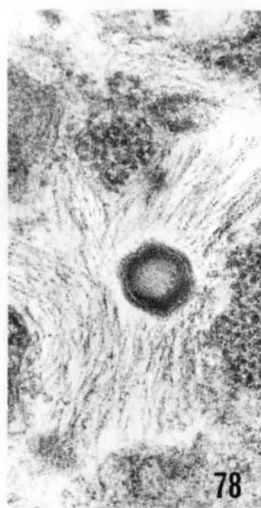
Figs. 78 to 80. 68,000 X.

Fig. 81. 100,000 X.

Figs. 82 and 83. Regular (equilateral) and non-regular hexagonal profiles at same magnification. 88,000 X.

Fig. 84. Regular pentagonal profiles. 68,000 X.

Fig. 85. Circular profile. 68,000 X.



profiles of virus particles. Hexagonal particles, when sectioned, resulted in the appearance of two classes of polygons, regular (Fig. 82) and irregular (Fig. 83).

Models of the regular solids were constructed of bristol board and an attempt was made to visually relate these models, viewed along various axes of symmetry, with virus particle profiles as seen in sectioned material. It was immediately obvious that the virus resembled an icosahedron. Methods similar to those outlined by Wrigley (142) were used to determine the relative numbers of particles seen along axes of 2-, 3-, or 5-fold symmetry. Assumptions made were that intracellular viruses were randomly orientated with respect to one another, and that quadrangular and pentagonal profiles were tangential sections of particles lying in 2- and 5-fold projection, respectively. Of 257 particles interpreted as showing recognizable symmetry, the ratios of those photographed along axes of 2-, 3-, and 5-fold symmetry were, respectively, 30:16.8:12.2. Expected ratios for an icosahedron are 30:20:12, since there are 30 axes of 2-, 20 of 3-, and 12 of 5-fold symmetry.

Negatively-stained virus particles were often distorted, presumably during the process of drying on the grid. However, particles with outlines typical of icosahedra were seen (Fig. 86). Size measurements (diameters) were taken only of virus particles in exact 3-fold orientation<sup>1</sup>.

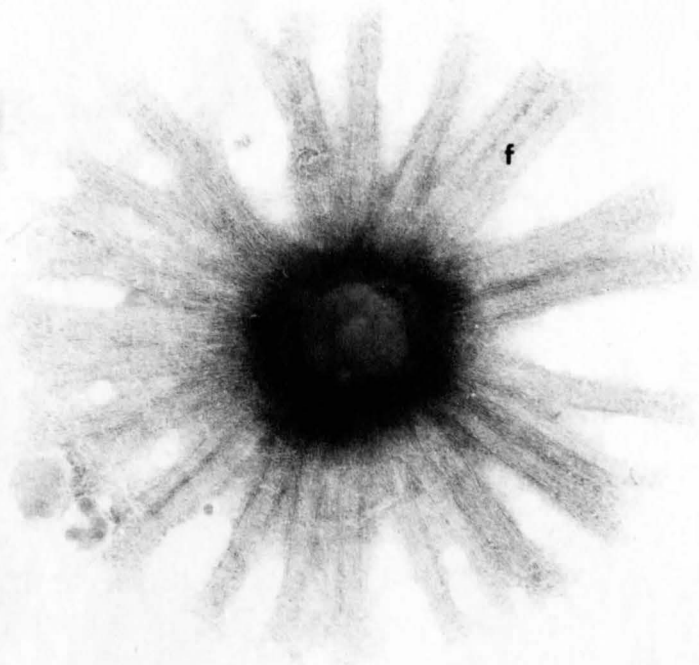
---

<sup>1</sup> This implies that the shortest distances between any three successive corners will be equal. In addition, all enclosed angles are equal (see Fig. 141).

This limited the number of measurable particles but eliminated that variation, as much as 13% (86), known to be due to differences in orientation. About 20 particles were measured in each case. In negatively-stained preparations, latex spheres (188 m $\mu$ ) were used as an internal marker. This allowed only a rough estimate of size since, excluding variation inherent in virus particles, latex spheres themselves can vary as much as 7.6 m $\mu$  in diameter (Dow Chemical specifications). CpV-1 particles were found to measure approximately 175 - 180 m $\mu$  in diameter, excluding fibrils. Capsids were approximately 5 m $\mu$  thick. Sectioned CpV-1 particles were similar in size to those which were negatively stained. Capsids, however, appeared to be thicker, in the order of 15-20 m $\mu$ . Cores, although irregular in shape, were estimated as having an average diameter of 60 - 70 m $\mu$ . These values can only be taken as approximate, since it was impossible to exactly determine the plane of sectioning of virus particles. Cores were not measured in negatively-stained particles, since they were usually poorly delineated.

The Toronto isolate (CpV-1-Toronto) appeared to be somewhat smaller (approximately 155-160 m $\mu$ ). This virus also had either long or short fibrils. In comparison, a virus (probably Chilo iridescent virus) obtained from the Insect Pathology Research Institute, Sault Ste. Marie, Ontario,

Figure 86. Negatively-stained virus particle in exact 3-fold projection. Virus particle is a regular hexagon. Note fibrils (f) attached to the capsid. 123,000 X.



f

measured only 135 - 140 m $\mu$  in diameter, and lacked detectable fibrils. These viruses are shown, negatively-stained in Figures 87 to 90.

(e) Degradation of Virus Particles

Suspensions of purified CpV-1 were treated with various chemical agents in an attempt to expose details of capsid morphology. It was hoped that treatments with enzymes and other protein-denaturing agents for short periods of time might selectively destroy certain features of the capsid and, in so doing, perhaps enhance visibility of other structures. Nasal decongestants were used because of demonstrated ability of Nafrine to show capsomeric substructure on intact SIV particles (142). It was thought that agents which might alter the structure of water might affect the water of hydration of a virus particle, and indirectly affect its stability. Pronase gave the most interesting results. Capsids in many instances appeared to undergo disruption in a regular manner, resulting in the release of numerous equilateral triangular fragments (Figs. 91 and 92), together with other, amorphous, fragments (Figs. 93 to 95). Triangular fragments were seen in preparations of CpV-1, CpV-1-Toronto, and "CIV" treated with pronase. The maximum number of such fragments per disrupted capsid was 18; this is probably not a real maximum value, because of overlap. Untreated suspensions of CpV-1 and "CIV" contained only intact virions.

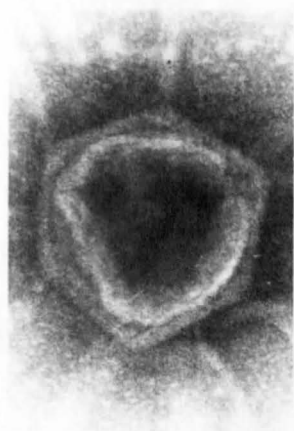
Figures 87 to 89. CpV-1 (Wisconsin), "CIV", and CpV-1  
(Toronto) at equivalent magnifications.  
200,000 X.

Fig. 87. CpV-1 (Wisconsin)

Fig. 88. "CIV"

Fig. 89. CpV-1 (Toronto)

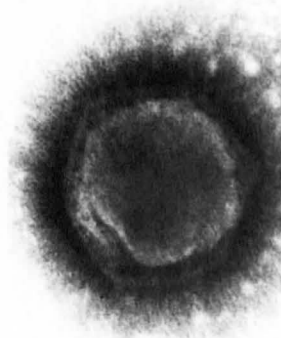
Figure 90. Mixture of CpV-1 (Wisconsin) and "CIV".  
168,000 X.



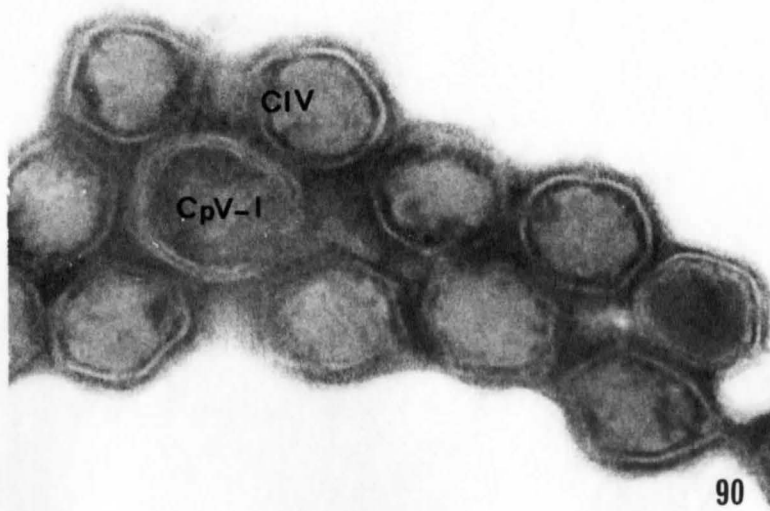
87



88



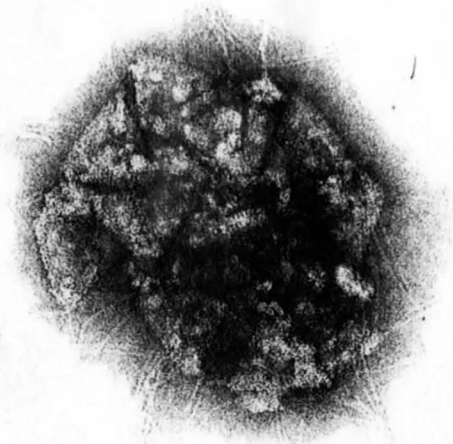
89



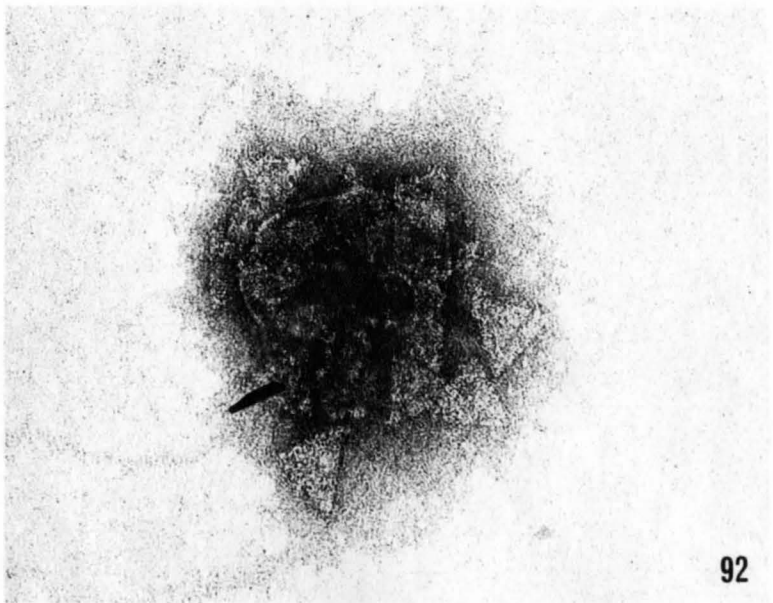
90

Figure 91. CpV-1 capsid disrupted by treatment with pronase. Many equilateral triangular fragments can be seen. 150,000 X.

Figure 92. Pronase-treated "CIV" capsid. Triangular fragments in this case are smaller than above; no fibrils are seen. 150,000 X.



91



92

A few triangular fragments were seen in the suspension of CpV-1-Toronto. This material (see METHODS) was not purified, and contained small numbers of bacteria as well as hemolymph. Treatment with pronase, however, increased the number of triangles seen. No triangular fragments were seen in negatively-stained pronase solutions.

At high magnifications (80-100,000 X), triangular fragments appeared to consist of regular hexagonal arrays of subunits (Figs. 93, 96 and 97). Unfortunately, while this appearance was often fairly clear in the electron microscope, it was almost impossible to reproduce the effect photographically. The pattern is perhaps best seen in reverse contrast (Fig. 93). Fibrils were clearly attached to triangular and other fragments derived from disrupted CpV-1 capsids (Fig. 93).

Triangular fragments from both CpV-1 and "CIV" capsids were often seen in close association with smaller fragments. The phenomenon was non-random: smaller fragments were invariably found in apposition to edges near corners of triangles (Figs. 94 and 95); they were not seen, for example, midway along sides of triangles. Occasionally, sharp well-defined angles could be measured on these fragments. Twelve such angles were measured, and gave a range of 103 to 125 degrees, with an average of 114 degrees.

In the absence of a suitable internal marker, accurate measurements of triangle size (i.e. edge length) were

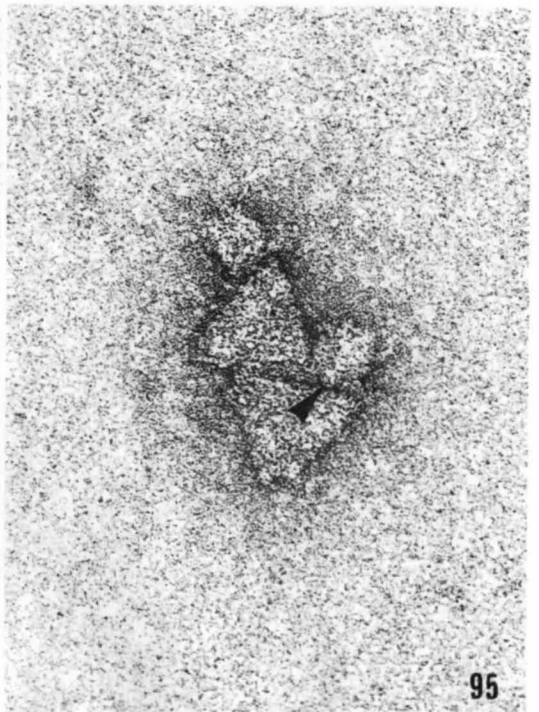
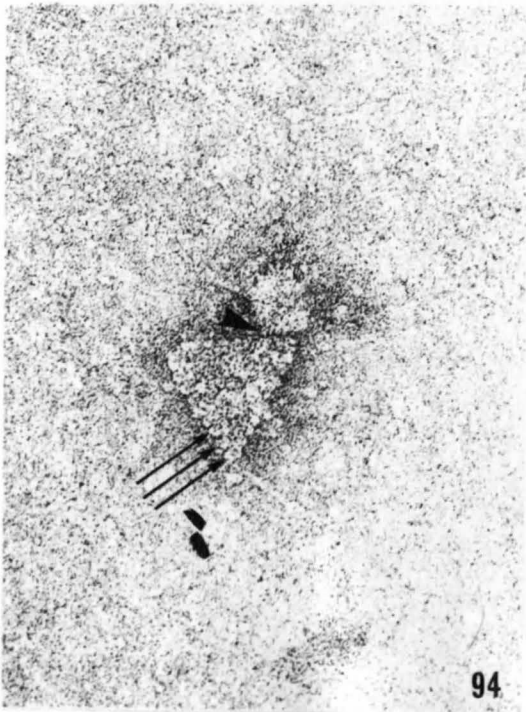
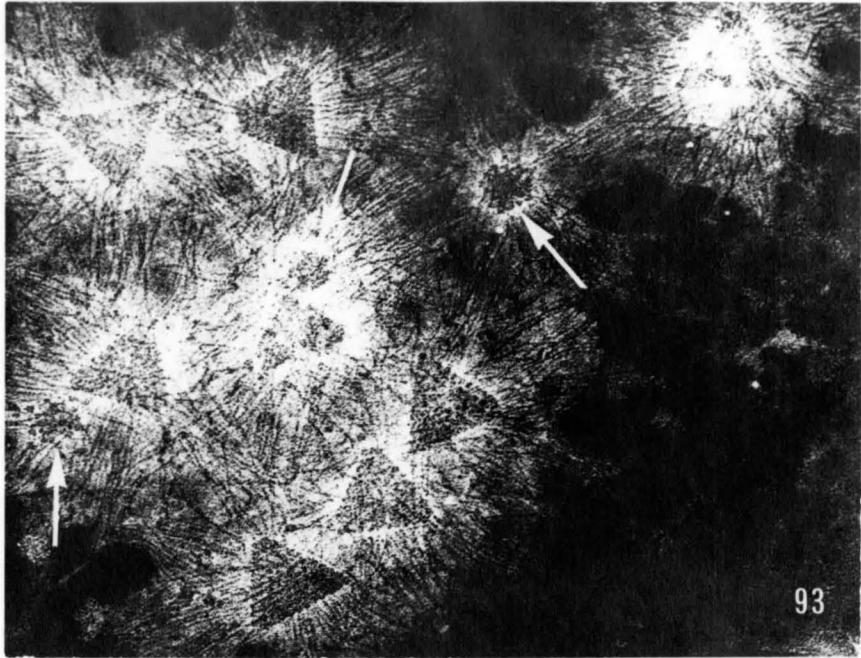
impossible. However, approximate dimensions can be given as 85 - 94  $\mu$  for CpV-1 and CpV-1-Toronto triangles (pooled results of measurements on 39 edges), and 73 - 77  $\mu$  for "CIV" triangles (12 edges measured). Measurements were made directly from electron microscope plates using a Bausch and Lomb comparator. The difference in size between "CIV" and CpV-1 triangles was reflected in the number of subunits per edge; the figures, respectively, are 10 and 12.

Triangular fragments derived from pronase-treated capsids were also on occasion observed to break up, resulting in free capsomeres (Fig. 98). The use of mercaptoethanol, however, always resulted in the production of suspensions of capsomeres (Figs. 99 and 100). "CIV" capsomeres appeared to have very short fibrils, while CpV-1 capsomeres bore very long fibrils, as was expected.

The effects of other chemicals on the virus were less instructive. Of the enzymes, the use of trypsin resulted in the appearance of a few triangles, but never as many as were seen in pronase-treated material. Pepsin at the concentration given completely destroyed virus capsids. Viruses treated with nasal decongestants or urea had very indistinct outlines, and showed no structural detail whatever. Chloroform, DMSO, and formamide had no effects on virus ultrastructure.

Figure 93. Fragments derived from disrupted CpV-1 capsid. Each triangle is made up of subunits in hexagonal array. Smaller arrays of subunits are visible (arrows). Fine fibrils are associated with triangular and other arrays of subunits. Negative contrast. 170,000 X.

Figures 94 and 95. Fragments derived from disrupted "CIV" capsids. Small fragments are associated with the corners of triangles; such fragments occasionally show sharply-defined angles (large arrows). Small arrows indicate rounded outlines of individual subunits; 200,000 X.

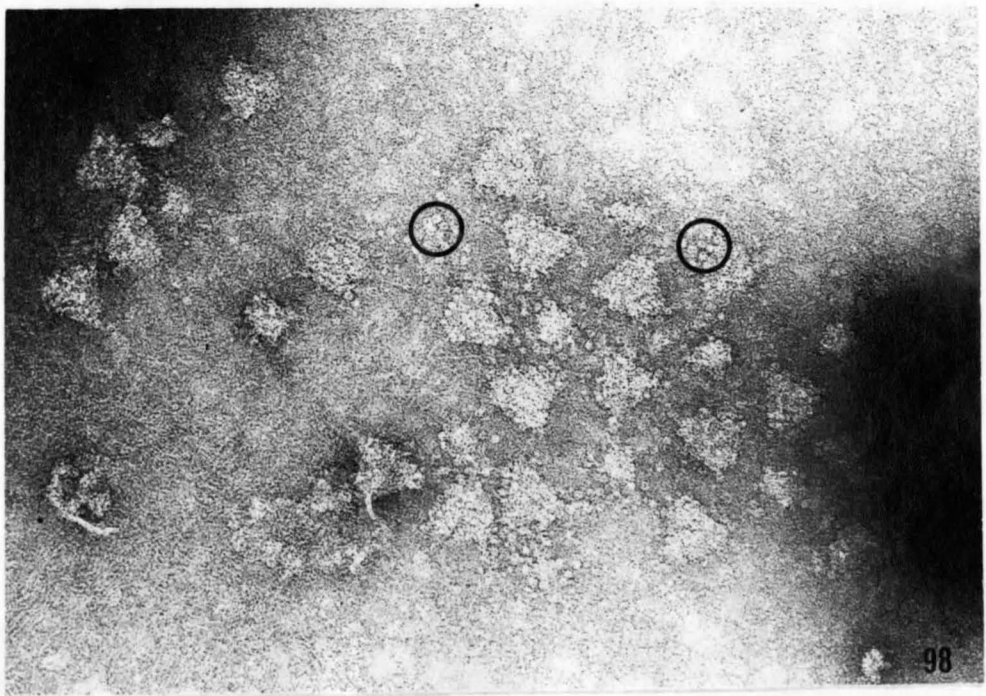
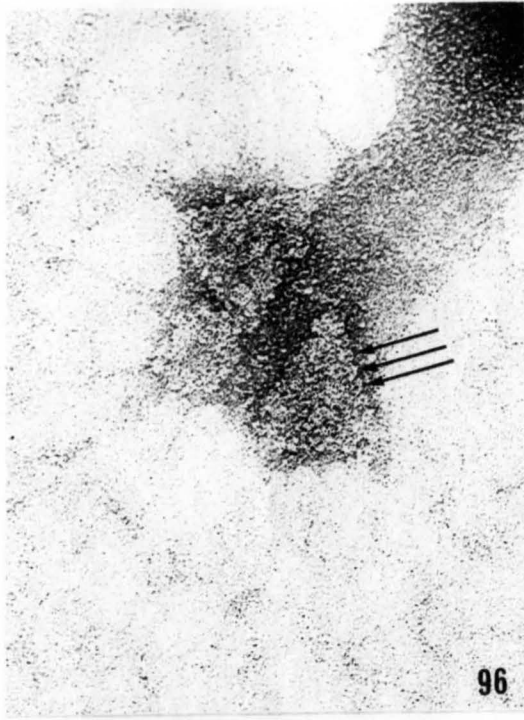


Figures 96 to 98. Triangular fragments derived from "CIV" and CpV-1 capsids treated with pronase. Figs. 96 and 97 are shown at equivalent magnifications.

Fig. 96. "CIV" triangle with 10 capsomeres (arrows) per edge, 250,000 X.

Fig. 97. CpV-1 triangle with 12 capsomeres (arrows) per edge. Note attached fibrils. 250,000 X.

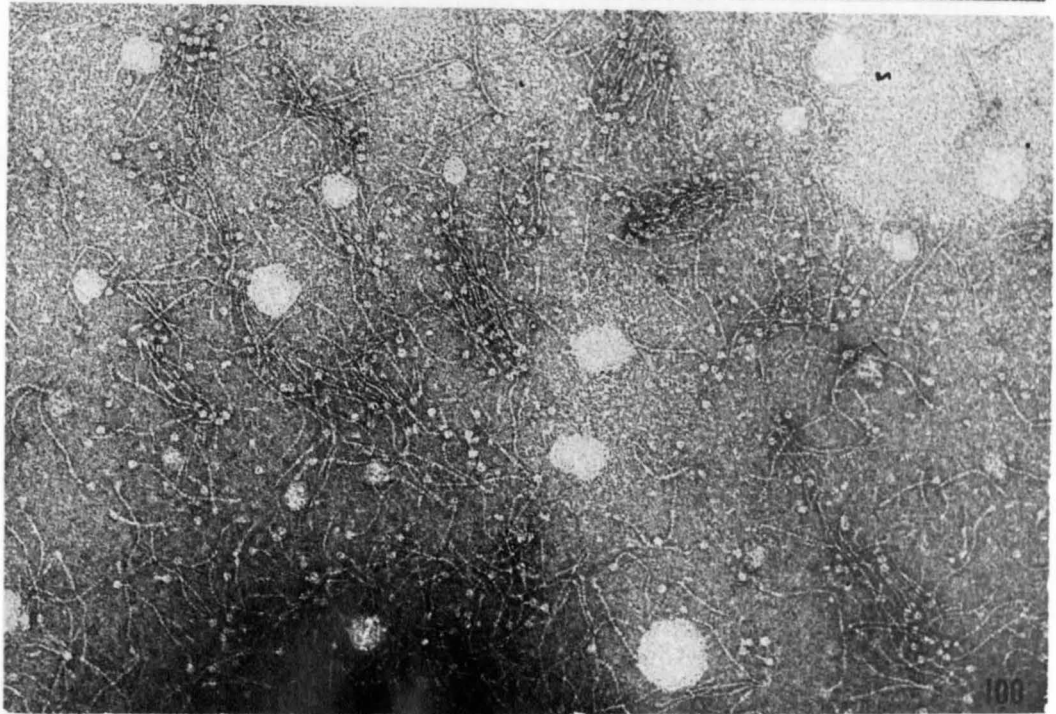
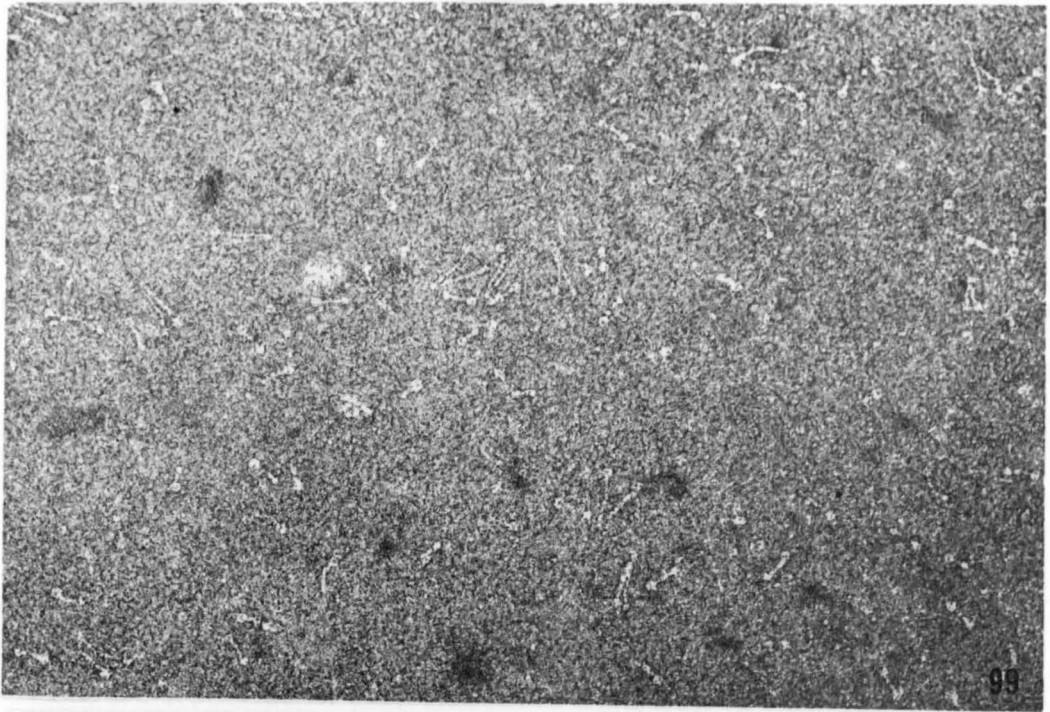
Fig. 98. Breakup of "CIV" fragments into subunits. Some free subunits (capsomeres) are encircled. 175,000 X.



Figures 99 and 100. Subunits released from mercapto-  
ethanol-treated viral capsids.

Fig. 99. "CIV" subunits with very short fibrils.  
135,000 X.

Fig. 100. CpV-1 subunits with attached fibrils.  
125,000 X.



(f) Colorimetric Determination of Nucleic Acids in  
CpV-1

Virus particles purified by sucrose density gradient centrifugation contained only one kind of nucleic acid, DNA. A suspension of virus containing 90  $\mu\text{gm}$  DNA/cc gave no measurable orcinol reaction for RNA (i.e., < 10  $\mu\text{gm}$  RNA/cc). The results of the tests are summarized below:

TABLE 1

Results of colorimetric tests for nucleic acids in  
CpV-1 virus particles

	Virus Sample Dilutions		
	Undiluted	1/2	1/4
DNA (viral) O.D. <sub>590</sub>	0.3	0.15	0.08
DNA ( amount) $\mu\text{gm}/\text{cc}$	90	46	25
RNA (viral) O.D. <sub>670</sub>	not measurable	-	-
RNA ( amount) $\mu\text{gm}/\text{cc}$	<10	-	-

## II. Cytoplasmic Polyhedrosis Virus in the Midgut Epithelium

### (a) Symptomatology

In this disease, the midgut had a chalky-white, opaque, appearance; normally this tissue appears translucent. The symptom of disease was readily apparent when viewed against the dark background normally provided by ingested material. In early stages of disease, before the entire gut becomes affected, individual infected cells could be seen with a dissecting microscope, again because of their white coloration. The disease affected primarily the midgut, but spread also into the foregut and hindgut epithelia.

Originally, only laboratory reared third-instar larvae were thought to contract disease. Recently, however, a fourth-instar larva field-collected from Lake Winnebago, Wisconsin, was found to be infected. This was the only infected larva that has ever been found under natural conditions. Infected larvae generally were somewhat more sluggish than others.

### (b) Cytology of Uninfected Midgut Epithelium

Only two papers containing micrographs of well-preserved midgut epithelia have been published (5, 106). Both of these were studies of moth tissue in which well-defined goblet cells are present. Neither these, nor tracheoles (since larvae are aquatic), are present in the midgut of chironomid larvae. For these reasons, preliminary observations of this material are given here in some detail.

The histology of the gut is well-shown in Figure 101. The epithelium was found to consist primarily of extremely large cells with well-defined apical brush borders. The basal cytoplasm of these cells appeared to contain extensive infoldings of the plasma membrane (Figs. 102 to 105). Small cells<sup>1</sup> with darkly-staining cytoplasm were found in this area (Figs. 101, 104 and 105). Nuclei of the large epithelial cells clearly contained polytene chromosomes (Figs. 102 to 105). Cells of intermediate dimensions occupied positions in the epithelium midway between the basement membrane and the lumen (Fig. 101). It appeared as though these cells might have been derived from the small peripheral cells, and might be involved in periodic replacement of mature epithelial cells. The gut wall was invested at apparently regular intervals by bands of striated circular muscle (Fig. 101). Longitudinal muscle fibers were also present, but their position relative to the circular bands was uncertain.

As seen in the electron microscope (Fig. 106), the apical cytoplasm of epithelial cells was packed with RER and mitochondria. Golgi apparatus, microtubules, multivesicular bodies, and myelin figures were also present. Larger organelles were excluded from the terminal web area immediately below the microvilli. Junctions between adjacent epithelial cells (Fig. 107) were invariably of the "septate" type (27). Nuclei

---

<sup>1</sup> These are probably comparable to the regenerative cells described by various authors (e.g., 136).

Figure 101. Combined transverse and tangential section of uninfected midgut epithelium. The gut has probably folded back upon itself in this area. Small regenerative cells at the periphery of the gut epithelium are circled. The brush border is indicated by an arrow. L, lumen; cm, circular muscle; lm, longitudinal muscle. 2000 X.



Figures 102 to 105. Detail of uninfected epithelial cells. All micrographs show apical infoldings of the plasma membrane, and polytene chromosomes in the largest nuclei.

Fig. 102. Long strands of material are circled. Granules, probably multivesicular bodies, are indicated by arrows.  
7000 X.

Fig. 103. lm, longitudinal muscle. 7000 X.

Fig. 104. Arrow indicates a regenerative cell.  
7000 X.

Fig. 105. Same as 104. 8000 X.

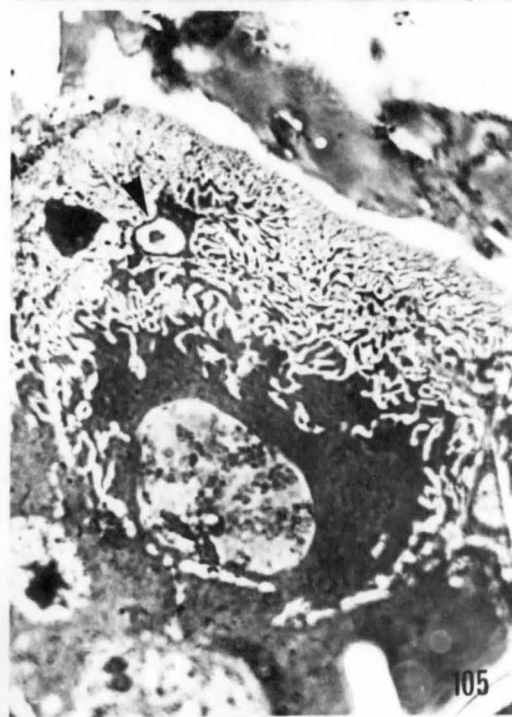
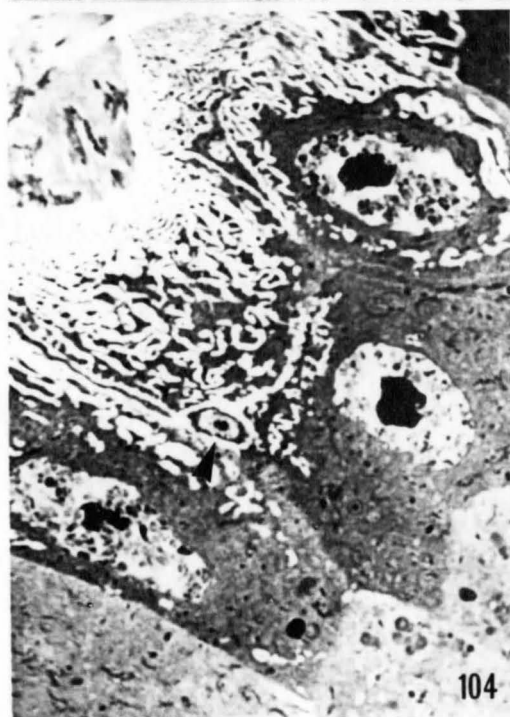
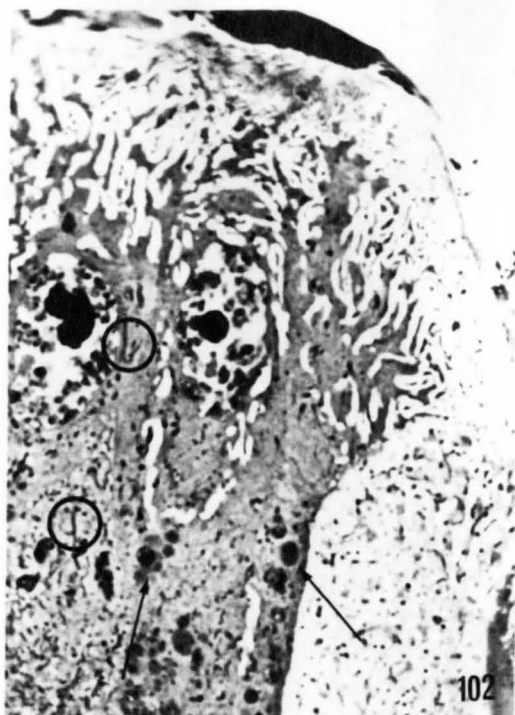


Figure 106. Uninfected midgut: ultrastructure of apical cytoplasm. ER, mitochondria (m), and microtubules (arrows) are abundant. G, Golgi apparatus; mv, microvillus; tw, terminal web area. 22,000 X.

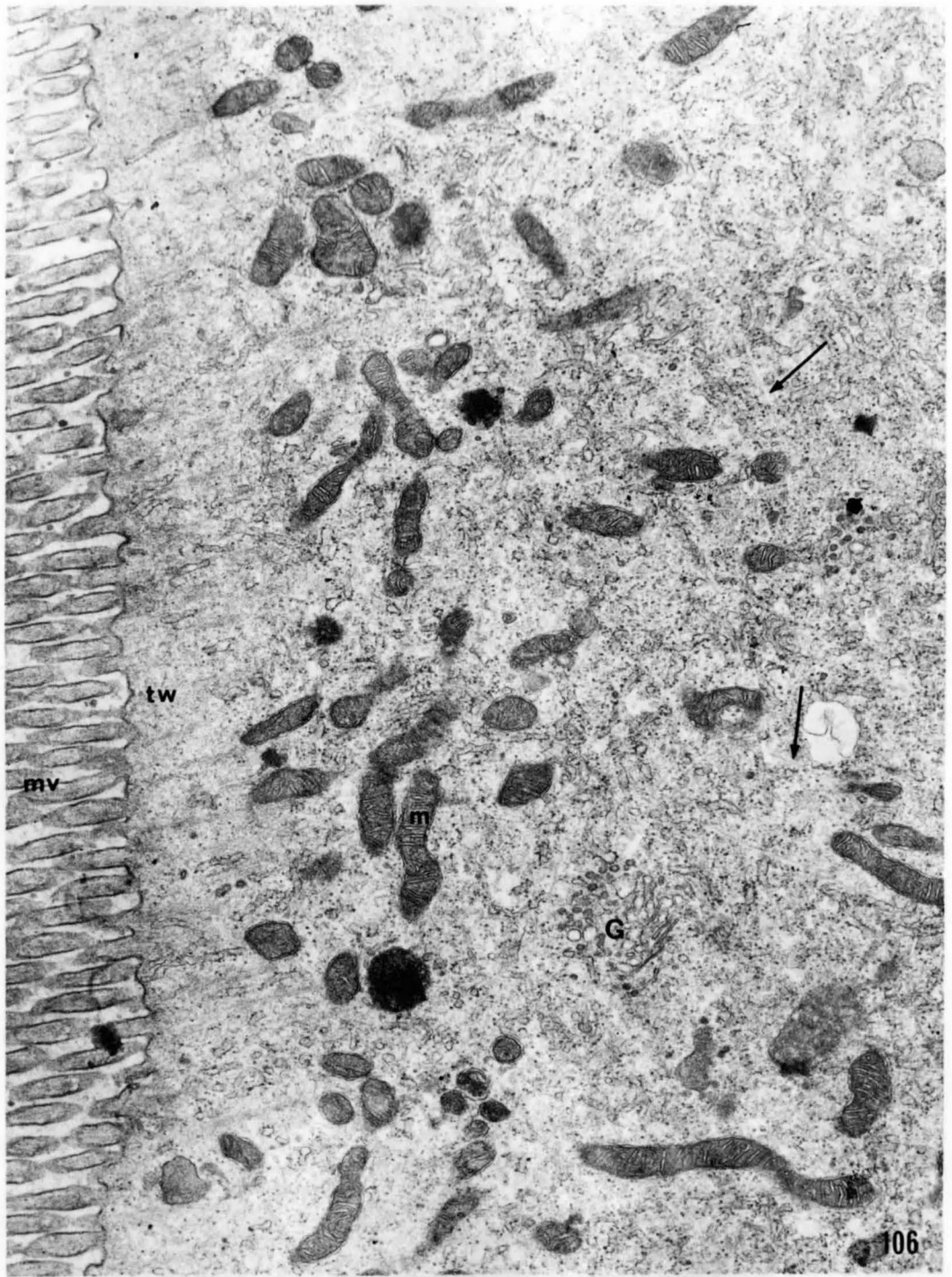
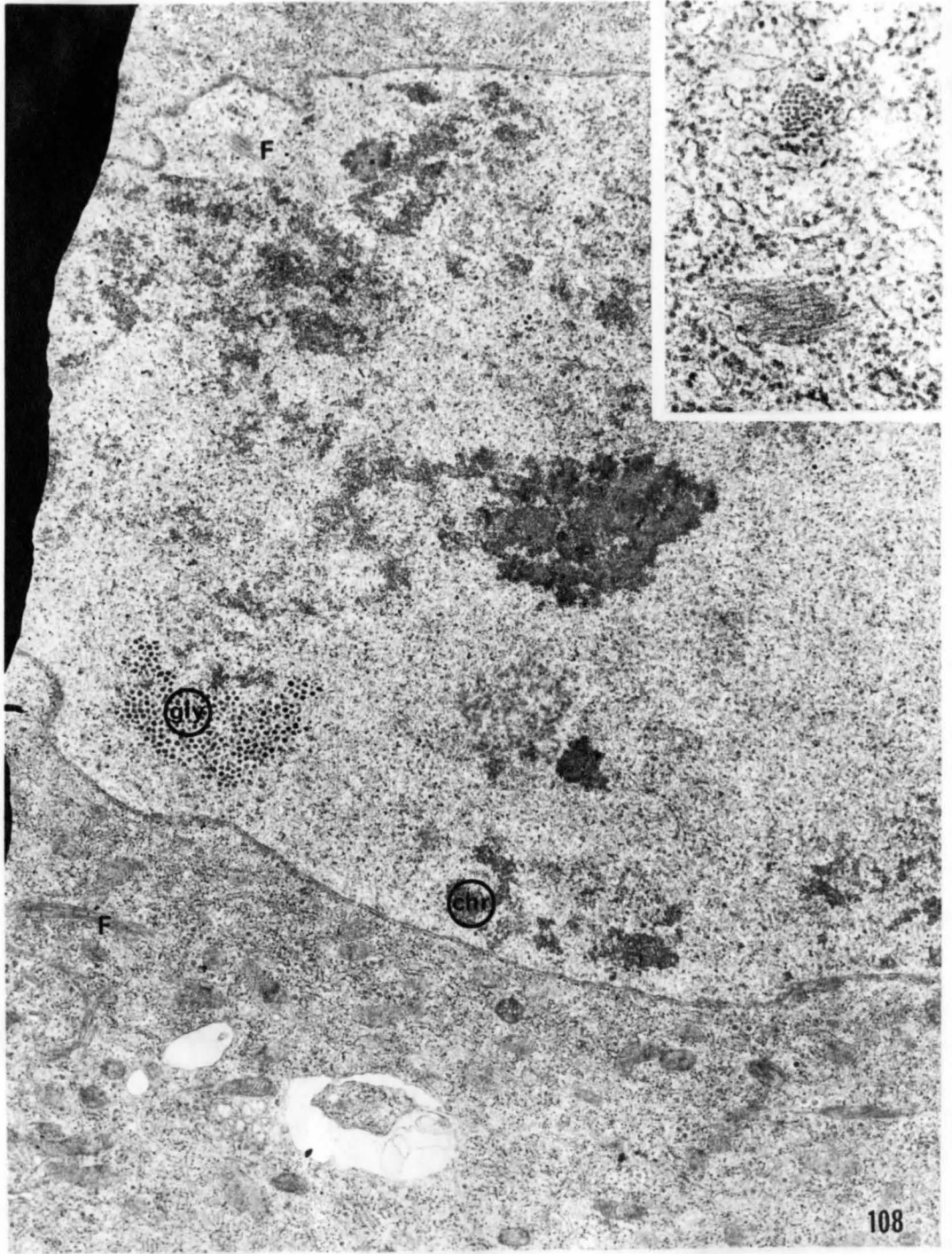


Figure 107. Uninfected midgut: lateral septate junctions between adjacent epithelial cells. The membranes are deeply infolded. 25,000 X. The inset shows detail of septate junctions (arrows). 40,000 X.



Figure 108. Uninfected midgut cell shown at the level of the nucleus. What appears to be glycogen (gly) is present in the nucleus. Bundles of fibers (F) are present in both nucleus and cytoplasm. nuc, nucleolus; chr, chromatin. 15,000 X.

The inset shows fiber bundles in longitudinal and cross-section. Individual fibers appear to be hollow. 75,000 X.



often contained, in addition to the usual components, accumulations of granules not unlike glycogen rosettes<sup>1</sup>, and bundles of fine filaments (Fig. 108). The latter were much more common in the cytoplasm. They were tubular, approximately 80 Å in diameter, and bore a striking resemblance to the filamentous component of elastin fibers (50). Basal cytoplasm (Fig. 109) differed in having extensive invaginations of the plasma membrane. In addition, this area of the cytoplasm contained a number of unusual organelles with dense crystalloids (Figs. 109 and 110). Some of these were attached to segments of RER (Fig. 110). Such organelles were never seen in the apical cytoplasm. They seemed remarkably similar in appearance to published micrographs of microbodies, or peroxisomes (36,105). What are probably regenerative cells were typically found at the periphery of the gut, but within the limiting basement membrane (Fig. 111). Such cells characteristically had an abundance of free ribosomes, but little RER.

### (c) Cytopolyhedrosis of the Midgut Epithelium

Infected midgut epithelium proved to be extremely delicate material to work with. The tissue had a tendency to fall apart on dissection. While cellular architecture was invariably destroyed in squash preparations, cytoplasmic inclusion bodies remained intact (Fig. 112). Two types of

---

<sup>1</sup> Nuclear glycogen has been observed in human hepatocytes (18).

Figure 109. Uninfected midgut: ultrastructure of the basal cytoplasm. The plasma membrane is deeply infolded. Many organelles having a dense crystalloid are present (arrows). m, mitochondrion; bm, basement membrane; M, muscle. 11,000 X.

The inset shows muscle A-band material cut transversely to show the arrangement of myosin (thick) and actin (thin) filaments. 55,000 X.

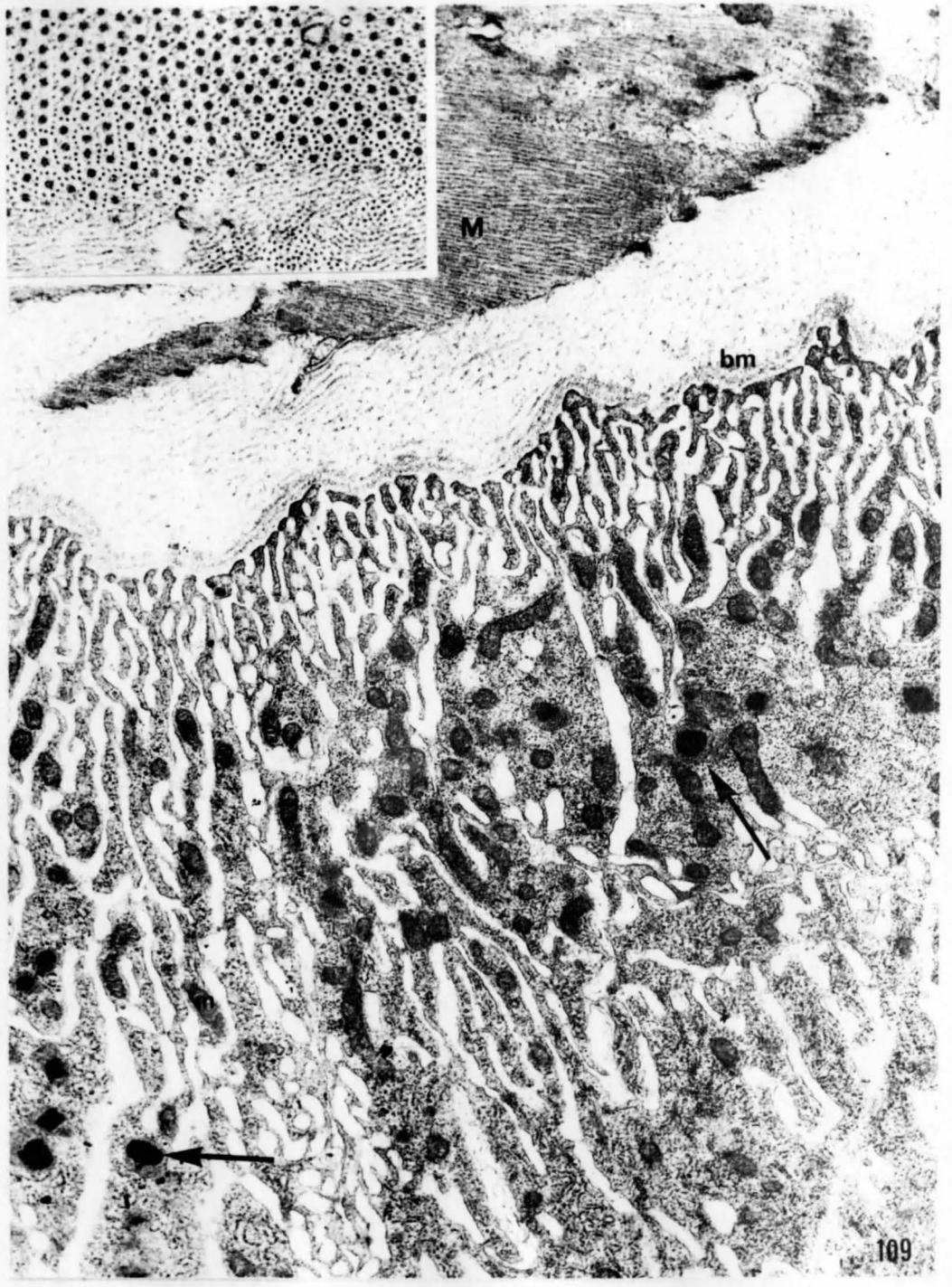


Figure 110. Uninfected midgut: microbodies in the basal cytoplasm. Note presence of a single limiting membrane and dense crystalloids (C). One microbody appears to be attached to the ER (arrows).  
45,000 X.

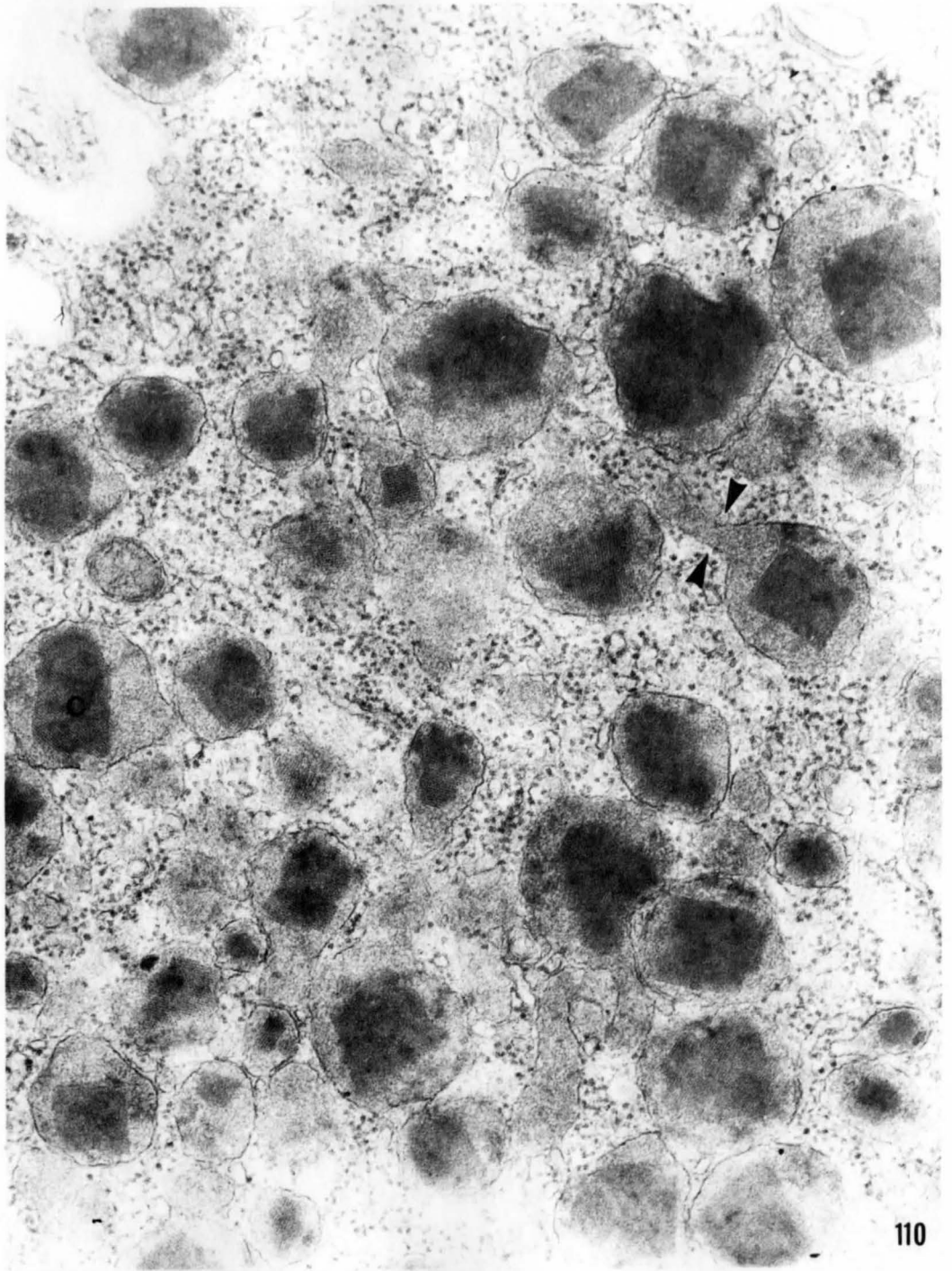


Figure 111. Regenerative cell at periphery of the gut. bm, basement membrane; M, muscle.  
21,000 X.



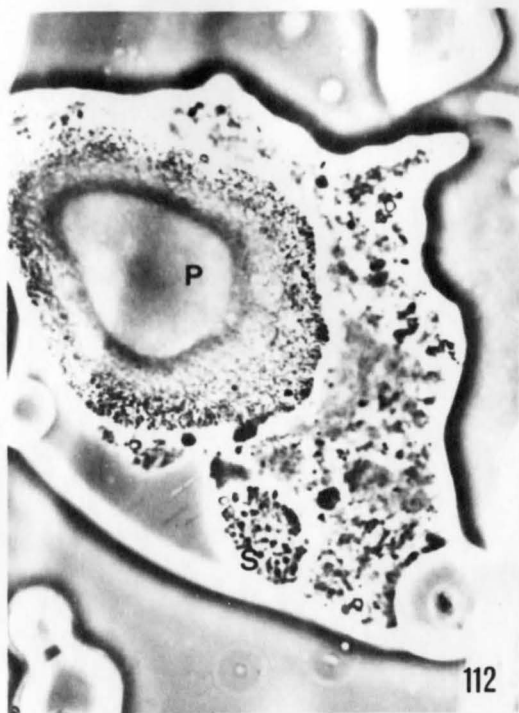
Figures 112 to 115. Infected midgut epithelial cells containing cytoplasmic inclusion bodies. P, large inclusion body corresponding to an accumulation of polyhedra. S, small inclusion body composed of virogenic stroma. Nuclei are not seen in these micrographs.

Fig. 112. Unfixed, squashed-cell preparation.  
6000 X.

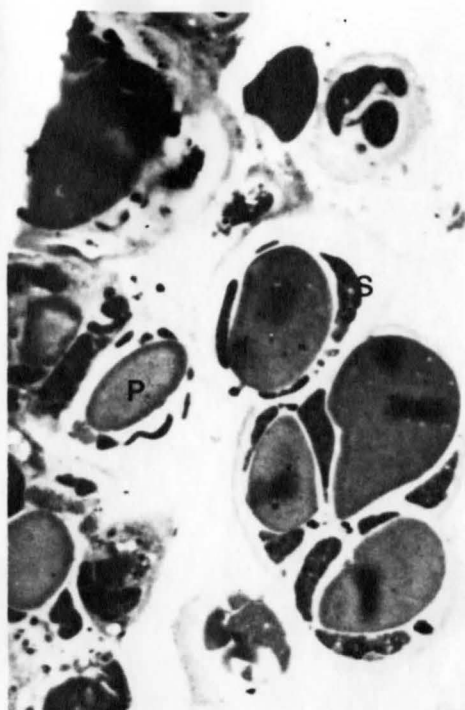
Fig. 113. Several infected cells with two kinds of cytoplasmic inclusion bodies.  
1700 X.

Fig. 114. Large inclusion bodies appear finely granular. Note masses of darkly-staining material within virogenic stromata. 7000 X.

Fig. 115. Remnants of virogenic stroma (arrows) are seen within larger inclusion bodies. 7000 X.



112



113



114



115

IB's could generally be recognized: larger ones with ovoid to circular outlines, which at higher magnification appeared finely granular; and smaller inclusions of more irregular outline, consisting of darkly staining masses within a lighter matrix (Figs. 112-115). What appeared to be remnants of the latter material were often detected within the large IB's (Fig. 115). The largest inclusions appeared to develop by means of a deposition of small granules within a preformed ovoid or circular mass of homogeneous material (Figs. 116 and 117).

In advanced stages of disease, the epithelium disintegrated, releasing inclusion bodies into the lumen of the gut (Fig. 118). At this time, extensive cytoplasmic vacuolization appeared (Figs. 116 and 118).

Nuclei of infected epithelial cells generally appeared to have a normal morphology; regenerative cells were also unaffected by the disease (Fig. 118). Inclusion bodies of the sort described above were never detected in the midguts of healthy larvae.

The two types of IB's detected by light microscopy were readily distinguished in the electron microscope (Figs. 119 to 121). It was immediately clear that the large inclusions corresponded to accumulations of polyhedra. IB's composed of polyhedra were invariably smooth in outline, though unbounded. At higher magnifications, polyhedra were seen to be composed of crystalline material within which virus

Figures 116 and 117. Formation of large cytoplasmic inclusion bodies.

Fig. 116. Granules are seen to be embedded in a preformed homogeneous matrix (arrow). 7000 X.

Fig. 117. Increased number of granules in matrix (arrow). 6000 X.

Figure 118. Breakdown of infected midgut epithelium. Note extensive cytoplasmic vacuolization. Two regenerative cells are indicated by arrows. N, nuclei. 2000 X.

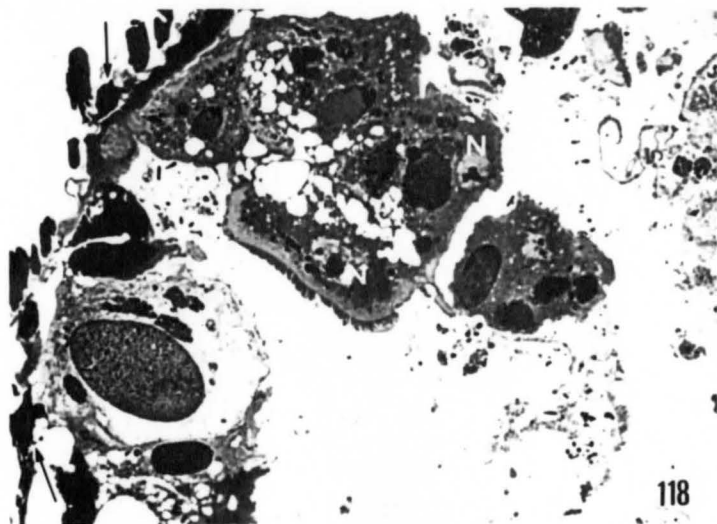
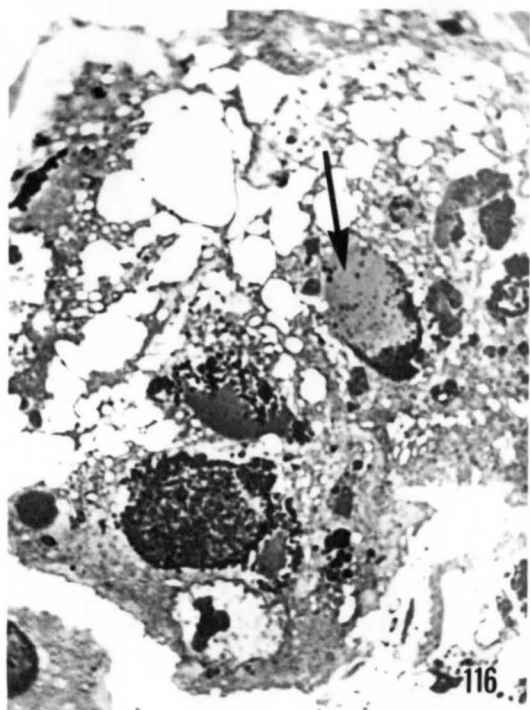


Figure 119. Low power electron micrograph distinguishing two kinds of cytoplasmic inclusion body. One, the larger, consists of a massive accumulation of small polyhedra (P). The other is a virogenic stroma (S) in which many small virus particles can be seen. 7000 X.

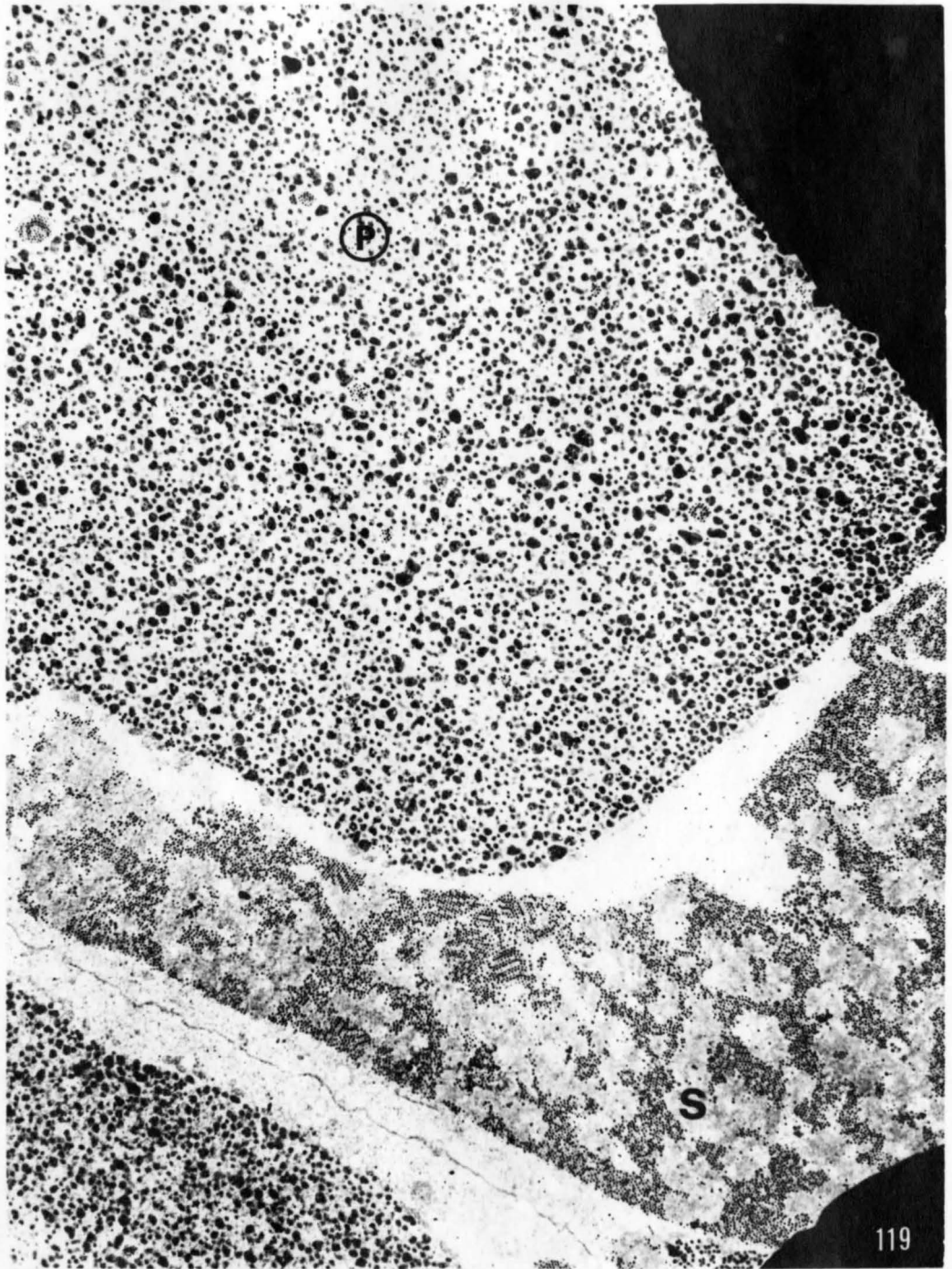
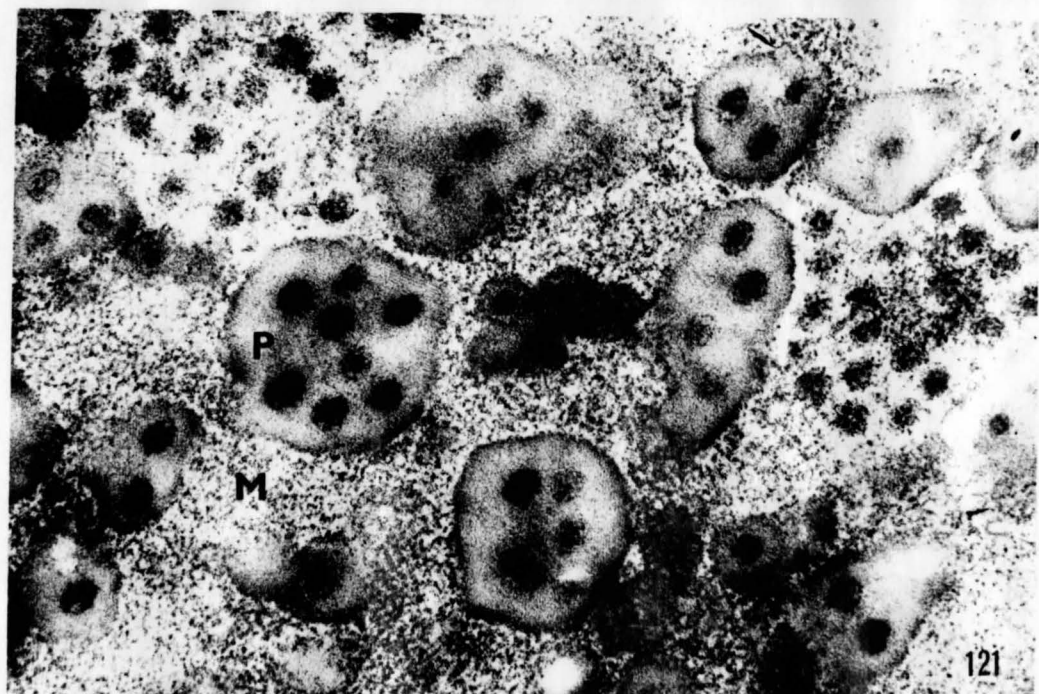
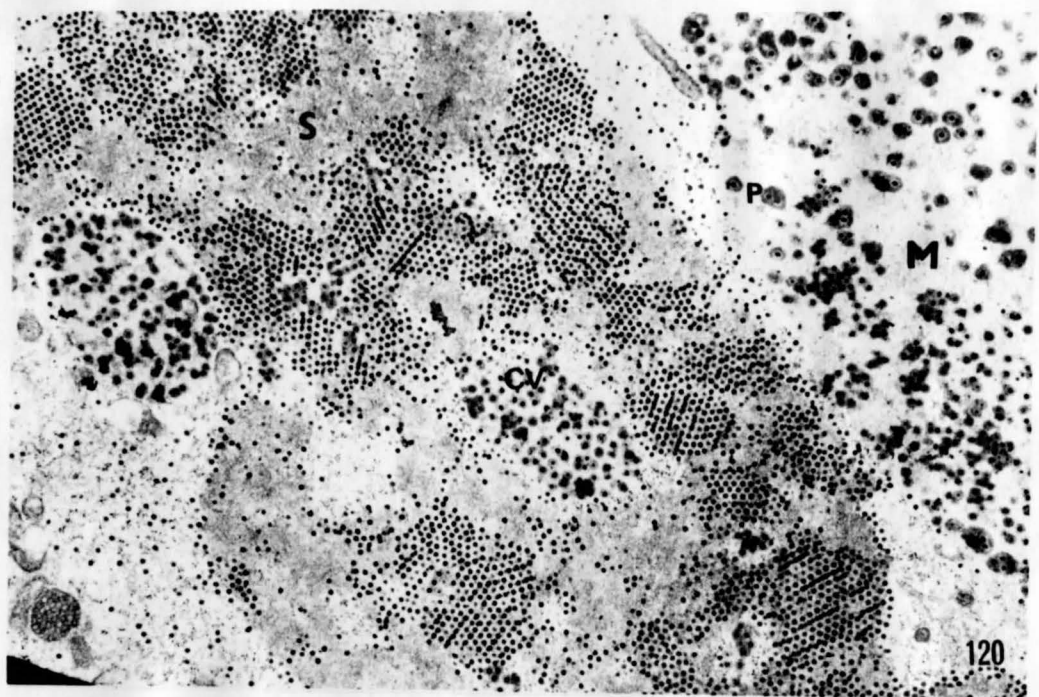


Figure 120. Developmental forms of virus. Free virus particles are largely in crystalline arrays. CV, "coated" virus particles; M, preformed occluding matrix; P, polyhedron; S, virogenic stroma. 16,500 X.

Figure 121. Polyhedra (P) composed of crystalline protein, and containing occluded virus particles. Polyhedra are embedded in an amorphous matrix (M). 75,000 X.

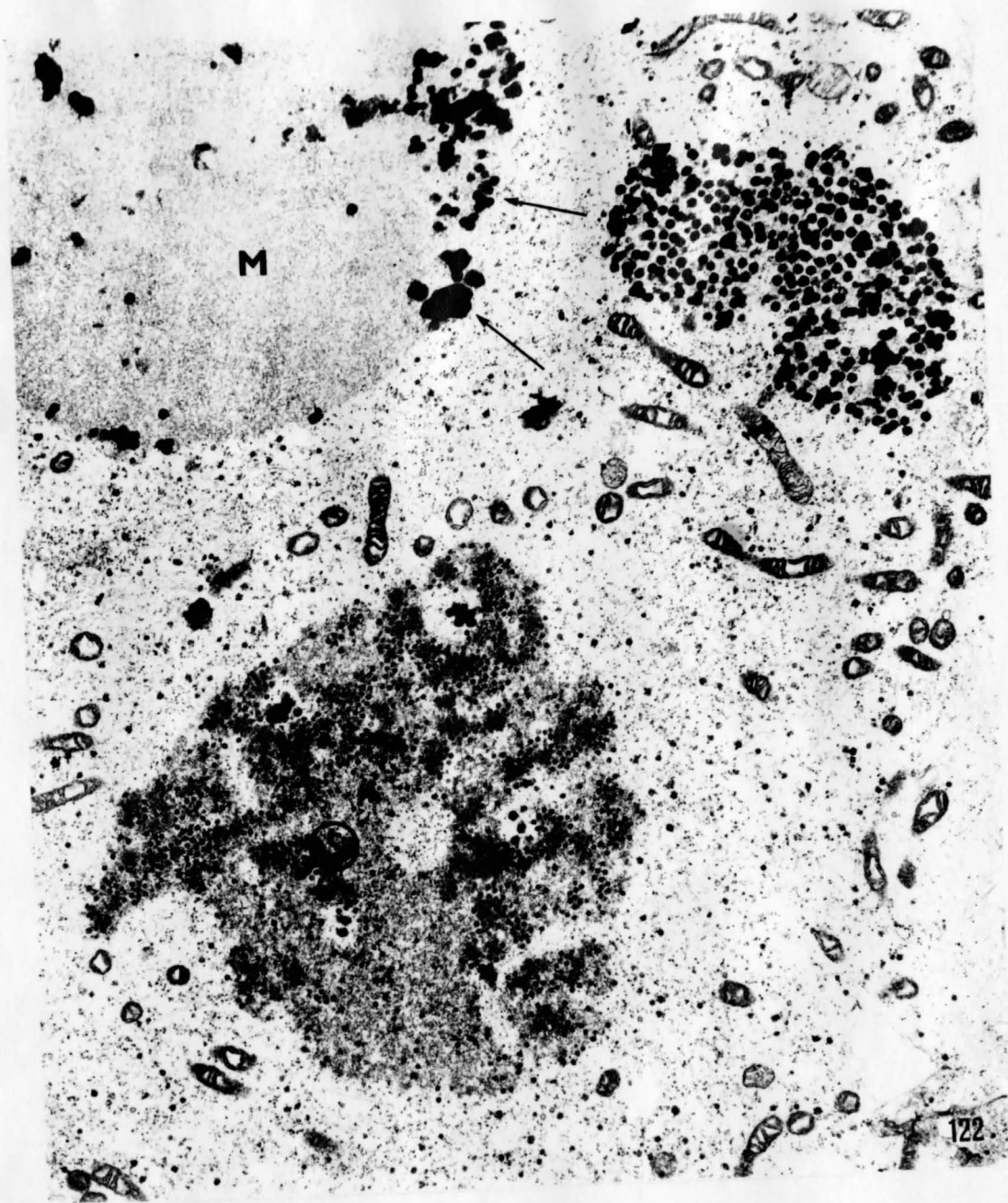


particles were occluded (Fig. 121). Polyhedra themselves appeared to be occluded within an amorphous matrix.

The smaller IB's corresponded to areas of viral multiplication. The darkly staining clumps seen within such IB's when examined by light microscopy probably represent masses of free virus particles; free virions were often oriented in microcrystalline array (Figs. 119 and 120). Virus particles which measured approximately 50-60  $\mu$  in diameter were interspersed with feltlike masses of material which was presumed, by association, to be virogenic. Ribosomes and other normal cytoplasmic constituents were never detected within such areas. In cells which appeared to be at an earlier stage of infection, virus particles were found to be associated primarily with a more electron-dense component of the virogenic stroma (Fig. 122).

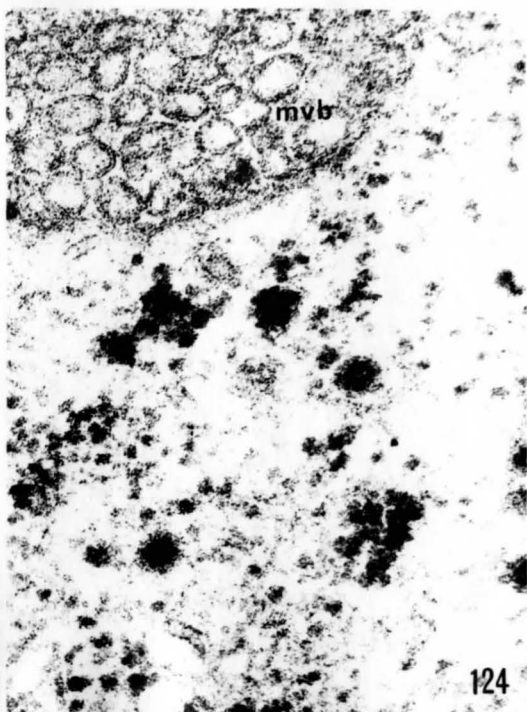
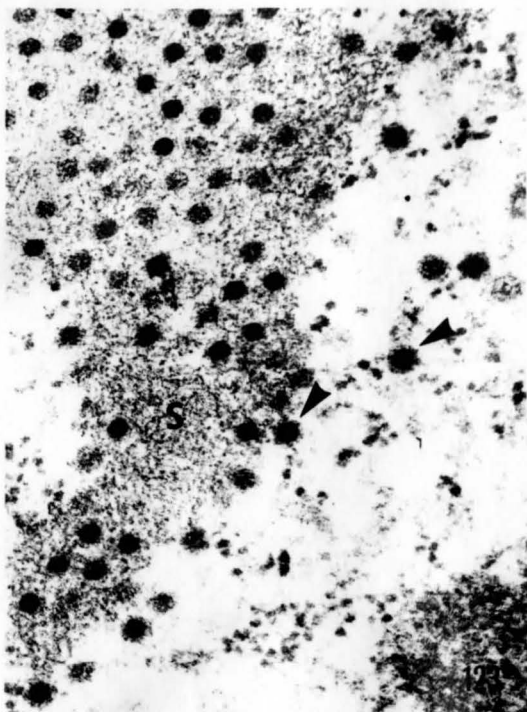
At higher magnifications, some viruses were surrounded by a lighter area of uniform width but rather indistinct morphology (Figs. 123 and 124). Extracellular particles either in situ or as detected in negatively-stained supernate of minced midgut bore 6 projections or spikes (Figs. 125 and 126). Such spikes varied in length from approximately 10-20  $\mu$ , they could only with difficulty be detected on some intracellular virions. Apparent thickenings of the capsid were evident at the bases of the projections; core material seemed to be attached to such plaques (Fig. 126). Particles of this nature were never detected in negatively-

Figure 122. Developmental forms of CPV. Presumably newly-formed virus particles are associated with a more electron-dense component of the stroma (S). Coated viruses and polyhedra (arrows) appear to become embedded in a circular matrix (M) of lighter electron density than stromal components. Cytoplasm is sparse and lacks RER. 20,000 X.

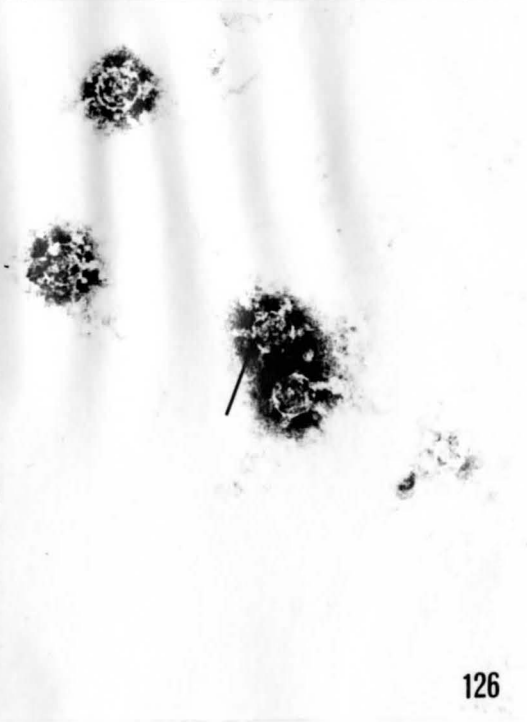
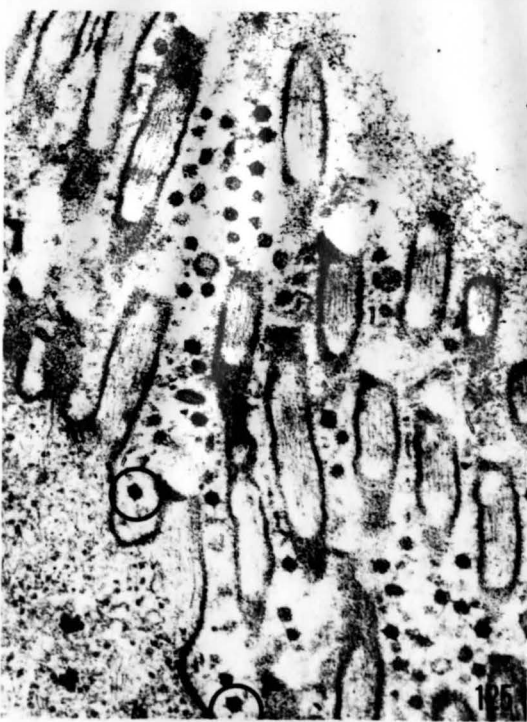


Figures 123 to 126. Ultrastructure of intra- and extra-cellular virions.

- Fig. 123. Viruses in vicinity of stroma (S) appear to have a thin layer around them (arrows). 75,000 X.
- Fig. 124. Same at higher magnification. mvb, multivesicular body. 100,000 X.
- Fig. 125. Extracellular sectioned particles with six projections or spikes (circled). 45,000 X.
- Fig. 126. Negatively-stained virus showing six projections. There seems to be a light "plaque" at the base of each spike. Core material appears to be attached (arrow) to shell of virion at bases of spikes. 125,000 X.



124



126

Figure 127. Developmental forms of CPV. Two free unoccluded virions are circled.  
S, virogenic stroma; CV, coated virions;  
P, polyhedra in occluding matrix;  
m, swollen mitochondrion. 60,000 X. .

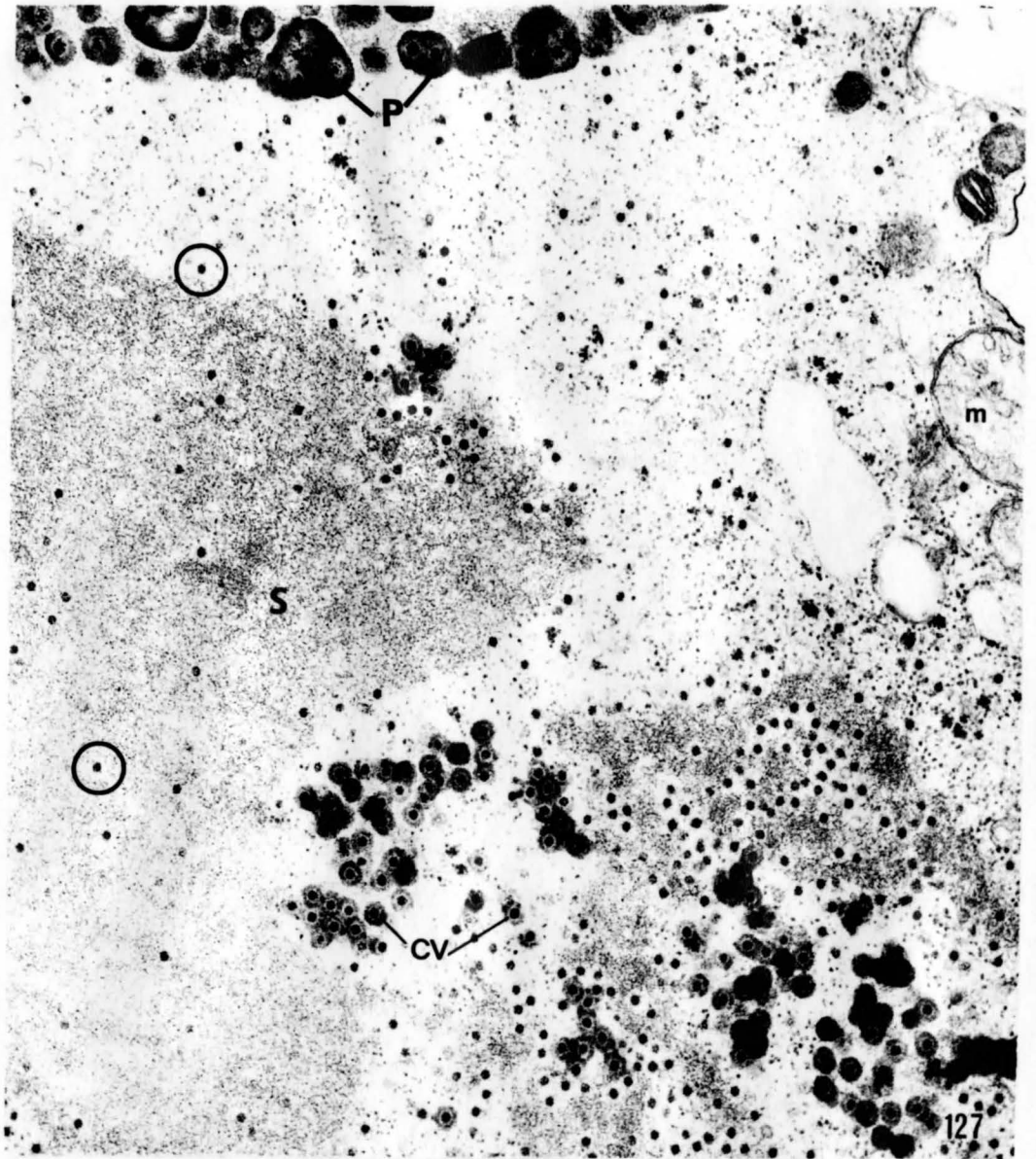
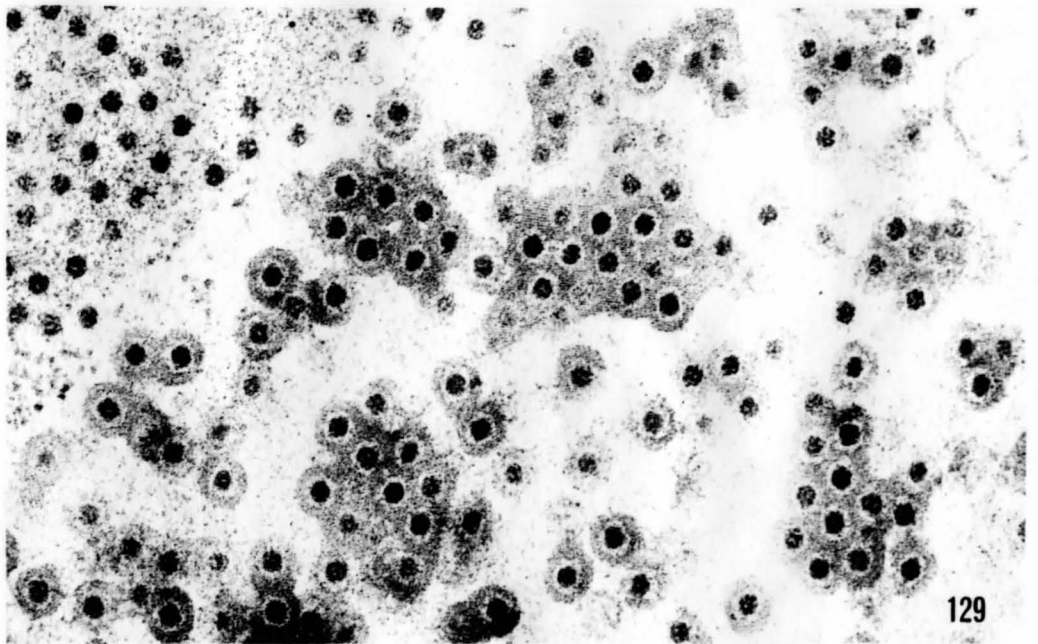
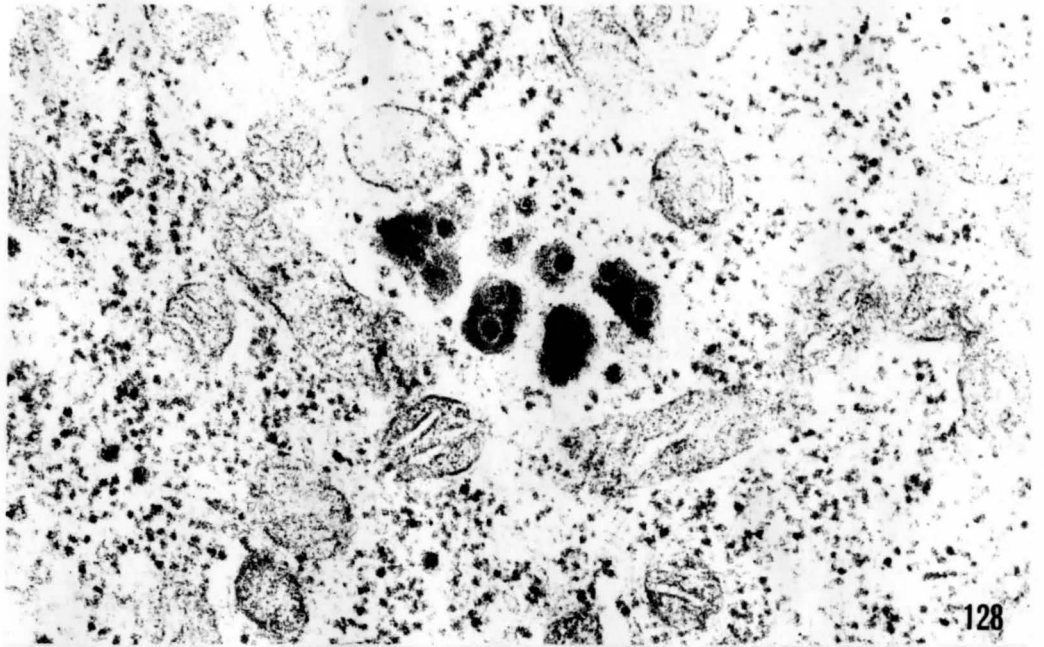


Figure 128. Free virions in the process of being occluded by polyhedral protein. 70,000 X.

Figure 129. Aggregations of coated virus particles, formed by fusion of coats of adjacent particles. The occluding protein of these aggregates appears uniformly crystalline. Note halos around occluded virions. 80,000 X.



stained preparations made from minced tissue derived from midguts of normal appearance. Virus particles were not detected in the hemolymph of infected or uninfected larvae.

Also present in, or, more commonly, at the periphery of virogenic stromata were small groups of virus particles which had acquired individual thick coats (Figs. 127 to 129). "Coated" virions measured approximately 110  $\mu$  in diameter. While such particles were occasionally seen as separate entities in sectioned material (Fig. 127), they were more commonly in direct contact with one or more other coated particles. In larger accumulations of adjacent coated particles, the limits of individual virus coats were not evident, so that the viruses seemed to become embedded in a homogeneous matrix; such matrices appeared crystalline (Fig. 129). The lattice structure of the crystals was not disturbed by the presence of occluded virus particles. Occluded virions were surrounded by a light halo of approximately the same width as the layer of material seen around some free virions (see Figs. 123 and 124).

Both coated virus particles, usually in aggregates, and polyhedra were themselves observed to become occluded in what appeared to be preformed circular or oval, amorphous, matrices (Figs. 120, 122 and 130)<sup>1</sup>. This material was always less electron-dense, and of a coarser structure, than components of virogenic stromata.

---

<sup>1</sup> The same material shown in Figure 130 is also represented in Figure 116 and can be found in Figure 118.

Polyhedra were of variable size and shape; larger ones rarely exceeded  $0.85 \mu$  in any dimension. Depending on the plane of sectioning, polyhedra appeared to consist of crystalline material (Figs. 121 and 131). Small islands of coated viruses and polyhedra were occasionally seen within virogenic stromata; more often, remnants of stroma could be detected within accumulations of polyhedra (Fig. 119).

Polyhedra and coated virus particles, en masse, and free virus particles were regularly seen in the lumen of infected midguts (Figs. 113, 118 and 125). Occasionally, free virus particles were seen inside microvilli; in such cases the ends of the microvilli appeared to enlarge and detach into the gut lumen as virus-containing vesicles (Fig. 132). Coated viruses and polyhedra apparently gained entrance to the lumen following breakdown of the midgut epithelium and disruption of cell membranes. Extracellular virus particles were never seen at the periphery of the gut, or in the investing muscularis.

Figure 130. Occlusion of polyhedra (P) in an oval matrix (M). S, virogenic stroma.

15,000 X.

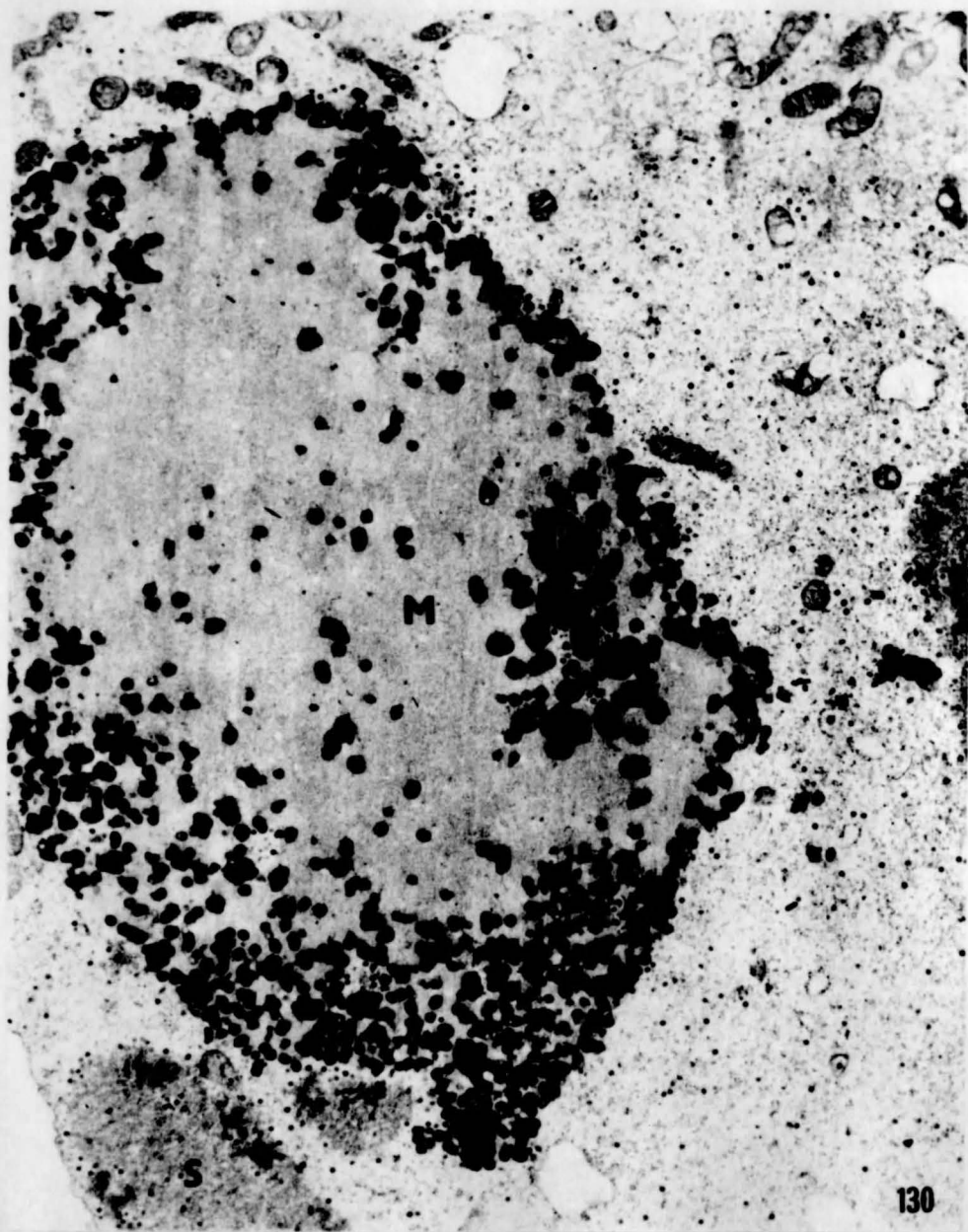


Figure 131. Polyhedra (P) and coated virus particles (CV) at edge of occluding matrix (M). The crystalline lattice of the polyhedral protein can be seen in both polyhedra and coated particles (arrows). V, free virus particle. 145,000 X.

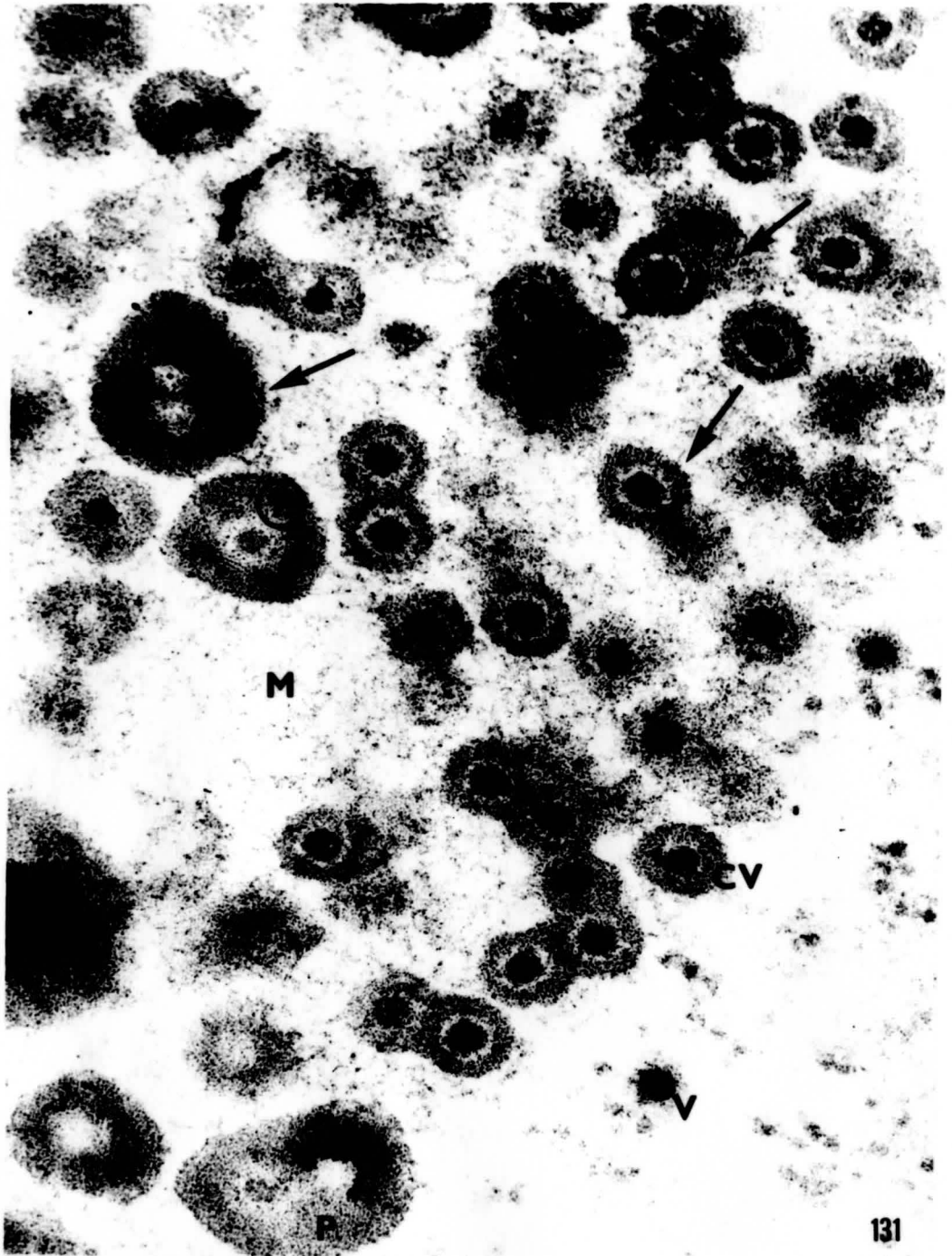
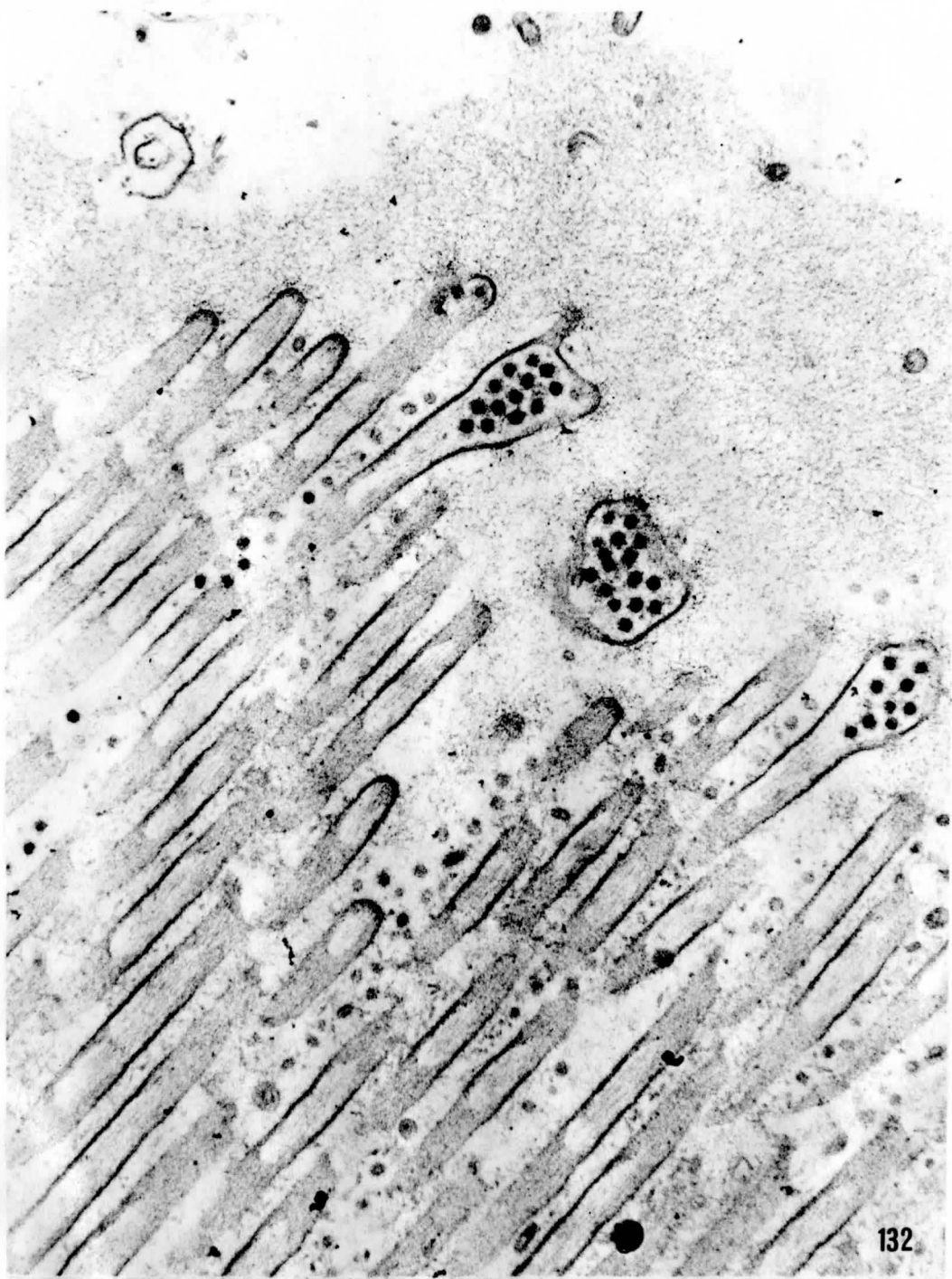


Figure 132. Virus particles in microvilli. Note that projections cannot be seen on intracellular particles. 55,000 X.



### III. Cytoplasmic Polyhedrosis of the Fat Body

A shipment of approximately 100 fourth-instar larvae collected from Lake Winnebago, Wisconsin, was received in March of 1969 from Dr. Hilsenhoff. Of these, one larva appeared to have symptoms of CpV-1 infection of the fat body (Figs. 133 and 134). This would have been unusual since that disease had never previously been found in larvae taken from Lake Winnebago. Symptoms of disease were, however, somewhat different from those seen with CpV-1 infections. Whereas fat body infected with CpV-1 appears mottled (Fig. 4), in this case the affected tissue was uniformly chalky-white. Upon dissection in tissue culture medium, CpV-1-infected tissue remains intact; this did not, but instead dissolved into innumerable, finely dispersed granules.

Epon-embedded material was examined by both phase-contrast and electron microscopy (Figs. 135 to 137). The cytoplasm of fat body cells was filled with large (up to 5  $\mu$ ) polyhedra, containing occluded virions. Fixation of this material was poor, presumably because of the late stage of the disease and consequent cellular fragility. For this reason, and for the lack of time, this disease has not been examined in detail; in addition, no other infected larvae have as yet been found.

Hemolymph from the infected larva was examined for the presence of virus particles by negative staining. Large

numbers of particles of homogeneous appearance and size (about 60  $\mu$ ) were seen. Particles in 2-, 3-, and 5-fold orientation could be distinguished (Figs. 138 to 140). Spikes of about 12  $\mu$  in length projected from the particle shells. No such particles were ever detected in the hemolymph of larvae lacking symptoms of this disease.

Figures 133 and 134. Larvae with cytopolyhedrosis  
infection of the fat body.

Fig. 133. 7 X.

Fig. 134. 15 X.

Figure 135 and 136. Large cytoplasmic polyhedra  
in fat body at late stage of  
infection.

Fig. 135. 2000 X.

Fig. 136. 7000 X.

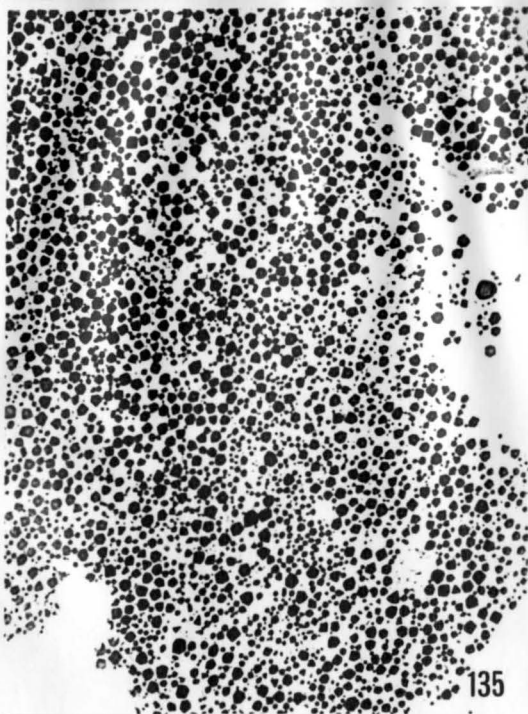


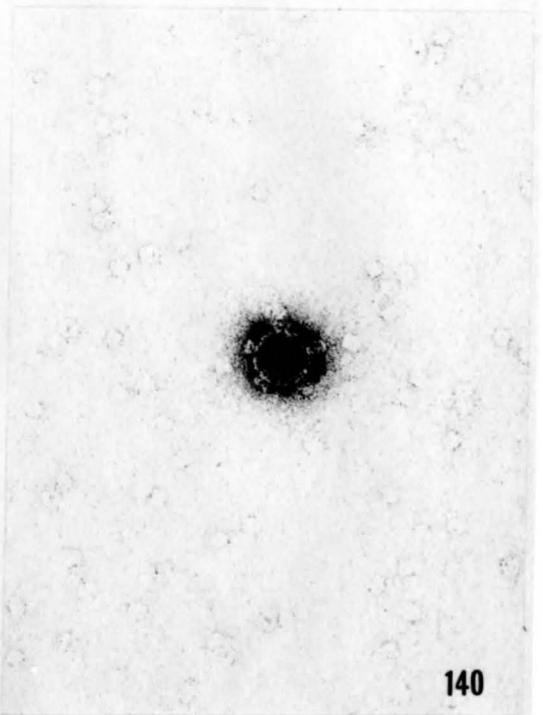
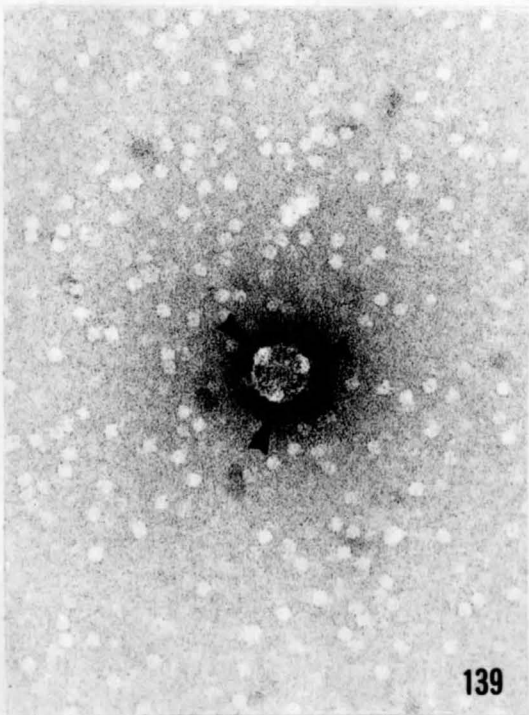
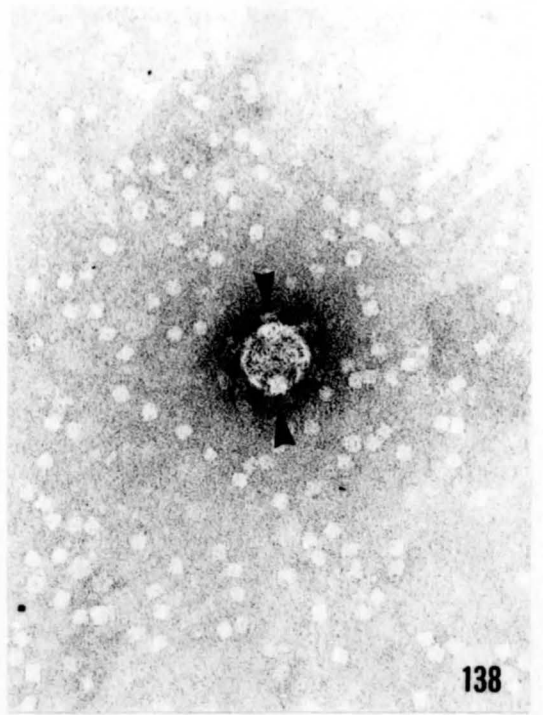
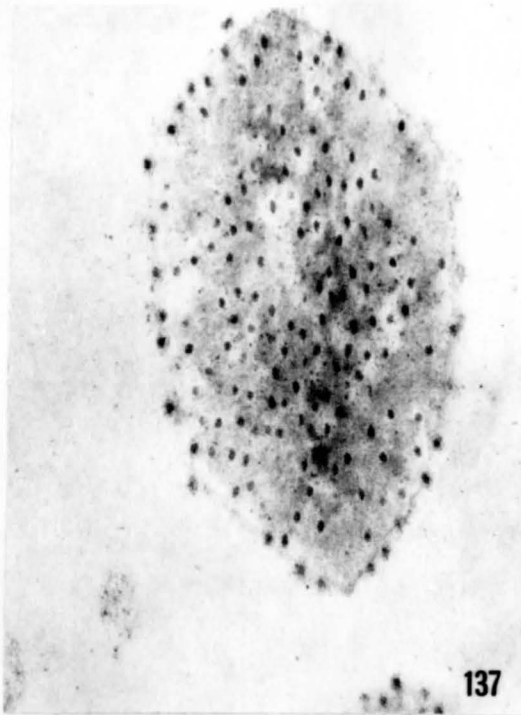
Figure 137. Polyhedron containing occluded virus particles. 50,000 X.

Figures 138 to 140. Negatively-stained virions viewed along different axes of symmetry. Electron-translucent areas (arrows) are probably projections or spikes at vertices of the capsid.

Fig. 138. Particle in 2-fold orientation.  
200,000 X.

Fig. 139. Particle in 3-fold orientation.  
165,000 X.

Fig. 140. Particle in 5-fold orientation.  
165,000 X.



## DISCUSSION

The question naturally arises as to whether the particles described in this thesis are, in fact, viruses. Only for the first type of particle discovered (CpV-1) was some evidence for infectivity obtained. While the numbers of larvae involved in experiments designed to show transmission of this virus were too small for meaningful interpretation, it is important to note that all injected larvae were from Lake Winnebago, in which the disease has never been found. It thus seems likely that the two cases of infection found in these larvae resulted from the multiplication of injected particles. Purified particles were found to contain only one kind of nucleic acid (DNA; this suggests that they were indeed virus particles. In addition, CpV-1 particles were similar in morphology to several previously-described viruses (Table 2).

The evidence for a viral etiology of two other diseases in C. plumosus larvae rests at present on morphological evidence only, since an insufficiency of material precluded transmission experiments. It is of interest, however, that only from tissues showing a clear histopathology could suspensions of particles having the morphology of typical insect cytoplasmic polyhedrosis

viruses (60) be obtained. Such particles were uniform in both size and shape, and showed icosahedral symmetry. Like the known cytoplasmic polyhedrosis viruses, they became occluded in crystalline polyhedra.

There seems, therefore, to be no compelling reason to avoid use of the word "virus" in the present contexts. Observations on three new virus diseases in C. plumosus are summarized and discussed separately below.

## I. Chironomus plumosus Virus-1 (CpV-1)

### 1. Characteristics of the Virion

A comparison of sectioned profiles of virus particles with models of the regular solids revealed that the CpV-1 capsid was in the shape of an icosahedron. The presumed derivation from an icosahedron of observed sectional profiles of virus particles is shown in Figure 141. Particles sectioned in 2-, 3- and 5-fold orientation were in the ratio of 30:17.8:12.2. Thus virus particles are not orientated in any specific manner in the cell cytoplasm.

The present study shows that sectional profiles of a large virus can be visualized in situ, and readily characterized as to symmetry. The same method would have been feasible with viruses such as TIV or SIV. A somewhat different approach was adopted by Wrigley (142) in a study of Sericesthis iridescent virus. In this case, intact negatively-stained virions were examined. The usual drawback

Figure 141. Diagrammatic representation of sectional profiles derived from an icosahedron. MED, median section; TAN, tangential sections.

A, icosahedron viewed along 2-fold axis of symmetry. The median profile is a non-regular hexagon, while the tangential is roughly diamond-shaped

$$X_1 = X_2$$

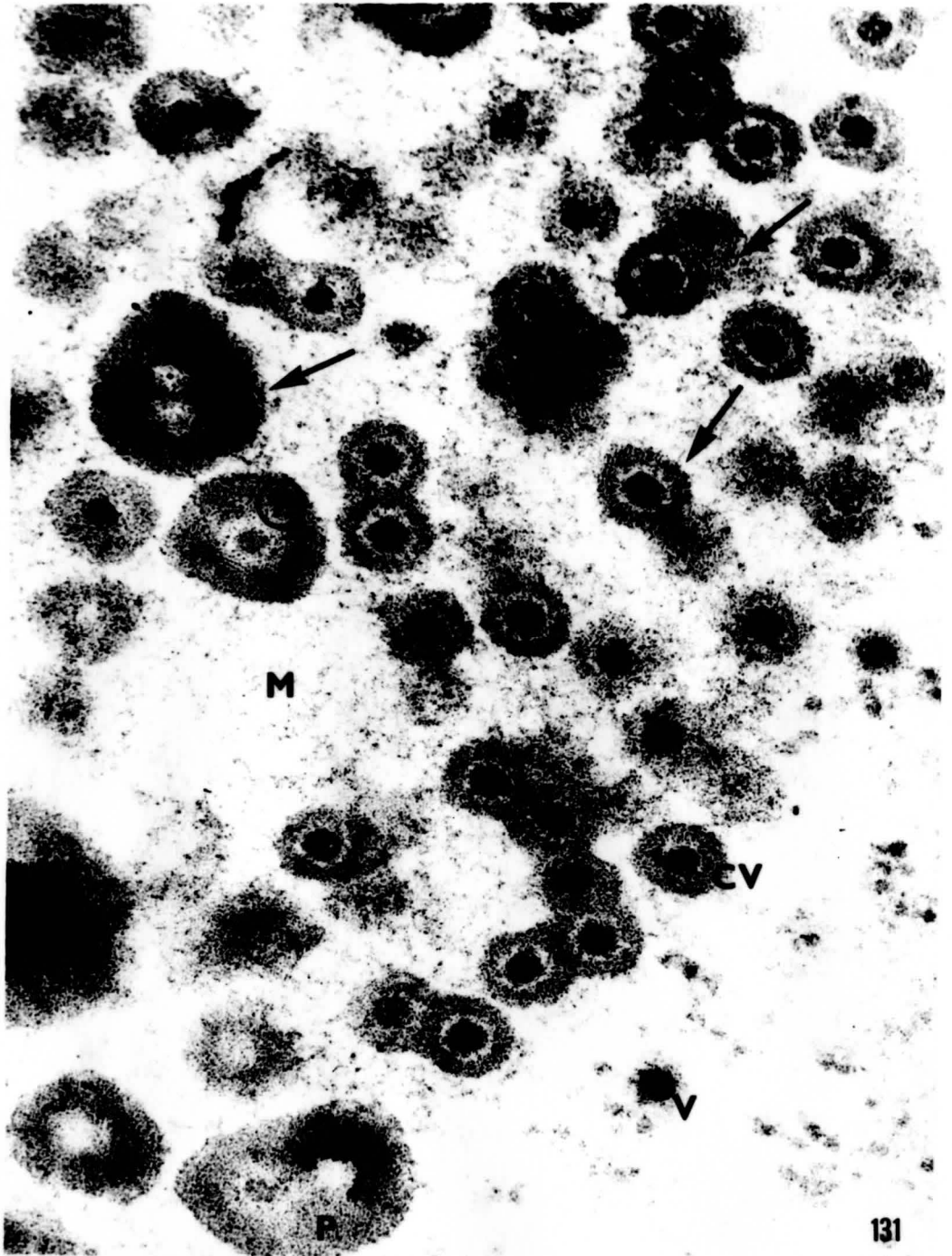
B, icosahedron viewed along 3-fold axis of symmetry. The median profile is a regular hexagon, while the tangential is a triangle<sup>1</sup>.

$$Y_1 = Y_2 = Y_3 = X_1$$

c, icosahedron viewed along 5-fold axis of symmetry. The median profile is more or less circular, while the tangential is a regular pentagon.

---

<sup>1</sup> Triangular virus profiles were rarely seen; they were too small to be recognized as such with any degree of accuracy.



of this method is that only two dimensions can be seen and can be interpreted in terms of 3-dimensional organization either with difficulty or not at all. The problem can be solved by shadowing in two directions as was done with Tipula iridescent virus (137), or by Wrigley's modification in which the images of virions seen are related to X-radiograms of icosahedral models built from Perspex. Such techniques, while ingenious, are also in a sense indirect.

Capsids treated with pronase were observed to collapse and undergo fragmentation. The most common and distinctive fragments were equilateral triangles of uniform size.

"Triangles" were never detected in either negatively-stained pronase solutions, or in untreated suspensions of purified CpV-1. They were most commonly seen in proximity to what clearly were disrupted capsids, and occasionally too in capsids that were apparently just starting to break up. Isolated intact virions bear a fringe of fine fibrils; so do the fragments. For these reasons, there can be little doubt as to their origin. Fragments appear to be composed of capsomeres in hexagonal array; capsomeres dispersed by mercaptoethanol clearly showed attached fibrils.

It was difficult to count the number of triangles per fragmented capsid, due to overlap and/or proximity to other capsids. As many as 18 were, however found, in association with what appeared to be a single disrupted capsid; this figure is close to the number of triangular

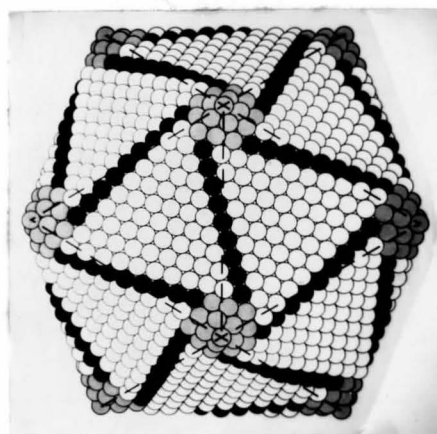
faces (twenty) of an icosahedron. Most of the triangles seen were complete, homogeneous in size, and without regular defects. The observations taken together suggest that the outer shell of the virus is an icosahedron, composed of 20 equilateral triangular assemblies, with no sharing of capsomeres along the edges of the triangles. This suggests that other capsomeres may exist along the icosahedral edges and certainly at the vertices in order to complete the capsid.

Fine fibrils definitely appear to be integral components of the virus particle. All fragments derived from CpV-1 capsids bore attached fibrils, so that it is likely that all capsomeres have them. The observation of very short fibrils associated with "CIV" capsomeres is difficult to explain. Wrigley (142) claims however to have seen a fringe of short fibrils around SIV particles.

Wrigley has recently published a brilliant analysis of the structure of Sericesthis iridescent virus (142). For the purpose of making more clear the following discussion, his structural model for SIV is reproduced below:

Figure 142

Diagram of proposed structure of Sericesthis iridescent virus capsid composed of 1562 capsomeres. Trisymmetrons ( $t = 55$ ) are shown in white, disymmetrons ( $d = 9$ ) in black, and pentasymmetrons ( $p = 16$ ) in grey. The geometrical edges of the icosahedron are marked by heavy broken lines. Note skew packing of triangular facets. Reproduced from Wrigley (142).



He was able to observe not only regular triangular but, in addition, regular pentagonal arrays of capsomeres, apparently resulting from spontaneous capsid disruption. The size and spacing of capsomeres in such arrays were similar to those observed on intact capsids which had been treated with a nasal decongestant, the active ingredient of which is unknown. In Wrigley's scheme, the triangles (his "trisymmetrons") represent the main component of the icosahedral face, and are packed in a skewed fashion; pentagonal fragments ("pentasymmetrons") represent groups of capsomeres at vertices of the capsid; and linear fragments ("disymmetrons") represent edge capsomeres, excluding those in the pentasymmetrons.

Wrigley counted 55 capsomeres per trisymmetron, and calculated a value of 16 per pentasymmetron. With these values together with an accurate edge length (vertex to vertex) for the icosahedron, and using a modified Goldberg<sup>1</sup> diagram, he was able to arrive at an approximate value of 1562 capsomeres for the capsid. Since disymmetrons were not clearly observed, this figure can be regarded only as a rather good approximation.

Fragments with definite pentagonal outlines were not seen in the present study of CpV-1 virus particles. However, amorphous fragments of more or less uniform size,

---

<sup>1</sup> A graphical method for showing all possible ways of arranging capsomeres in hexagonal array on an icosahedral surface with pentagonal packing at the vertices (43).

and approximately the right size to be expected for pentasymmetrons from Wrigley's model were often seen in association with triangles. This association was non-random and similar to that seen between tri- and pentasymmetrons in the proposed SIV structure. A few of the smaller fragments had well-defined angles, averaging 114 degrees; this is close to the value (108 degrees) expected for angles enclosed by a regular pentagon. Therefore, such fragments may well be analogous to Wrigley's pentasymmetrons. If so, judging from their size, they must have had at least 3 capsomeres per edge (or, at least 16 per fragment).

Trisymmetrons differed from those in SIV capsids in having 12, rather than 10, capsomeres per edge, or a total of 78. This disparity in number of capsomeres is reflected in both trisymmetron and capsid dimensions. CpV-1 is in both respects measurably larger than SIV. In the absence of accurate icosahedral edge length measurements, however, the Goldberg diagram cannot be used to estimate the total number of capsomeres in CpV-1.

Nevertheless, some probable estimates can be given, assuming that the edge length would be somewhat longer, and higher values for "t", "p", and "d"<sup>1</sup> obtained. Even discounting possible values for "p" and "d", there must be 20 x 78 or 1560 capsomeres in the trisymmetrons alone.

---

<sup>1</sup> Short for tri-, penta- and disymmetron.

Assuming that values for  $p$  and  $d$  are not larger, but equal to those in SIV capsids,  $N$  (total number of capsomeres) increases to  $1560 + (30 \times 9) + (12 \times 16)$ , or 2022. This value is not found in the Goldberg diagram. However, it is close to numbers predicted for capsids with trisymmetrons having 78 capsomeres, as follows:

- (a) 1752 ( $p = 16$ ;  $d = 0$ )
- (b) 1932 ( $p = 31$ ;  $d = 0$ )
- (c) 2082 ( $p = 16$ ;  $d = 11$ )
- (d) 2232 ( $p = 31$ ;  $d = 10$ ).

It is tempting, following the SIV model, to eliminate the  $d = 0$  categories. However, recognizable disymmetrons were in fact not seen so that any of the four values given (or others) might be correct. It is felt that neither Wrigley's work, nor the present study, either proves or disproves the existence of disymmetrons. An intensive study will be necessary to elucidate this point.

Suspensions of an insect iridescent virus, presumably Chilo iridescent virus, were also treated with pronase. Triangular assemblies of 55 capsomeres were seen, but not with the clarity that Wrigley illustrates in his micrographs of SIV. Nevertheless, these results are taken as confirmation in part of Wrigley's observations, and indicate a structural relationship between the iridescent viruses and CpV-1. This will be discussed further, in respect to classification of the virus.

Work of this nature has previously been attempted only with adenovirus, for which the number of capsomeres is in any case obvious. Adenovirus capsids can also be induced to break up into regular fragments (70, 100, 112), but these are not equilateral triangles.

## 2. Classification

The most commonly accepted scheme of virus classification, originally developed by Lwoff, Horne and Tournier (78), provides for the naming of virus families according to the following criteria: nature of the nucleic acid, type of symmetry of the nucleocapsid, presence or absence of an envelope, number of capsomeres (for cubical viruses), and diameter of the nucleocapsid (helical viruses). Only one insect virus, Tipula iridescent virus, is represented in this scheme at present. TIV became the type species of the genus Iridovirus, from which the family name, Iridoviridae, can be derived. The family was defined by the following characteristics: presence of DNA, cubical symmetry, absence of an envelope and a capsid containing 812 capsomeres. The latter value can now be regarded as erroneous (15,142); it was never based on good evidence in the first place.

An alternative scheme of viral classification, the cryptogram, has been proposed by Gibbs et al. (42), who proposed that, for purposes of classification, equal importance be attached to all characters of a virus, at least for the present. The cryptogram scheme was recently

vigorously refuted by Lwoff (80). Nevertheless, a few of the characters mentioned by Gibbs et al. should be added to the LHT system, and seem to be of some importance in respect to classification to the level of a virus family. These are: strandedness of the nucleic acid, site of replication in the (eucaryotic) cell, and in some cases at least (11), number of proteins. It would perhaps, be premature to erect as a viral taxon the arrangement of capsomeres in regular degradation products of capsids, where such products occur. Nevertheless, it seems reasonable to propose that where the capsids of different viruses can be disrupted into similar regular arrays of capsomeres, this be taken as further evidence of relatedness, other things being equal.

Regular triangular fragments (trissymmetrons) of the sort here described for CpV-1, and by Wrigley (142) for SIV, are unprecedented in the virological literature. Evidence for the existence of similar trissymmetrons in two other viruses, namely TIV and African swine fever virus (ASFV), can be extracted from a paper by Almeida et al. (3); this paper was apparently overlooked by Wrigley. The implication is that all these viruses are closely related, at least in a structural sense. If the synthesis and assembly of a particular type of structure is genetically determined, then one might expect that these viruses are also genetically related.

While the names Iridovirus and Iridoviridae have, outside of the papers of Lwoff et al. (78,79,80), never appeared in the literature, it now seems that the "Iridescent Virus Group" (15) may include viruses other than Tipula, Chilo, and Sericesthis iridescent viruses. To these can reasonably be added the mosquito iridescent viruses, of which there are several (29,30,134), and possibly viruses in Simulium ornatum (135) and Formica lugubris (119).

In recent years, several other icosahedral cytoplasmic DNA viruses have been discovered in animals other than insects (30,35,39,131,138); in most cases, the authors have noted a close resemblance in size and morphology between such viruses and the iridescent viruses (3,24,28,35,77,87,118,148). The known icosahedral cytoplasmic DNA viruses and their hosts are given in Table 2. Almeida et al. (3) have proposed on structural grounds that ASFV is closely related to TIV. A microvesicular element, similar to that described in this study, is also apparently involved in the development of ASFV (24,25). FV-1, a frog virus, shows aberrant capsids identical to those described for CpV-1 (35). It is suggested here that all the viruses listed above are related and can be included in the family Iridoviridae. Further studies are clearly required to establish any relationships that may exist. The proposal simply has the purpose of including in one group a number of previously unclassified viruses which have several features in common. It is implicit in the

Table 2  
The Icosahedral<sup>1</sup> Cytoplasmic DNA Viruses<sup>2</sup>

Virus <sup>3</sup>	Natural Host(s)	References
<u>Tipula iridescent virus (TIV)</u>	<u>Tipula paludosa</u> (Insect: Diptera)	143
<u>Sericesthis iridescent virus (SIV)</u>	<u>Sericesthis pruinosa</u> (Insect: Lepidoptera)	120
<u>Chilo iridescent virus (CIV)</u>	<u>Chilo suppressalis</u> (Insect: Lepidoptera)	41
Mosquito iridescent virus (MIV)	Several species (Insect: Diptera)	29,30,134
	<u>Simulium ornatum<sup>4</sup></u> (Insect: Diptera)	135
	<u>Chironomus plumosus</u> (Insect: Diptera)	present study
	<u>Formica lugubris<sup>4</sup></u> (Insect: Hymenoptera)	119
Frog viruses (FV-1)	<u>Rana pipiens</u> (Frog)	35
Frog viruses (FV-3)	<u>Rana pipiens</u> (Frog)	49
Lucke tumor viruses (LT-1 - LT-5)	<u>Rana pipiens</u> (Frog)	30
Tadpole edema virus	<u>Rana catesbeiana</u> (Frog)	138
African swine fever virus (ASFV)	(Swine)	24
Lymphocystis virus	<u>Lepomis macrochirus</u> (Fish)	87
Lymphocystis virus	<u>Stizostedion vitreum</u> (Fish)	131
	<u>Gehyra variegata</u> (Lizard)	118

<sup>1</sup> Icosahedral symmetry is in most cases unproven, but seems likely from published micrographs.

<sup>2</sup> All these viruses are quite large, ranging in size from 120-220 m $\mu$ .

<sup>3</sup> Some viruses have not as yet been given a common, or vernacular, name.

<sup>4</sup> Presence of DNA as yet unknown.

suggestions made here that "host species" should not be regarded as an important criterion in virus classification.

To be sure, differences between many of these viruses have been noted. For example, FV-3 DNA differs markedly in G + C content from iridescent virus DNA (15). It is, however, difficult to draw any conclusions from this since in DNA/RNA hybridization experiments, nucleic acids from CIV and TIV, which have very similar G + C contents (14), hybridized only minimally (16). Comparative serological studies have not been done. The main objection to inclusion of lymphocystis virus, ASFV, and the frog viruses in a single family with the iridescent insect viruses seems to be a matter of ether-sensitivity; the former are sensitive, while the latter are not (15). Nevertheless, detailed comparative data are not yet at hand, so that the question of relatedness of these viruses must remain open.

What exactly is the taxonomic position of CpV-1? In common with SIV, this virus contains DNA, has icosahedral symmetry with, probably, a similar arrangement of the triangular facets, and multiplies in the cytoplasm. For these reasons, it can undoubtedly be included in the Iridoviridae. It differs, however, from the type genus<sup>1</sup> in

---

<sup>1</sup> Iridovirus - TIV, the type species, is the same size as SIV, and thus can be presumed to have 55 capsomeres per trisymmetron, given that the capsids of the two viruses are similar, as is likely (142).

the following characteristics: 78 capsomeres per trisymmetron (hence a larger capsid), and the presence of long fibrils attached to the capsid. In addition, tissues infected with CpV-1 do not iridesce; iridescence is on the other hand typical of all tissues infected with Tipula, Chilo or Sericesthis iridescent viruses (41,120,143). The presence of fibrils on CpV-1 particles may prevent the formation of microcrystalline arrays of virus particles, known to be responsible for iridescence in Iridovirus-infected tissue (66,111). In the absence of serologic and/or biochemical data, it is not possible to further define, or deny, any possible relationships that may exist between these viruses. It is however safe to predict that CpV-1 will eventually be found to be more closely related to the known iridoviruses than is indicated here.

### 3. Intracellular Development

The use of  $H^3$ - $CH_3$ -thymidine as a marker for viral DNA synthesis made it possible to distinguish different types of cytoplasmic inclusion bodies, and relate them to stages in viral maturation. Since virus particles were visible at the level of the light microscope, they could also be used effectively as markers in such studies.

Observations on the intracytoplasmic development of the virus in both fat body and muscle can best be interpreted as follows: the first sign of infection is the appearance of a small homogeneous cytoplasmic matrix,

surrounded by a rim of RER and free ribosomes. Such matrices are Feulgen-positive and incorporate  $H^3-CH_3-$ thymidine, presumably into replicating viral DNA. Hence, these matrices can be regarded as virogenic. As they enlarge, internal fenestrations appear, presumably so as to provide a greater surface area for the elaboration and assembly of subviral components; fenestrations are lined primarily with polyribosomes. In infected fat body cytoplasm, distended vesicular profiles derived from the peripheral RER enter the virogenic matrix and apparently liberate their contents into it. Virus particles first appear on the outer edges of stromata, or in association with internal islands of polyribosomes.

Immature virus particles are in the form of angular, incomplete shells which, in the process of closure, acquire an amorphous content derived from the stroma. This material appears fibrillar in some complete capsids and, on the basis of similar observations (102), can be regarded as being at least in part viral DNA. The DNA or nucleoprotein, as the case may be, then apparently condenses to form electron-dense cores. Core "transformation", such as described here, is of course only hypothetical. While capsids undoubtedly enclose some material derived from the matrix in which they develop, the possibility of entry and progressive accumulation after closure of some components involved in core formation cannot be discounted.

Complete shells containing fibrillar material are probably analogous to the "empty" capsids of other authors (21,145). Such shells did indeed appear empty at low magnification. Since, however, they were most commonly seen in close association with virogenic stromata, they are best interpreted as developmental forms of virus. It is of interest to note that these capsids were always larger in diameter than those containing electron-dense cores. Capsids of adenovirus "ghosts" similarly are larger than those of complete virions (95). Clearly, the core in some manner influences at least the size, or "tightness", of the capsid in both cases.

It was impossible to detect any substructure in the capsids of sectioned particles. Incomplete, angular shells appeared to originate from a relatively thick microvesicular element which did not resemble membranes of the ER. Microvesicular elements have also been implicated by Xeros (145) in the development of TIV. Contra Xeros' interpretation, his microvesicles appear to have been derived from RER. Profiles of both rough and smooth ER were seen in CpV-1 stromata. It is felt that they are either involved in the synthesis of viral proteins and/or result from interpenetration of stroma into normal cytoplasmic materials. In any case, recognizable cytoplasmic unit membranes do not become incorporated into viral shells.

It is not known at which stage fibrils are attached to the capsids. It does appear, however, that most particles do not acquire fibrils while in intimate association with the virogenic stroma, but at some distance from it.

Certain cases of abnormal viral maturation are of some interest. In one case, it was apparent that core material was either not synthesized or else not assembled properly within developing capsids. While capsid material was clearly present, no complete or closed shells were formed (observations based on one cell only). This of course bears on the interesting problem of viral morphogenesis; it may be possible in this case that shell closure generally requires contained core material, perhaps in a particular configuration or having a certain composition. Whether in the case of CpV-1 the required material is DNA, maturation proteins, both, or a particular association of the two, is impossible to determine from the present electron microscopic observations. Kellenberger et al. (64) have claimed a morphogenetic function for a core material, presumably protein, in the T-even phages. It is clear that complete phage capsids containing no DNA can be constructed (65, 140).

Viral maturation in fat body, but not muscle, cells is accompanied by marked nuclear changes. These usually begin to appear when large numbers of virus particles are visible in inclusion bodies. Characteristic changes include the

appearance of what seems to be nuclear lipid, and "spotting" of the nucleolus. Nuclear lipid has been detected in the liver of rats suffering from acute amino acid deficiency (104) and ethionine (125) or thioacetamide (139) poisoning. It has also, however, been seen occasionally in normal liver cell nuclei (139). The significance of the phenomenon in the present context is uncertain, except that it appears to be part of a virus-induced pathology.

"Spotted" nucleoli appear to result from a condensation of the granular portion of the nucleolus; the phenomenon is common in virus infections (48,59,71). Nucleolar fragmentation follows, presumably as a result of dispersal of clumped granular material. Similar appearances have been noted in cells poisoned with actinomycin D (99,101,122), and are undoubtedly related to an interference with, or cessation of, ribosomal RNA synthesis (98,101,122). It is of interest in this regard that those cytoplasmic IB's which contained numerous mature virus particles did not incorporate  $H^3-CH_3$ -thymidine. Thus, taking into account the nucleolar anomalies seen in such cells, it seems likely that this type of IB is a site of assembly, rather than synthesis of viral components.

#### 4. Transmission and Ecology of CpV-1: Some Speculations

As has been stated, CpV-1 infects fat body and muscle. However, while these tissues are certainly present in all larval instars, they show signs of being infected only in the fourth. Mosquito larvae infected with mosquito

iridescent virus present an analogous situation: larvae fed virus in the early instars show signs of disease and die only in the fourth-instar (74). Clearly CpV-1 and MIV can be present in a "latent" form, though what exactly this form takes is unknown. It seems reasonable to suppose that whatever factors render early instar fat body immune to virus disease are similar in both insects.

Of interest with respect to the question of temporary latency followed by induction of virus multiplication is the data of Hilsenhoff (unpublished) concerning numbers of virus-infected larvae found at different times of the year in Lake Pepin, Wisconsin. Data for 1967-68 indicate a dramatic rise in infection rate during the winter months. Similar behaviour is shown by a herpes-type virus associated with Lucké renal adenocarcinomas of the frog, Rana pipiens (91,113). This virus replicates only during hibernation of the host; in laboratory experiments, prolonged maintenance of tumors at cold temperatures depresses host DNA synthesis, but stimulates that of the virus. Before cold treatment, virus particles cannot be detected in tumor nuclei. While the parallel is satisfying, factors other than temperature are undoubtedly involved. It may be, for example, that in the cases of CpV-1 and MIV, fat body has to reach a certain size and/or composition before it will support viral proliferation. In support of this are data (again unpublished) from the winter of 1968-69, in which almost no cases of viral infection were

found. Hilsenhoff (personal communication) reports that larvae had "unusually small fat bodies".

How is the virus spread? Limited laboratory feeding tests with all instars suggested only very low rates of transmission per os (i.e., <1%). In order to explain the epidemic proportions of the disease in some years (up to 40% infected), one must postulate a highly effective mode of transmission. As a working hypothesis, it is proposed that CpV-1 is transmitted transovarially, with occasional reinfection occurring primarily by cannibalism; this is more or less exactly how MIV is maintained in mosquito populations (75). Cannibalism of dead or moribund C. plumosus larvae was observed in the present study. There is as yet no evidence for this hypothesis. It is deemed useful by virtue of the fact that MIV is transmitted in this way, so that a mechanism obviously exists for the transovarial passage of at least one cytoplasmic icosahedral DNA virus. Further, the larvae of both mosquitoes and midges are aquatic; one might reasonably surmise that such an environment might predispose towards a particular mode of transmission for non-occluded viruses in both types of insect.

Transovarial passage of several plant viruses in leafhoppers has been reported (124). The viruses involved are not transmitted by sperm. Sylvester (124) points out that "the lack of sperm transmission may be related to the mechanism by which eggs are infected," and goes on to discuss

some possible mechanisms. It is possible, for example, that rice dwarf virus enters the egg on the membrane surface of a mycetomal microorganism of the green rice leafhopper vector (94). Such bacteria-like symbiotes are passed through the maternal line only, either by invasive forms or by fusion of maternal mycetocytes with the follicular epithelium (124); similar symbiotes are known in many species of insects (69,81,93,146). What are presumably symbiotes or commensals were also observed in the fat body of both infected and uninfected C. plumosus larvae. They were morphologically identical to members of the Rickettsiae, as characterized in micrographs published recently by several authors (4,81). The possibility of transmission of both MIV and CpV-1 in association with rickettsial microorganisms should be investigated.

CpV-1-infected larvae are known from only one lake, Pepin, in Wisconsin. According to Hilsenhoff (personal communication), it would be virtually impossible for adult flies to reach even the nearest lake, which is 20 miles away. Lake Pepin, however, is a widening of the Mississippi River, so that infected larvae might have been distributed far and wide by this system in the past. There is no reason to believe therefore, that the disease is limited only to Lake Pepin populations of insects. Indeed, a similar, if not identical, virus (CpV-1-Toronto) has been found in larvae collected from Lake Ontario.

## II. Cytopolyhedrosis of the Midgut in *C. plumosus*

As previously mentioned, this disease is thought to have a viral etiology on morphological grounds only. Negatively-stained particles from diseased tissue were indistinguishable from published micrographs of cytoplasmic polyhedrosis virus particles (34,60,90).

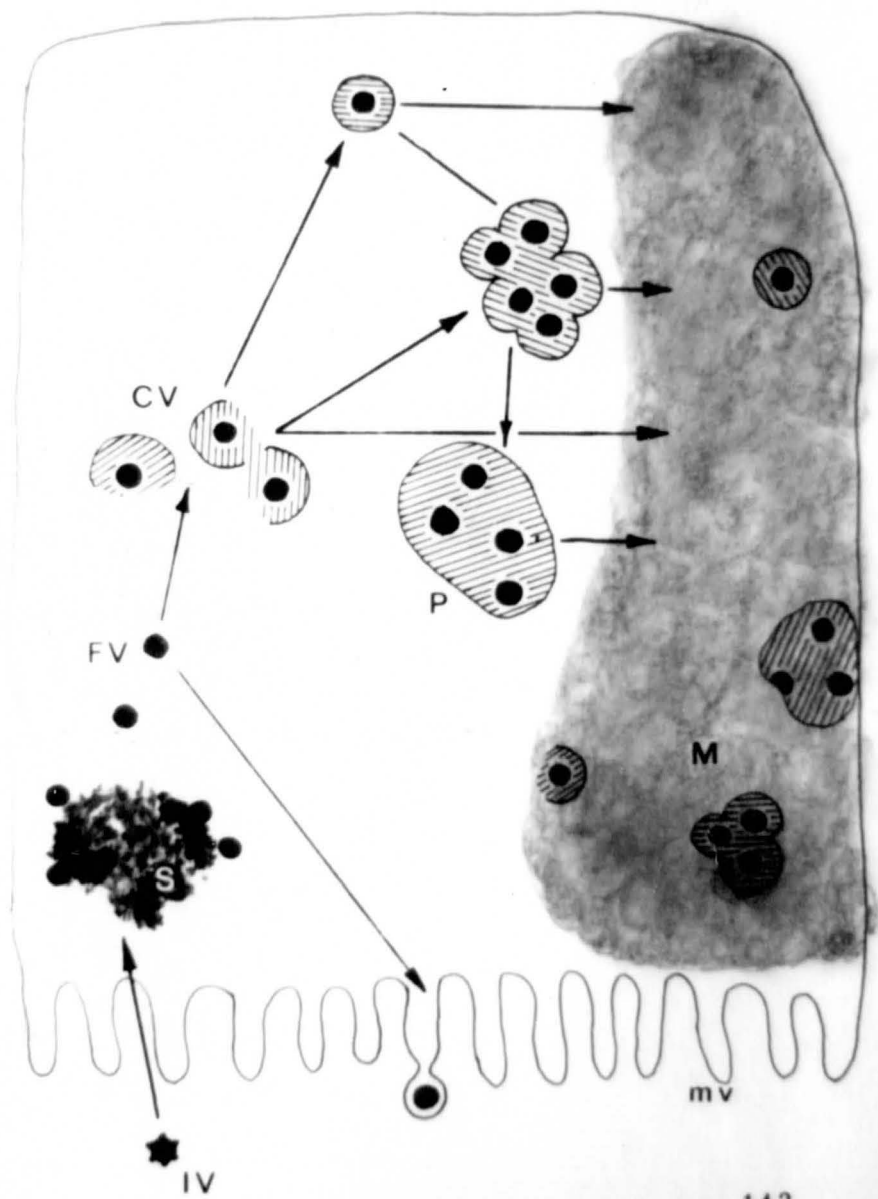
### 1. Intracytoplasmic Development of the Virion

The intracellular development of a typical insect cytoplasmic polyhedrosis virus can be summarized as follows: virions are produced from a virogenic stroma and are then, in some unknown fashion, occluded by masses of crystalline protein. These crystals, called polyhedra, enlarge to a final diameter of from 2-5  $\mu$ , and may individually contain as many as 10,000 occluded virus particles (110,111,8).

The present observations suggest a second mode of development for a cytoplasmic polyhedrosis virus, in which two cycles of occlusion occur. Briefly, the sequence of events, shown diagrammatically in Figure 143 is as follows: free virions are individually invested, or occluded within, a uniform layer of crystalline polyhedral protein to become "coated" viruses. These aggregate to form polyhedra. Both polyhedra and coated virions are then occluded in large amorphous matrices.

Coated viruses have not been previously described in insect cytopolyhedroses. They are of particular interest inasmuch as they would seem to form part of a logical sequence

Figure 143. Diagrammatic representation of CPV maturation in the midgut cytoplasm of C. plumosus. Although the early stages of infection are unknown in this case, what is known about other cytopolyhedroses (110,111) probably applies. Polyhedra originally gain entrance to the lumen of the gut per os, and infective virions (IV) are liberated. Two cycles of occlusion occur within the infected cell. Details are given in the text. S, virogenic stroma; FV, free virion, CV, coated virion; P, polyhedron; M, matrix in which polyhedra and coated virions are occluded; mv, microvillus.



of events in viral development and, possibly, phylogeny: they represent an intermediate stage between the free (unoccluded) virus and the polyhedron of the typical cytopolyhedrosis. It is not unreasonable to suggest that a disease resulting only in the production of a coated form of cytoplasmic polyhedrosis virus (CPV) might exist in nature. If so, such an ancestral form could conceivably have given rise to the typical CPV by way of a virus such as is seen in C. plumosus. Possible evolutionary pathways among the cytoplasmic polyhedrosis viruses are outlined in Figure 144.

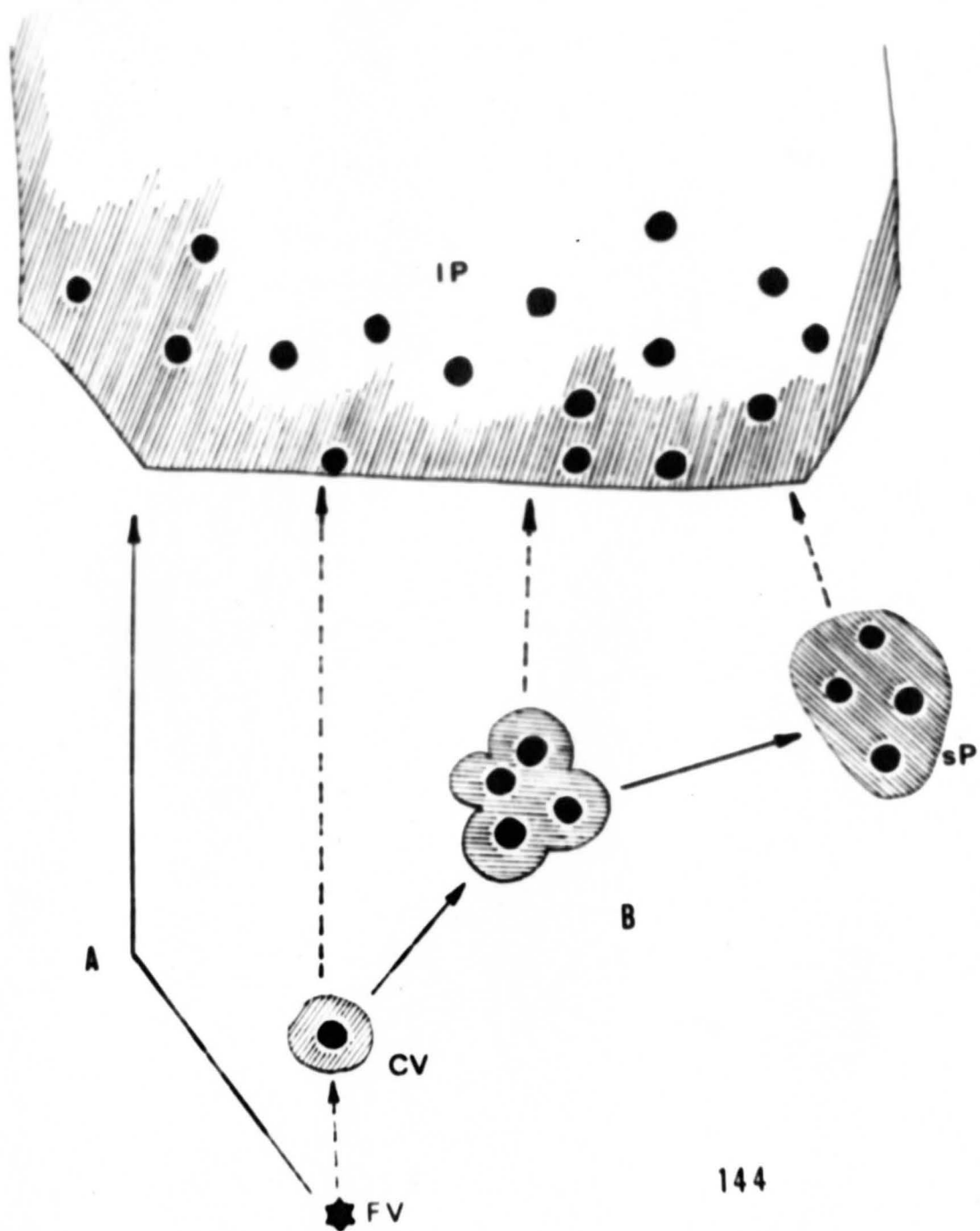
It is of interest to point out that a similar evolutionary sequence has been proposed for the nuclear polyhedrosis viruses<sup>1</sup> which, like the typical cytoplasmic polyhedrosis viruses, lack intermediate developmental forms of the "coated" variety. Arnott and Smith (7) propose that nuclear polyhedrosis viruses may have evolved from granulosis viruses<sup>2</sup> by way of abnormal multiparticulate forms of the latter. This would account for the usual form of nuclear polyhedrosis in which bundles of virus particles are occluded (1,22,52). The same authors have also described an aberrant multicapsular form of GV; although the possibility

---

<sup>1</sup> Nuclear polyhedrosis viruses contain DNA, have helical symmetry, and are enveloped, either singly or in bundles. Many virions in either case are occluded within a single polyhedron.

<sup>2</sup> Granulosis viruses also contain DNA and have helical symmetry. Usually, each virus has an envelope, and is occluded singly in "capsules" of crystalline polyhedral protein.

Figure 144. Diagrammatic representation of possible evolutionary pathways among the cytoplasmic polyhedrosis viruses. Solid arrows indicate events that have been observed to occur during the maturation of known viruses. Broken arrows represent pathways which may exist, or may have had some evolutionary significance. FV, free infective virion; CV, ancestral coated virus; A, typical CPV maturation pathway; B, maturation pathway of CPV in C. plumosus; lP, large (typical) polyhedron; sP, small polyhedron.

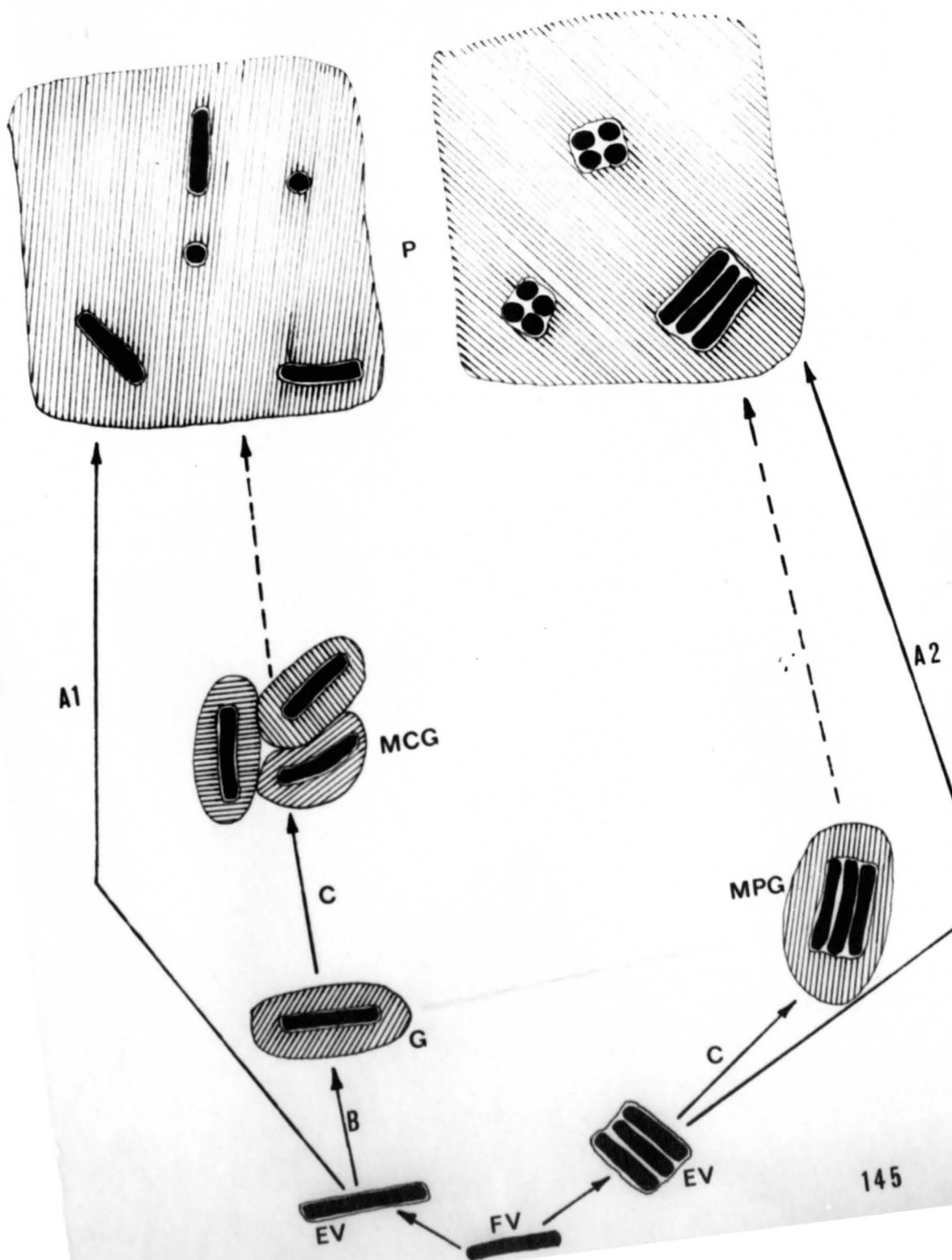


was not mentioned, such a form presumably could have given rise to those nuclear polyhedroses in which virions are occluded singly (38,51,52,76), rather than in bundles. The granulosus and nuclear polyhedrosis viruses appear to be genetically related (17); thus, while the schemes outlined above are highly speculative, they are nevertheless within the realm of possibility. Suggested evolutionary pathways among the granulosus and nuclear polyhedrosis viruses are indicated in Figure 145.

Clearly, the "coated" form of CPV is the structural analogue of the capsules seen in granulosus infections. However, before any evolutionary analogies can be proposed, it will be necessary to show some genetic similarity between the CPV of C. plumosus and other CPV's.

Remaining to be elucidated is the process of occlusion itself. Both round and cubic strains of polyhedra and capsules are known, and seen to breed true (7,8,114). It is likely, therefore, that the form of a capsule of polyhedron is a viral function (7,8,9,114). Size, on the hand, may in many cases be regulated in part by factors attributable to the host cell environment (10,84). What is not clear is how possible control systems might operate. Occlusion of virus particles must somehow involve a specific recognition between the virus and the occluding protein, since components other than viruses are not occluded (8). This site seems to be located on the envelope in the case of GV's

Figure 145. Diagrammatic representation of possible evolutionary pathways among the granulosis and nuclear polyhedrosis viruses. Arrows as in Fig. 144. A1, maturation pathway for NPV in which single virions are enveloped and occluded; A2, maturation pathway for NPV in which bundles of virions are enveloped and occluded; B, normal maturation pathway of granulosis virus; C, abnormal granulosis maturation pathways; FV, unenveloped virion; EV, enveloped virion(s); P, polyhedron; G, encapsulated granulosis virus; MCG, abnormal multicapsular form of GV; MPG, abnormal multiparticulate form of GV.



and the NPV's. Either the capsid, or an as yet unidentified layer, must act as a condensation site for cytoplasmic polyhedral protein; the layer seen in the present study around free virions, and represented by a halo around occluded virions, may represent such a site.

In many granulosis and polyhedrosis infections, relatively precise control over crystal size is often exhibited. The reason for this is puzzling. As Arnott and Smith (7) point out, cessation of crystal growth is unlikely to be due to a lack of polyhedral protein. These authors suggest that an interposing barrier on the crystal surface may be responsible. An electron-dense layer is indeed seen around capsules and polyhedra in some micrographs (1,6,8,52,116,122) but may represent only a differential deposition of osmium during fixation (8). Such a layer was rarely seen around polyhedra in C. plumosus, and never around coated particles. It is of interest to note here that the size of the coated particle seems to be more precisely regulated than that of polyhedra or capsules in general.

A double occlusion, first of virions and then of polyhedra, occurs during the development of cytopolyhedrosis in C. plumosus. Nothing analogous to the second occlusion event is known in the literature concerning insect viruses. A similar phenomenon is however, seen in ectromelia and cowpox infections, in which mature virions become occluded in a preformed

non-crystalline amorphous matrix, the Marchal body (63)<sup>1</sup>. Several strains of ectromelia and cowpox viruses make such inclusion bodies; in not every strain, however, are the virions occluded in them. The authors concluded that there was an occlusion factor,  $V$ ;  $V^+$  was found to be dominant over  $V^-$ . The formation of Marchal bodies is thought to be a viral function, since the protein(s) in it differ antigenically from those of the host (62). It is tempting to speculate that the matrices in which polyhedra become occluded are similar to the Marchal bodies. Both types of matrices are indeed similar in morphology, and both are apparently involved only in processes of occlusion; apparently neither is involved in any way in viral replication.

## 2. Transmission and Ecology

Cytoplasmic polyhedroses are very common among the Lepidopterous insects (110,111), in populations of which the viruses may under some conditions be latent (9, but see 20). However, several reports (47,108) of activation of supposedly latent viruses can be discounted because of possible contamination of the "inducer" (e.g. NPV) by CPV's (1,76).

It seems likely that the predominant mode of transmission of polyhedroses among the Lepidoptera is by contamination of egg and leaf surfaces with polyhedra (26,111). Transovarial

---

<sup>1</sup> It is of interest to note that the insect pox viruses have a pattern of development much like that of the typical insect polyhedrosis, in which virions are occluded in crystalline polyhedra (44). Marchal bodies are not seen.

transmission of virus has been suggested to occur (20), but no direct evidence substantiates this proposal. Recent reports suggest that mechanical transmission by insect parasites may also be an extremely important factor in the spread of insect virus diseases (20,68,116).

Transmission would be expected to be more effective if larvae were able to excrete polyhedra over a long period of time. This is more likely to occur with debilitating, rather than lethal, diseases. Cytoplasmic polyhedrosis viruses, while highly infective, are in fact generally lethal for only a minority of larvae, unless polyhedra are ingested during the very early instars (26,117,130). It is possible that regenerative cells, which are apparently immune to both NPV (19,115) and CPV (26,83) infections, may be in part responsible for the relatively low lethality associated with cytopolyhedroses. Stairs (116) suggests that "since these embryonic cells are essential to the survival of the insect, and, since the survival of the insect may be essential to the survival of the virus, the resistance of the embryonic cells probably has arisen to ensure the survival of both ...."

The present study constitutes the first well-documented case of a cytopolyhedrosis in the Diptera. The disease has been found to date in only a small number of larvae. All were heavily infected, and it seems likely that most larvae with the disease would not survive to the fourth instar. Indeed all infected larvae except one were

in the third instar. No information can be given concerning the mode of transmission of the virus. A possible advantage (for the virus) to be derived from the occlusion of polyhedra, however, may be that they thereby become associated with structures large enough ( $>12\mu$ ; 132) to be retained on the larval filter-feeding apparatus.

### 3. Classification

The cytoplasmic polyhedrosis viruses have not been classified, even in the LHT system (78). It is recognized however, that they do form a distinct and unique group or family of viruses, based on observations that they have double-stranded RNA (73,89), exhibit icosahedral symmetry (60), and are without exception occluded (110). The number of capsomeres is uncertain.

### III. Cytopolyhedrosis of the Fat Body in *C. plumosus*

This disease was found in a single fourth-instar larva; for reasons previously given, it cannot be discussed in any detail. It is noteworthy, however, that this is the first known instance of a cytopolyhedrosis in an organ other than the gut in any insect. It had previously seemed likely that other organs were immune, even to virus injected directly into the hemocoel (40).

Since polyhedra were large and readily visible in the light microscope, and since no intermediate developmental forms (e.g. "coated" particles) were seen, it would appear

that this disease progresses in a manner typical of most cytopolyhedroses, as described by several authors (8,23,110, 117).

Cytoplasmic polyhedrosis viruses are thought to have icosahedral symmetry and form (60). Hence, the diameter of the particle will vary depending on its orientation. Hosaka and Aizawa (60) were able to visualize particles in 2- and 5-, but not 3-fold, orientation; the latter were assumed to exist from the classes of particle diameters measured. What appear to be particles seen along axes of 3-fold symmetry are reported here for the first time. Hosaka and Aizawa have also proposed that CPV has a double capsid consisting of an inner and an outer shell, both icosahedral, and each consisting of 12 (i.e., 1/vertex) pentagonal capsomeres. Capsomeres on the outer shell bear long tapering spikes which according to these authors, are hollow and made up of four segments. Several authors have presented evidence in support of part of all of such a structure (8,23,34,90,111). However, the published micrographs remain unconvincing. The proposal of a capsid composed of 2 concentric icosahedral shells in particular appears doubtful, at least from the

evidence given. The present study gives no evidence for a double capsid, although segmented projections were seen.

What is of particular interest in the present case is the fact that particles seen along various axes of (icosahedral) symmetry are almost identical in appearance, if not size, to  $\emptyset$  X 174 particles in similar orientation (37). Published micrographs of both types of virus (8,37) reveal an apparent permeability of the capsid to material resembling nucleic acid; it seems possible that the "leaky" sites are the vertex projections (37).  $\emptyset$  X 174 has icosahedral symmetry, and appears to have 12 vertex capsomeres bearing spikes<sup>1</sup>, and 20 additional capsomeres to complete the shell (37). The capsid, then, is regarded as being composed of a single shell of capsomeres. If this virus is, as has been reported (129), much smaller than CPV particles, then it seems reasonable to expect that the latter should have more than 32 capsomeres in the outer shell alone. Contra Hosaka and Aizawa (60), it would seem that the structure of the CPV particle remains to be elucidated in its entirety; it is quite possible that CPV will eventually be found to be constructed according to a plan similar to that which has been proposed (37) for  $\emptyset$  X 174.

---

<sup>1</sup> Whether or not these are similar in structure to those associated with vertices of the CPV capsid is unknown.

## CONCLUSIONS

1. Three new virus diseases have been discovered in larvae of the midge, Chironomus plumosus.
2. It is proposed that one of these, CpV-1, be included in the family Iridoviridae, as defined by the Lwoff, Horne, and Tournier system of viral classification.
3. All the known icosahedral cytoplasmic DNA viruses in both invertebrate and vertebrate animals are probably related, at least in a structural sense.
4. Two other diseases in C. plumosus are cytopolyhedroses; one of these is unique in that it infects fat body. The other has an unusual developmental cycle in which two different occlusion events occur.
5. The commonly accepted proposal that cytoplasmic polyhedrosis virus particles have a double capsid with a total of 24 capsomeres is regarded as being unsubstantiated. Limited evidence suggests that the capsid may instead be based on a plan similar to that proposed for the bacteriophage  $\phi$  X 174. If so, CPV particles would have in excess of 32 capsomeres.
6. What is probably a rickettsial symbiote or commensal is found in the fat body cytoplasm of C. plumosus larvae.

## REFERENCES

1. Adams, J. R., Wallis, R. L., Wilcox, T. A., and Faust, R. M. A previously undescribed polyhedrosis of the zebra caterpillar, Ceramica picta. J. Invert. Pathol. 11: 45-58, 1968.
2. Adler, I. "A New Look at Geometry", John Day Co., New York, 1966.
3. Almeida, J. D., Watson, A. P., and Plowright, W. The morphological characteristics of African swine fever virus and its resemblance to Tipula iridescent virus. Arch. ges. Virusforsch. 20: 392-396, 1967.
4. Anderson, D. R., Hopps, H. E., Barile, M. F., and Bernheim, B. C. Comparison of the ultrastructure of several rickettsial, ornithosis virus, and mycoplasma in tissue culture. J. Bact. 90: 1387-1404, 1965.
5. Anderson, E., and Harvey, W. R. Active transport by the Cecropia midgut. II. Fine structure of the midgut epithelium. J. Cell Biol. 31: 107-134, 1966.
6. Arnott, H. J., and Smith, K. M. An ultrastructural study of the development of a granulosis virus in the cells of the moth Plodia interpunctella (Hbn.). J. Ultrastruct. Res. 21: 251-268, 1968.
7. Arnott, H. J., and Smith, K. M. Ultrastructure and formation of abnormal capsules in a granulosis virus of the moth Plodia interpunctella (Hbn.). J. Ultrastruct. Res. 22: 136-158, 1968.
8. Arnott, H. J., Smith, K. M., and Fullilove, S. L. Ultrastructure of a cytoplasmic polyhedrosis virus affecting the monarch butterfly, Danaus plexippus. I. Development of virus and normal polyhedra in the larva. J. Ultrastruct. Res. 24: 479-507, 1968.
9. Aruga, H., Hukuhara, T., Yoshitake, N., and Ayudhya, I. N. Interference and latent infection in the cytoplasmic polyhedrosis of the silkworm, Bombyx mori (Linn.). J. Insect. Pathol. 3: 81-92, 1961.

10. Aruga, H., Yoshitake, N., and Watanabe, H. Some factors controlling the size of the cytoplasmic polyhedra of Bombyx mori (Linnaeus). J. Insect Pathol. 5: 72-77, 1963.
11. Baltimore, D. How to define "picornavirus". Proc. 1st Intern. Conf. Comp. Virol., unpublished, 1969.
12. Beerman, W., and Clever, Y. Chromosome puffs. Scient. Amer. 210: April, 1964.
13. Bellett, A. J. D., and Mercer, E. H. The multiplication of Sericesthis iridescent virus in cell cultures from Antheraea eucalypti Scott. I. Qualitative experiments. Virology 24: 645-653, 1964.
14. Bellett, A. J. D., and Inman, R. B. Some properties of deoxyribonucleic acid preparations from Chilo, Sericesthis, and Tipula iridescent viruses. J. Mol. Biol. 25: 425-432, 1967.
15. Bellet, A. J. D. The iridescent virus group. Adv. Virus Res. 13: 225-246, 1968.
16. Bellett, A. J. D., and Fenner, F. Studies of base-sequence homology among some cytoplasmic deoxyriboviruses of vertebrate and invertebrate animals. J. Virol. 2: 1374-1380, 1968.
17. Bellett, A. J. D. Relationships among the polyhedrosis and granulosis viruses of insects. Virology 37: 117-123, 1969.
18. Biempica, L. Human hepatic microbodies with crystalloid cores. J. Cell Biol. 29: 383-386, 1966.
19. Bird, F. T. The effect of metamorphosis on the multiplication of an insect virus. Can. J. Zool. 31: 300-303, 1953.
20. Bird, F. T. Transmission of some insect viruses with particular reference to ovarian transmission and its importance in the development of epizootics. J. Insect Pathol. 3: 352-380, 1961.
21. Bird, F. T. On the development of the Tipula iridescent virus particle. Can. J. Microb. 8: 533-534, 1962.
22. Bird, F. T. On the development of insect polyhedrosis and granulosis virus particles. Can. J. Microb. 10: 49-52, 1964.

23. Bird, F. T. On the morphology and development of insect cytoplasmic-polyhedrosis virus particles. *Can. J. Microb.* 11: 497-501, 1965.
24. Breese, S. S. Jr., and DeBoer, C. J. Electron microscope observations of African swine fever virus in tissue culture cells. *Virology* 28: 420-428, 1966.
25. Breese, S. S. Jr., and DeBoer, C. J. Effect of hydroxyurea on the development of African swine fever virus. *Am. J. Pathol.* 55: 69-77, 1969.
26. Bucher, G. E., and Harris, P. Virus diseases and their interaction with food stress in *Calophasia lumula*. *J. Invert. Pathol.* 10: 235-244, 1968.
27. Bullivant, S., and Loewenstein, W. R. Structure of coupled and uncoupled cell junctions. *J. Cell Biol.* 37: 621-632, 1968.
28. Came, P. E., and Dardiri, A. H. Host specificity and serologic disparity of African swine fever virus and amphibian polyhedral cytoplasmic viruses. *Proc. Soc. Exptl. Biol. Med.* 130: 128-132, 1969.
29. Chapman, H. C., Clark, T. B., Woodard, D. B., and Kellen, W. R. Additional hosts of the mosquito iridescent virus. *J. Invert. Pathol.* 8: 545-546, 1966.
30. Clark, H. F., Brennan, J. C., Zeigel, R. F., and Karzon, D. T. Isolation and characterization of viruses from the kidneys of *Rana pipiens* with renal adenocarcinoma before and after passage in the red eft (*Triturus viridescens*). *J. Virol.* 2: 629-640, 1968.
31. Clark, T. B., Kellen, W. R., and Lum, P. T. M. A mosquito iridescent virus (MIV) from *Aedes taeniorhynchus* (Weidemann). *J. Invert. Pathol.* 7: 519-521, 1965.
32. Clark, T. B., Chapman, H. C., and Fukuda, T. Nuclear-polyhedrosis and cytoplasmic-polyhedrosis virus infections in Louisiana mosquitoes. *J. Invert. Pathol.* 14: 284-286, 1969.
33. Clever, U., and Karlson, P. Induktion von puffveränderungen in den speicheldrüsenchromosomen von *Chironomus tentans* durch ecdyson. *Expt. Cell Res.* 20: 623-626, 1960.
34. Cunningham, J. C., and Longworth, J. F. The identification of some cytoplasmic-polyhedrosis viruses. *J. Invert. Pathol.* 11: 196-202, 1968.

35. Darlington, R. W., Granoff, A., and Breeze, D. C. Viruses and renal carcinoma of Rana pipiens. II. Ultrastructural studies and sequential development of virus isolated from normal and tumor tissue. Virology 29: 149-156, 1966.
36. DeDuve, C., and Baudhuin, P. Peroxisomes (microbodies and related particles). Physiol. Rev. 46: 323-357, 1966.
37. Edgell, M. H., Hutchison III, C. A., and Sinsheimer, R. L. The process of infection with bacteriophage  $\phi$  X 174 XXVIII. Removal of the spike proteins from the phage capsid. J. Mol Biol. 42: 547-557, 1969.
38. Entwistle, P. F., and Robertson, J. S. An unusual nuclear-polyhedrosis virus from larvae of a hepialid moth. J. Invert. Pathol. 11: 487-495, 1968.
39. Faust, R. M., and Adams, J. R. The silicon content of nuclear and cytoplasmic viral inclusion bodies causing polyhedrosis in Lepidoptera. J. Invert. Pathol. 8: 526-530, 1966.
40. Faust, R. M., and Cantwell, G. E. Inducement of cytoplasmic polyhedrosis by the intra-hemocoelic injection of freed viral particles into the silkworm, Bombyx mori. J. Invert. Pathol. 11: 119-122, 1968.
41. Fukaya, M., and Nasu, S. A Chilo iridescent virus from the rice stem borer, Chilo suppressalis walker (Lepidoptera: Pyralidae). Appl. Entomol. Zool. 1: 69-72, 1966.
42. Gibbs, A. J., Harrison, B. D., Waton, D. H., and Wildy, P. What's in a virus name? Nature 209: 450-454, 1966.
43. Goldberg, M. A class of multi-symmetric polyhedra. Tôhuka math. J. 43: 104, 1937.
44. Goodwin, R. H., and Filshie, B. K. Morphology and development of an occluded virus from the black-soil scarab, Othnonius batesi. J. Invert. Pathol. 13: 317-329, 1969.
45. Gotz, P., Huger, A. M., and Krieg, A. Uber ein insektenpathogenes virus ans der gruppe der pockenviren. Naturwissenschaften 56: 145, 1969.
46. Grace, T. D. C. Establishment of 4 strains of cells from insect tissues grown in vitro. Nature 195: 788-789, 1962.

47. Grace, T. D. C. The development of a cytoplasmic polyhedrosis in insect cells grown in vitro. Virology 18: 33-42, 1962.
48. Granboulan, N., Tournier, P., Wicker, R., and Bernhard, W. An electron microscope study of the development of SV40 virus. J. Cell Biol. 17: 423-441, 1963.
49. Granoff, A., Came, P. E., and Rafferty, K. The isolation and properties of viruses from Rana pipiens: their possible relationships to the renal adenocarcinoma of the leopard frog. Ann. N. Y. Acad. Sci. 126: 237-255, 1965.
50. Greenlee, T. K., Jr., Ross, R., and Hartman, J. L. The fine structure of elastic fibers. J. Cell Biol. 30: 59-71, 1966.
51. Harrap, K. A., and Robertson, J. A. A possible infection pathway in the development of a nuclear polyhedrosis virus. J. gen. Virol. 3: 221-225, 1968.
52. Heimpel, A. M., and Adams, J. R. A new nuclear polyhedrosis of the cabbage looper, Trichoplusia ni. J. Invert. Pathol. 8: 340-346, 1966.
53. Hendrickson, A., Kunz, S., and Kelly, D. E. NaOH-HIO<sub>4</sub> treatment of osmium-collidine fixed, epoxy sections to facilitate staining after autoradiography. Stain Techn. 43: 175-177, 1968.
54. Hilsenhoff, W. L. Predation by the leech Helobdella stagnalis on Tendipes plumosus (Diptera: Tendipedidae) larvae. Ann. Entomol. Soc. Am. 56: 252, 1963.
55. Hilsenhoff, W. L. The biology of Chironomus plumosus (Diptera: Chironomidae) in Lake Winnebago, Wisconsin. Ann. Entomol. Soc. Am. 59: 465-473, 1966.
56. Hilsenhoff, W. L. Infection of Chironomus plumosus (Diptera: Chironomidae) by a microsporidian (Thelohania sp.) in Lake Winnebago, Wisconsin. J. Invert. Pathol. 8: 512-519, 1966.
57. Hilsenhoff, W. L. Ecology and population dynamics of Chironomus plumosus (Diptera: Chironomidae) in Lake Winnebago, Wisconsin. Ann. Entomol. Soc. Am. 60: 1183-1194, 1967.
58. Hilsenhoff, W. L., and Narf, R. P. Colonization of Chironomus plumosus (Diptera: Chironomidae). Mosquito News 27: 363-366, 1967.

59. Hinz, R. N., Barski, G., and Bernhard, W. An electron microscopic study of the development of encephalomyocarditis (EMC) virus propagated in vitro. Expt. Cell Res. 26: 571-586, 1962.
60. Hosaka, Y., and Aizawa, K. The fine structure of the cytoplasmic polyhedrosis virus of the silkworm, Bombyx mori (Linnaeus). J. Insect Pathol. 6: 53-77, 1964.
61. Huxley, H. E. Electron microscope studies on the structure of natural and synthetic protein filaments from striated muscle. J. Mol. Biol. 7: 281-308, 1963.
62. Ichihashi, Y., and Matsumoto, S. Studies on the nature of Marchal bodies (A-type inclusion) during ectromelia virus infection. Virology 29: 264-275, 1966.
63. Ichihashi, Y., and Matsumoto, S. The relationship between poxvirus and A-type inclusion body during double infection. Virology 36: 262-270, 1968.
64. Kellenberger, E., Eiserling, F. A., and Boy de la Tour, E. Studies on the morphopoiesis of the head of phage T-even III. The cores of head related structures. J. Ultrastruct. Res. 21: 335-360, 1968.
65. King, J. Assembly of the tail of bacteriophage T4. J. Mol. Biol. 32: 231-262, 1968.
66. Klug, A., Franklin, R. E., and Humphreys-Owen, S. P. F. The crystal structure of Tipula iridescent virus as determined by Bragg reflection of visible light. Biochim. Biophys. Acta 32: 203-219, 1959.
67. Kopriva, B. M., and Leblond, C. P. Improvements in the coating technique of radioautography. J. Histochem. Cytochem. 10: 269-284, 1962.
68. Kurstak, E., and Vago, C. Transmission du virus de la denonucleose par le parasitisme d'un hymenoptere. Rev. Can. Biol. 26: 311-316, 1967.
69. Lanham, U. N. The Blochmann bodies: hereditary intracellular symbionts of insects. Biol. Rev. 43: 269-286, 1968.
70. Laver, W. G., Pereira, H. G., Russell, W. C., and Valentine, R. C. Isolation of an internal component from adenovirus type 5. J. Mol. Biol. 37: 379-386, 1968.

71. Leduc, E. H., and Bernhard, W. Electron microscope study of mouse liver infected by ectromelia virus. *J. Ultrastruct. Res.* 6: 466-488, 1962.
72. Leutenegger, R. Early events of Sericesthis iridescent virus infection in hemocytes of Galleria mellonella (L.). *Virology* 32: 109-116, 1967.
73. Lewandowsky, L. J. Structure of the nucleic acid of cytoplasmic polyhedrosis virus; RNA polymerase activity associated with purified CPV. Proc. 1st Intern. Conf. Comp. Virol., unpublished, 1969.
74. Linley, J. R., and Nielsen, H. T. Transmission of a mosquito iridescent virus in Aedes taeniorhynchus I. Laboratory experiments. *J. Invert. Pathol.* 12: 7-16, 1968.
75. Linley, J. R., and Nielsen, H. T. Transmission of a mosquito iridescent virus in Aedes taeniorhynchus II. Experiments related to transmission in nature. *J. Invert. Pathol.* 12: 17-24, 1968.
76. Longworth, J. F., and Cunningham, J. C. The activation of occult nuclear-polyhedrosis viruses by foreign nuclear polyhedra. *J. Invert. Pathol.* 10: 361-367, 1968.
77. Lunger, P. D. Amphibian-related viruses. *Adv. Virus Res.* 12: 1-33, 1966.
78. Lwoff, A., Horne, R., and Tournier, P. A system of viruses. *Cold Spr. Hbr. Symp. Quant. Biol.* 27: 51-55, 1962.
79. Lwoff, A., and Tournier, P. The classification of viruses. *Ann. Rev. Microb.* 20: 45-74, 1966.
80. Lwoff, A. Reflexions sur la classification des virus. Le Phanerogramme. Proc. 1st Intern. Conf. Comp. Virol., unpublished, 1969.
81. Maramorosch, K., Shikata, E., and Granados, R. R. Structures resembling mycoplasma in diseased plants and in insect vectors. *Trans. N. Y. Acad. Sci.* 30: 841-855, 1968.
82. Martignoni, M. E., and Longston, R. L. Supplement to an annotated list and bibliography of insects reported to have virus diseases. *Hilgardia* 30: 1-40, 1960.
83. Martignoni, M. E., Iwai, P. J., Hughes, K. M., and Addison, R. B. A cytoplasmic polyhedrosis of Hemerocampa pseudotsugata. *J. Invert. Pathol.* 13: 15-18, 1969.

84. Mathad, S. B., Splittstresser, C. M., and McEwen, F. L. Histopathology of the cabbage looper, Trichoplusia ni, infected with a nuclear polyhedrosis. J. Invert. Pathol. 11: 456-464, 1968.
85. Mejbaum, W. Uber die bestimum kleiner pentosemengen inshesondere in derivaten der adenylsamen. Z. Physiol. Chem. 258: 117, 1939.
86. Mercer, E. H., and Day, M. F. The structure of Sericesthis iridescent virus and its crystals. Biochem. Biophys. Acta 102: 590-599, 1965.
87. Midlige, F. H., Jr., and Malsberger, R. G. In vitro morphology and maturation of lymphocystis virus. J. Virol. 2: 830-835, 1968.
88. Mitsuhashi, J. Infection of leafhopper and its tissues cultivated in vitro with Chilo iridescent virus. J. Invert. Pathol. 9: 432-434, 1967.
89. Miura, K., Fujii, I., Sakaki, T., Fuke, M., and Kawase, S. Double-stranded ribonucleic acid from CPV of the silkworm. J. Virol. 2: 1211-1222, 1968.
90. Miura, K., Fujii-Kawata, I., Iwata, H., and Kawase, S. Electron-microscopic observations of a cytoplasmic-polyhedrosis virus from the silkworm. J. Invert. Pathol. 14: 262-265, 1969.
91. Mizell, M., Stackpole, C. W., and Halperen, S. Herpes-type virus recovery from "virus-free" frog kidney tumors. Proc. Soc. Exptl. Biol. Med. 127: 808-814, 1968.
92. Muscatello, U., and Horne, R. E. Effect of the tonicity of some negative-staining solutions on the elementary structure of membrane-bounded systems. J. Ultrastruct. Res. 25: 73-83, 1968.
93. Musgrave, A. J. Insect mycetozoa. Can. Entomol. 96: 377-389, 1964.
94. Nasu, S. Electron microscopic studies on transovarial passage of rice dwarf virus. J. Appl. Entom. Zool. 9: 225-237, 1965.
95. Norrby, E. Biological significance of structural adenovirus components. Current Topics Microb. Immunol. 43: 1-43, 1968.

96. Odhiambo, T. R. The fine structure and histochemistry of the fat body in the locust, Schistocerca gregaria. J. Cell Sci. 2: 235-242, 1967.
97. Pavan, C., and DaCunha, A. B. Chromosomal activities in Rhynchosciara and other Sciaridae. Ann. Rev. Genet. 3: 425-450, 1969.
98. Reich, E. Actinomycin: correlation of structure and function of its complexes with purines and DNA. Science 143: 684-689, 1964.
99. Reynolds, R. C., Montgomery, P. O'B., and Hughes, B. Nucleolar "caps" produced by actinomycin D. Cancer Res. 24: 1269-1277, 1964.
100. Russell, W. C., Valentine, R. C., and Pereira, H. G. The effect of heat on the anatomy of the adenovirus. J. gen. Virol. 1: 509-522, 1967.
101. Schoefl, G. I. The effect of actinomycin D on the fine structure of the nucleolus. J. Ultrastruct. Res. 10: 224-243, 1964.
102. Schreil, W. H. Studies on the fixation of artificial and bacterial DNA plasms for the electron microscopy of thin sections. J. Cell Biol. 22: 1-20, 1964.
103. Sekiguchi, M., and Takagi, Y. Effect of mitomycin C on the synthesis of bacterial and viral deoxyribonucleic acid. Biochim. Biophys. Acta 41: 434-443, 1960.
104. Shinozuka, H., Verney, E., and Sidransky, H. Alterations in the liver due to acute amino acid deficiency. An electron microscopic study of young rats force-fed a threonine-devoid diet. Lab. Invest. 18: 72-85, 1968.
105. Shnitka, T. K. Comparative ultrastructure of hepatic microbodies in some mammals and birds in relation to species differences in uricase activity. J. Ultrastruct. Res. 16: 598-625, 1966.
106. Smith, D. S., Compher, K., Janners, M., Lipton, C., and Wittle, L. W. Cellular organization and ferritin uptake in the midgut of a moth, Ephestia kuhniella. J. Morph. 127: 41-72, 1969.
107. Smith, K. M., and Wyckoff, R. W. G. Structure within polyhedra association with insect virus diseases. Nature 166: 861-862, 1950.

108. Smith, K. M., and Rivers, C. F. Some viruses affecting insects of economic importance. *Parasitology* 46: 235-242, 1956.
109. Smith, K. M., and Hills, E. J. Further studies on the electron microscopy of the Tipula iridescent virus. *J. Mol. Biol.* 1: 277-280, 1959.
110. Smith, K. M. The cytoplasmic virus diseases. In "Insect Pathology" (E. A. Steinhaus, ed.), Vol. 1, p. 478. Academic Press, New York, 1963.
111. Smith, K. M. "Insect Virology", Academic Press, New York, 1967.
112. Smith, K. O., Gehle, W. D., and Trousdale, M. D. Architecture of the adenovirus capsid. *J. Bact.* 90: 254-260, 1965.
113. Stackpole, C. W. Herpes-type virus of the frog renal adenocarcinoma I. Virus development in tumor transplants maintained at low temperature. *J. Virol.* 4: 75-93, 1969.
114. Stairs, G. R. Selection of a strain of granulosis virus producing only cuboidal inclusion bodies. *Virology* 24: 520-521, 1964.
115. Stairs, G. R. The effect of metamorphosis on nuclear-polyhedrosis virus infections in certain Lepidoptera. *Can. J. Microb.* 11: 509-512, 1965.
116. Stairs, G. R. Inclusion-type insect viruses. *Current Topics Microb. Immunol.* 42: 1-23, 1968.
117. Stairs, G. R., Parrish, W. B., and Allietta, M. A histopathological study involving a cytoplasmic-polyhedrosis virus of the salt-marsh caterpillar, Estigmene acrea. *J. Invert. Pathol.* 12: 359-365, 1968.
118. Stehbens, W. E., and Johnston, M. R. L. The viral nature of Pirhemocytion tarentolae. *J. Ultrastruct. Res.* 15: 543-554, 1966.
119. Steiger, U., Lamparter, H. E., Sandri, C., and Akert, K. Virus-ähnliche partikel im zytosol von nerven- und gliazellen der waldameise. *Arch. ges. Virusforsch.* 26: 271-282, 1969.
120. Steinhaus, E. A., and Leutenegger, R. Icosahedral virus from a scarab (Sericesthis). *J. Insect. Pathol.* 5: 266-270, 1963.

121. Stevens, B. J., and Swift, H. RNA transport from nucleus to cytoplasm in Chironomus salivary glands. J. Cell Biol. 31: 55-77, 1966.
122. Stevens, B. J. The effect of actinomycin D on nucleolar and nuclear fine structure in the salivary gland cell of Chironomus thummi. J. Ultrastruct. Res. 11: 329-353, 1964.
123. Summers, M. D. Apparent in vivo pathway of granulosis virus invasion and infection. J. Virol. 4: 188-190, 1969.
124. Sylvester, E. S. Evidence of transovarial passage of the sowthistle yellow vein virus in the aphid Hyperomyzus lactucae. Virology 38: 440-446, 1969.
125. Thoenes, W. Fett in nucleolus. J. Ultrastruct. Res. 10: 194-206, 1964.
126. Thomas, R. S. The chemical composition and particle weight of Tipula iridescent virus. Virology 14: 240-250, 1961.
127. Thomas, R. S., and Williams, R. C. Localization of DNA and protein in Tipula iridescent virus by enzymatic digestion and electron microscopy. J. Biophys. Biochem. Cytol. 11: 15-29, 1961.
128. Tojo, S., and Kodama, T. Purification and some properties of Chilo iridescent virus. J. Invert. Pathol. 12: 66-72, 1968.
129. Tromans, W. J., and Horne, R. W. The structure of bacteriophage  $\phi$  X 174. Virology 15: 1-7, 1961.
130. Vail, P. V., Hall, I. M., and Gough, D. Influence of a cytoplasmic polyhedrosis on various developmental stages of the cabbage looper. J. Invert. Pathol. 14: 237-244, 1969.
131. Walker, R. Fine structure of lymphocystis virus of fish. Virology 18: 503-505, 1962.
132. Walshe, B. M. Feeding mechanisms of Chironomus larvae. Nature 160: 474, 1947.
133. Warren, R. H., and Porter, K. R. An electron microscope study of differentiation of the molting muscles of Rhodnius prolixus. Am. J. Anat. 124: 1-30, 1969.
134. Weiser, J. A new virus infection of mosquito larvae. Bull. World Health Organ. 33: 586-588, 1965.

135. Weiser, J. Iridescent virus from the blackfly Simulium ornatum Meigen in Czechoslovakia. J. Invert. Pathol. 12: 36-39, 1968.
136. Wigglesworth, V. B. "The Principles of Insect Physiology", Methuen and Co., Ltd., London, 1950.
137. Williams, R. C., and Smith, K. M. The polyhedral form of the Tipula iridescent virus. Biochim. Biophys. Acta 28: 464-469, 1958.
138. Wolf, K., Bullock, G. L., Dunbar, C. E., and Quimby, M. C. Tadpole edema virus: a viscerotropic pathogen for anuran amphibians. J. Inf. Dis. 118: 253-262, 1968.
139. Wood, R. L. Effect of ethionine on the ultrastructure of developing liver cells. J. Ultrastruct. Res. 19: 100-115, 1967.
140. Wood, W. B., Edgar, R. S., King, J., Lielausis, I., and Henninger, M. Bacteriophage assembly. Fed. Proc. 27: 1160-1166, 1968.
141. Woodard, D. B., and Chapman, H. C. Laboratory studies with the mosquito iridescent virus (MIV). J. Invert. Pathol. 11: 296-301, 1968.
142. Wrigley, N. G. An electron microscope study of the structure of Sericesthis iridescent virus. J. gen. Virol. 5: 123-134, 1969.
143. Xeros, N. A second virus disease of the leather-jacket Tipula paludosa. Nature 174: 562-564, 1954.
144. Xeros, N. The virogenic stroma in nuclear and cytoplasmic polyhedroses. Nature 178: 412-413, 1956.
145. Xeros, N. Development of the Tipula iridescent virus. J. Insect. Pathol. 6: 261-283, 1964.
146. Yanders, A. F., Brewer, J. G., Peacock, W. J., and Goodchild, D. J. Meiotic drive and visible polarity in Drosophila spermatocytes. Genetics 59: 245-253, 1968.
147. Yunker, C. E., Vaughn, J. L., and Cory, L. Adaptation of an insect cell line (Grace's Antheraea cells) to medium free of insect hemolymph. Science 155: 1565-1566, 1967.
148. Zwillenberg, L. O., and Wolf, K. Ultrastructure of lymphocystis virus. J. Virol. 2: 393-399, 1968.

## APPENDIX

Preliminary observations on two of the viruses described in this thesis appear in the following published papers:

1. Stoltz, D. B., Stich, H. F., and Hilsenhoff, W. L.  
A virus disease in Chironomus plumosus. J. Invert. Pathol. 12: 118-128, 1968.
2. Stoltz, D. B., and Hilsenhoff, W. L. Electron-microscopic observations on the maturation of a cytoplasmic-polyhedrosis virus. J. Invert. Pathol. 14: 39-48, 1969.